TOJSAT
The Online Journal of Scince and Technology

ISSN 2146-739

The Online Journal of Science and Technology

Volume 4 Issue 4
October 2014

Prof. Dr. Aytekin İşman
Editor-in-Chief

Prof. Dr. Mustafa Şahin Dündar
Editor

Associate Editors:
Assist. Prof. Dr. İrfan Şimşek

www.tojsat.net
October 2014

Copyright © 2014 - THE ONLINE JOURNAL OF SCIENCE AND TECHNOLOGY
All rights reserved. No part of TOJSAT's articles may be reproduced or utilized in any form or by any means, electronic or mechanical, including photocopying, recording, or by any information storage and retrieval system, without permission in writing from the publisher.

Published in TURKEY

Contact Address:

Prof. Dr. Aytekin İŞMAN- TOJSAT, Editor in Chief Sakarya-Turkey

Message from the Editor-in-Chief

TOJSAT welcomes you. TOJSAT looks for academic articles on the issues of science and technology. The articles should discuss new methods and applications in science and technology. TOJSAT contributes to the development of both theory and practice in the field of science and technology. TOJSAT accepts academically robust papers, topical articles and case studies that contribute to the area of research in science and technology.

The aim of TOJSAT is to help students, teachers, academicians and communities better understand new developments in science and technology. The submitted articles should be original, unpublished, and not in consideration for publication elsewhere at the time of submission to TOJSAT. TOJSAT provides perspectives on topics relevant to the study, implementation and management of science and technology.

I am always honored to be the editor in chief of TOJSAT. Many persons gave their valuable contributions for this issue.

TOJSAT and Sakarya University will organize International Science and Technology Conference (ISTEC 2014) in December 2014 in Doha, Qatar. Please visit www.iste-c.net

For any suggestions and comments on the international online journal TOJSAT, please do not hesitate to contact with the editor.

October 1, 2014
Editor-in-Chief
Prof. Dr. Aytekin İŞMAN
Sakarya University

Dear Readers,

Now, we have reached to the end of fourth volume of the Tojsat journal. Nearly 4 years ago we have published the first issue of the journal on-line. Our goal is to rewiev and accept all kinds of scientific research paper, rewiev articles, etc. We are approaching to 5th istec 2014 conference held in Doha, Qatar between 18-20 December 2014. We are welcome all attendees coming and joining the conference.

I will thank to the readers all around the World for supports by sending their valuable scientific works to publish in the journal.

Prof. Dr. M. Şahin DÜNDAR

Editor, TOJSAT

Editor-in-Chief

Prof. Dr. Aytekin İŞMAN - Sakarya University, Turkey

Editor

Prof. Dr. Mustafa Şahin DÜNDAR - Sakarya University, Turkey

Associate Editors

Assist. Prof. Dr. Hayrettin EVİRGEN, Sakarya University, Turkey
Assist. Prof. Dr. İrfan ŞİMŞEK, Istanbul University, Turkey

Editorial Board

Abdülkadir MASKAN, Dicle University, Turkey
Ahmet AKSOY, Erciyes University, Turkey
Ahmet APAY, Sakarya University, Turkey
Ahmet BİÇER, Gazi University, Turkey
Ahmet ÖZEL, Sakarya University, Turkey
Ahmet Zeki SAKA, Karadeneniz Technical University, Turkey
Ali ÇORUH, Sakarya University, Turkey
Ali DEMIRSOY, Hacettepe University, Turkey
Ali Ekrem OZKUL, Anadolu University, Turkey
Ali GUL, Gazi University, Turkey
Ali GUNYAKTI, Eastern Mediterranean University, TRNC
Alparslan FIGLALI, Kocaeli University, Turkey
Antonis LIONARAKIS, Hellenic Open University, Greece
Arif ALTUN, Hacettepe University, Turkey
Atilla YILMAZ, Hacettepe University, Turkey
Aydın Ziya OZGUR, Anadolu University, Turkey
Bekir SALIH, Hacettepe University, Turkey
Belma ASLIM, Gazi University, Turkey
Bensafi Abd-El-Hamid, Abou Bekr Belkaid University of Tlemcen, Algeria.
Berrin ÖZÇELİK, Gazi University
Bilal GÜNEŞ, Gazi University, Turkey
Bilal TOKLU, Gazi University, Turkey
Burhan TURKSEN, TOBB University of Economics and Technology, Turkey
Cafer CELIK, Ataturk University, Turkey
Can KURNAZ, Sakarya University, Turkey
Canan LACIN SIMSEK, Sakarya University, Turkey
Cüneyt BİRKÖK, Sakarya University, Turkey
Elnaz ZAHED, University of Waterloo, UAE
Emine Sercen DARCIN, Sakarya University, Turkey
Eralp ALTUN, Ege University, Turkey
M. Şahin DÜNDAR, Sakarya University, Turkey
Mehmet Ali YALÇIN, Sakarya University, Turkey
Mehmet BAYRAK, Sakarya University, Turkey
Mehmet CAGLAR, Eastern Mediterranean University, TRNC
Mehmet TURKER, Gazi University, Turkey
Mehmet YILMAZ, Gazi University, Turkey
Melek MASAL, Sakarya University, Turkey
Metin BAŞARIR, Sakarya University, Turkey
Moinuddin Sarker, MCIC, USA
Moinuddin Sarker, Natural State Research, Inc., USA
Muhammed JAVED, Islamia University of Bahawalpur,Pakistan
Muharrem TOSUN, Sakarya University, Turkey
Murat DIKER, Hacettepe University, Turkey
Murat TOSUN, Sakarya University, Turkey
Mustafa BÖYÜKATA, Bozok University, Turkey
Mustafa DEMİR, Sakarya University, Turkey
Mustafa GAZI, Eastern Mediterranean University, TRNC
Mustafa GAZİ, Near East University, TRNC
Mustafa GUL, Turkey
Mustafa KALKAN, Dokuz Eylul Universiy, Turkey
Mustafa YILMAZLAR, Sakarya University, Turkey
Nabi Bux JUMANI, Allama Iqbal Open University, Pakistan.
Nilgun TOSUN, Trakya Üniversitesi, Turkey
Nureddin KIRKAVAK, Eastern Mediterranean University, TRNC
Nursen SUCSUZ, Trakya Üniversitesi, Turkey
Oğuz SERİN, Cyprus International University, TRNC
Orhan ARSLAN, Gazi University, Turkey
Orhan TORKUL, Sakarya University, Turkey
Osman ÇEREZCİ, Sakarya University, Turkey
Phaik Kin, CHEAH Universiti Tunku Abdul Rahman,

Ercan MASAL, Sakarya University, Turkey
Ergun KASAP, Gazi University, Turkey
Ergun YOLCU, Istanbul University, Turkey
Fatime Balkan KIYICI, Sakarya University, Turkey
Fatma AYAZ, Gazi University, Turkey
Fatma ÜNAL, Gazi University, Turkey
Galip AKAYDIN, Hacettepe University, Turkey
Gilbert Mbotho MASITSA, Universirty of The Free State - South Africa
Gregory ALEXANDER, Universirty of The Free State - South Africa
Gülay BİRKÖK, Gebze Institute of Technology, Turkey
Gürer BUDAK, Gazi University, Turkey
Harun TAŞKIN, Sakarya University, Turkey
Hasan DEMIREL, Eastern Mediterranean University, TRNC
Hasan Hüseyin ONDER, Gazi University, Turkey
Hasan KIRMIZIBEKMEZ, Yeditepe University, Turkey
Hasan OKUYUCU, Gazi University, Turkey
Hayrettin EVİRGEN, Sakarya University, Turkey
Hikmet AYBAR, Eastern Mediterranean University, TRNC
Hüseyin EKİZ, Sakarya University, Turkey
Hüseyin Murat TÜTÜNCÜ, Sakarya University, Turkey
Hüseyin ÖZKAN, Sakarya University, Turkey
Hüseyin YARATAN, Eastern Mediterranean University, TRNC
Iman OSTA, Lebanese American Universiy, Lebanon
Işık AYBAY, Eastern Mediterranean University, TRNC
İbrahim OKUR, Sakarya University, Turkey
İlyas ÖZTÜRK, Sakarya University, Turkey
İsmail Hakkı CEDİMOĞLU, Sakarya University, Turkey
İsmail ÖNDER, Sakarya University, Turkey
Kenan OLGUN, Sakarya University, Turkey
Kenan OLGUN, Sakarya University, Turkey
Latif KURT, Ankara University, Turkey
Levent AKSU, Gazi University, Turkey
Malaysia
Piotr S. Tomski, Czestochowa University of Technology, Poland
Rahmi KARAKUŞ, Sakarya University, Turkey
Ratnakar Josyula, Yale University school of medicine, New Haven, USA
Ratnakar JOSYULA,Yale University, USA
Recai COŞKUN, Sakarya University, Turkey
Recep İLERİ, Bursa Orhangazi University, Turkey
Rıfat EFE, Dicle University, Turkey
Ridvan KARAPINAR, Yüzüncü Yıl University, Turkey
Sanjeev Kumar SRIVASTAVA, Mitchell Cancer Institute,USA
Seçil KAYA, Anadolu University, Turkey
Selahattin GÖNEN, Dicle University, Turkey
Senay CETINUS, Cumhuriyet University, Turkey
Serap OZBAS, Near East University, North Cyprus
Sevgi AKAYDIN, Gazi University, Turkey
Sevgi BAYARI, Hacettepe University, Turkey
Sukumar SENTHILKUMAR, South Korea
Süleyman ÖZÇELİK, Gazi University, Turkey
Şenol BEŞOLUK, Sakarya University, Turkey
Tuncay ÇAYKARA, Gazi University, Turkey
Türkay DERELI, Gaziantep University, Turkey
Uner KAYABAS, Inonu University, Turkey
Ümit KOCABIÇAK, Sakarya University, Turkey
Vahdettin SEVİNÇ, Sakarya University, Turkey
Vasudeo Zambare, South Dakota School of Mines and Technology, USA
Veli CELIK, Kırıkkale University, Turkey
Yusuf ATALAY,Sakarya University, Turkey
Yusuf KALENDER, Gazi University, Turkey
Yusuf KARAKUŞ, Sakarya University, Turkey
Yüksel GÜÇLÜ, Sakarya University, Turkey
Zawawi Bin Daud, Universiti Tun Hussein Onn Malaysia, Malaysia
Zekai SEN, Istanbul Technical University, Turkey

Table of Contents

Study on the Thermal Behavior of Mechanically Activated Malachite

Tuğba Tunç and Kenan Yıldız

Metallurgy and Materials Engineering, Engineering Faculty Sakarya University, Turkey
ttunc@sakarya.edu.tr, kenyil@sakarya.edu.tr

Abstract: Malachite, a copper carbonate hydroxide mineral with the formulation of $Cu_2CO_3(OH)_2$ was mechanically activated for different durations in a planetary mill. For comparison of structural changes, malachite was calcined at 400°C and 600°C. Morphological changes in both mechanically activated and calcined malachite were determined with scanning electron microscopy (SEM). From the X-ray diffraction (XRD) patterns, amorphization degrees were calculated for mechanically activated malachite and alteration of the ore structure with mechanical activation was demonstrated. With differential thermal analysis (DTA-TG), decomposition and dehydroxylation temperatures for mechanically activated samples were specified. Fourier transform infrared spectroscopy analysis was used for calcined malachite for understanding of the bond characteristic to heat. From the FT-IR analysis, the reasons of disappearing endotherms for mechanically activated samples were assigned.

Key words: malachite, mechanical activation, calcination, amorphization.

Introduction

In electrical and electronic industry, copper is the most preferable metal because of its higher conductivity. Beside this area, copper and its alloys are used in rolling industry, communication and aviation industry for electric production and distribution (Arzutug et al., 2004). Sulfide and oxidized copper ore exist in the world (Liu et al., 2012). Tenorite (CuO), chrystocolla ($CuSiO_3.2H_2O$) (Bingöl et al.) and chalcocite (Cu_2O) (Arzutug et al., 2004) are copper oxide minerals like azurite [$Cu_3(OH)_2(CO_3)_2$] and malachite [$Cu_2(OH)_2CO_3$]. In these minerals copper in the divalent state and they are completely soluble in acidic or alkaline medium at room temperature (Bingöl et al., 2005). Chalcopyrite ($CuFeS_2$), bornite (Cu_5FeS_4) (Arzutug et all., 2004), chalcocite (Cu_2S) (Watling, 2006), cubanite ($CuFe_2S_3$), and enargite (Cu_3AsS_4) (Moskalyk et all., 2003) get involved in the group of sulfide minerals. Copper oxide and carbonate ores represent 10% of the total world copper reserves (Samouhos et al., 2011). Metallic copper is produced from there ores by hydrometallurgical and pyrometallurgical process.

Malachite had been determined in ancient art works as a green painting (Molchan et al., 2008). Besides using as a painting material, malachite is used as stone in jewelry, employed in catalysts, coatings and pigments and considered as a source of copper to produce other copper compounds (Xu et al., 2005).

Stoilova et al. (2002) stated that the mineral malachite, $Cu_2(OH)_2CO_3$, crystallized in monoclinic system. According to Stoilova et al. Cu(1) is coordinated by two oxygen atoms from the carbonate ions and two OH^- ion, Cu(2) is coordinated by two oxygen atoms from the carbonate ions and four OH^- ions.

Mechanical activation process was studied by many researchers. Pourghahramani et al., (2007a) stated that mechanical activation process accelerates the leaching kinetics by increasing of the specific surface area, creating structural disordering and amorphization of the mineral particles. They are also stated that mechanical activation process affects the thermal process of sulfide. Another statement is with mechanical activation it is possible to reduce minerals reaction or their decomposition temperatures (Pourghahramani et al., 2007b).

Wieczorek et al. (2002) studied thermal behavior of mechanically activated for 5, 10, 15 min inorganic salts that were obtained by precipitation from aqueous solutions. They proposed that decomposition took place between 150°C and 400°C and there is not only one mechanism in the range of these temperatures, there are two overlapping mechanisms occurrences were detected related to –OH group liberation as H_2O molecules and CO_2 remotion according to Equation 1 and stated that theoretical malachite composition (%) is; CuO -72.0, H_2O-8.1 and CO_2-19.9.

Related decomposition temperatures shifted to lower value after mechanical activation and they grounded on the alteration of the crystal structure and formation of the new surface. This phenomenon accelerate the decomposition occurring.

$$Cu_2(OH)_2CO_3 \rightarrow 2CuO + H_2O + CO_2 \quad (1)$$

M. K. Seguin (1975) studied effect of different heating rate, kind of inert atmosphere and particle size and determine the decomposition temperature changing from 340°C to 425°C. M. Samouhos et al. (2011) studied microwave reduction of malachite concentrate and some part of this study is thermal and structural analysis of the material. From the X-ray analysis, quartz, hematite, talc, clinochlore, calcite, illite and azurite were detected. These compositions acted on the thermal analysis and decomposition temperatures found at 310°C and 422°C for malachite, at 587°C decomposition of clinochlore, 749°C for illite and 929°C for talc were detected.

Frost et al. (2002) stated that thermal decomposition of malachite took place in six overlapping stages at 250°C, 321°C that associate with the loss of water, 332°C, 345°C related to loss of water and carbon dioxide simultaneously, 362°C corresponds to loss of carbon dioxide and 842°C related to reduction of cupric oxide to cuprous oxide because of the using of nitrogen as inert atmosphere. Proposed thermal reaction of malachite by Frost et al. (2002) is as below;

Step 1	250°C	Loss of OH units as water	
Step 2	321°C	Loss of OH units-dehydroxylation	$Cu_2(OH)_2CO_3 \rightarrow 2Cu_2(OH)(CO_3)_2+H_2O$
Step 3	332°C		$2Cu_2(OH)(CO_3)_2 \rightarrow CuCO_3+CuO+CO_2+H_2O$
Step 4	345°C	Loss of water and carbon dioxide	$Cu_2(OH)(CO_3)_2 \rightarrow CuCO_3+CO_2+H_2O$
Step 5	362°C	Loss of carbon dioxide only	$CuCO_3 \rightarrow CuO+CO_2$
Step 6	842°C	Loss of oxygen	$CuO \rightarrow Cu_2O+O_2 Cu_2O \rightarrow Cu+O_2$

Materials and Method

For comparison of the structural changes, this study was subdivided into mechanical activation and calcination process.

Mechanical activation process was conducted with Planetary Mono Mill – Pulverisette 6. Grinding bowl and balls are made of tungsten carbide (WC). Grinding bowl has 250 ml capacity and balls have 10 mm diameter and 8.14 gr weight. Grinding process was performed in dry conditions. The speed of main disc and ball-to-mass ratio were kept constant for 15, 60 and 120 min durations at 600 rev.min^{-1} and 25 respectively.

Calcination was performed in muffule furnace with 10°C/min heating rate for 400°C and 600°C under atmospheric conditions. For both temperature, dwell times were chosen as two- hours and five- hours. Sample was put in the furnace and heated together and after furnace reached in the room temperature sample was taken.

For comparison of the structural alterations, X-ray diffraction (XRD), Differential thermal analysis and Thermogravimetric analysis (DTA-TG), Scanning electron microscopy and Fourier transform infrared spectroscopy were done. XRD was performed with Rigaku Ultima X-ray diffractometer and Cu Kα radiation. The degree of amorphization (A) of both mechanically activated and calcined malachite according to X-ray diffraction results was calculated from Equation (2),

$$A = \left(1 - \frac{I_x B_0}{I_0 B_x}\right).100 \quad (2)$$

where I_0 is the integral intensity of the diffraction peak for the untreated malachite, B_0 is the background of the diffraction peak for the untreated malachite, and I_x and B_x are the equivalent values for the treated malachite (Balaz, 2008). A JEOL 6060 LV scanning electron microscope (SEM) was used for morphological analysis of the treated malachite. DTA was performed using TA Instruments SDTQ 600 at heating rate of 10°C.min^{-1} under atmospheric conditions and Shimadzu FTIR spectroscopy was used for Fourier transform infrared spectroscopy analysis of the samples.

Results and Discussion

X-ray diffraction analysis of mechanically activated and calcined malachite samples are given in Figure 1(a), (c) and (d). Quartz is the dominant phase whereas malachite is the minor phase in the untreated malachite sample that coded in the figures as original.

In Figure 1(a), newly formed phase wasn't observed for mechanically activated samples but some significant differences in the peaks are clear. Increased mechanical activation duration caused decreased in intensity of quartz peaks accompanied by peak widening and switching in degree. Malachite peaks couldn't been determined for 60 and 120 min mechanically activated samples so it can be said that hundred percentage of amorphization degree was achieved after 15 min. While the peaks of malachite were disappearing, the peaks of quarts relatively preserved itself because of its hardness. Comparative amorphization degree diagram which was calculated from Equation 2 for quartz and malachite in terms of mechanical activation duration was given in Figure 1(b).

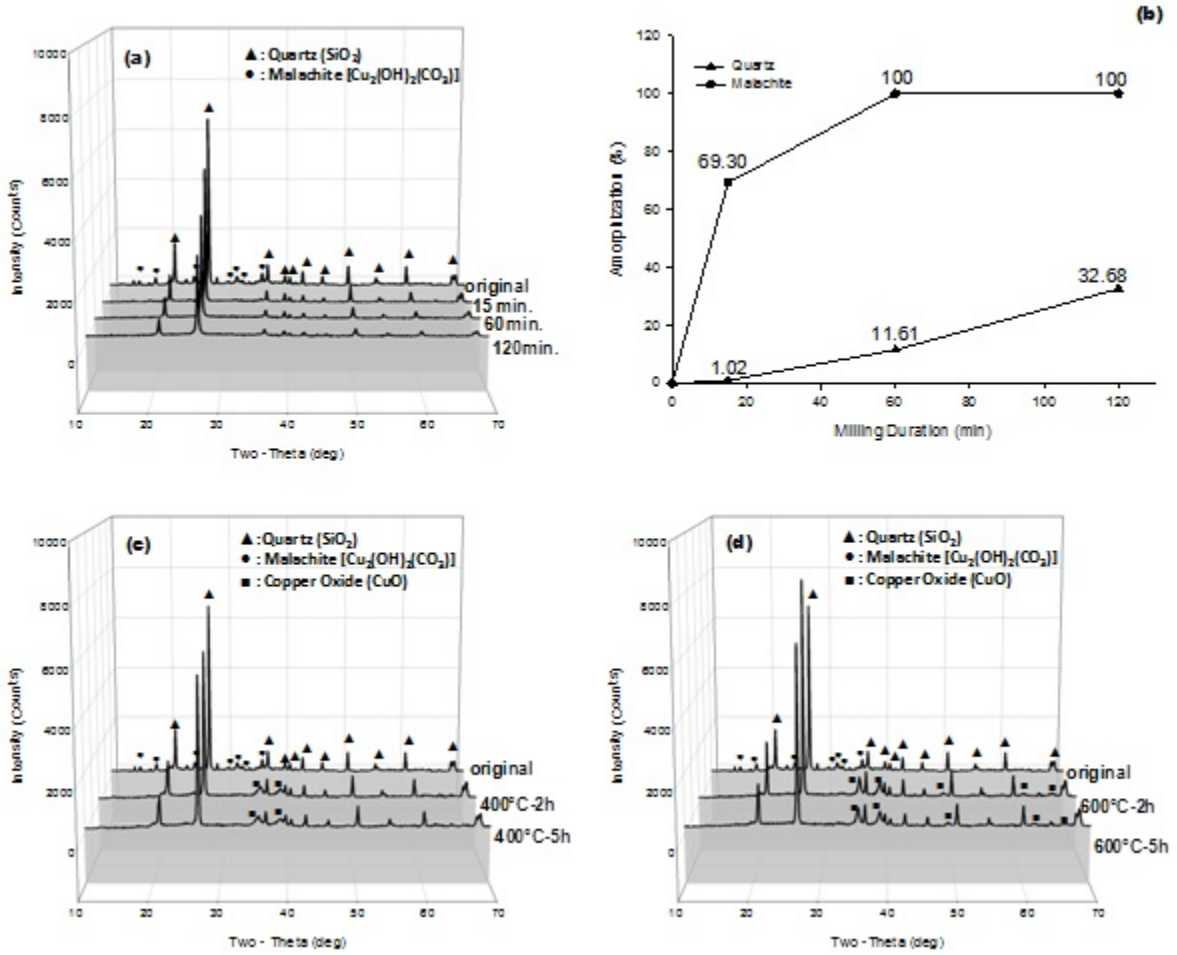

Figure 1: XRD patterns of the (a) mechanically activated malachite for different durations and (b) related amorphization degrees. XRD patterns of calcined malachite samples for 2 and 5 hours at (c) 400°C and (d) 600°C.

X-ray diffraction analysis of calcined malachite samples at 400°C for 2 and 5 hours are given in Figure 1 (c).

Malachite peaks couldn't be determined much the same as mechanically activated ones. But the differences between patterns are newly formed phase - copper oxide. It can be said that malachite structure decomposed and formed CuO partially because of the weak peaks of the copper oxide if taking into consideration that sharp peak is the indication of the crystallinity. The intensity of the quartz peaks decreased with prolonged calcination durations except located at 67.8°3 and 68.24°. These two peaks get strong with calcination at 400°C with prolonged duration.

X-ray diffraction analysis of calcined malachite samples at 600°C for 2 and 5 hours are given in Figure 1(d). Malachite phase couldn't been determined has been in mechanically activated ones and calcined at 400°C. Difference from calcined at 400°C samples is stronger copper oxide peaks. The other significant difference is the quartz peak that positioned at 26.74°. Initially the intensity of this peak increased for 2 hours and then decreased for 5 hours calcined sample. It may be due to the -OH liberation that may be bounded with the structure of quartz and copper oxide together. After liberation of -OH, quartz and copper oxide get their crystallinity completely and it caused increased in intensity but prolonged calcination at 600°C altered quartz crystallinity and decreasing in intensity occurred.

Thermal analyses of non-activated and activated samples for various durations including thermo gravimetric (TG) and differential thermal analyses (DTA) were given in Figure 2(a)-(d). For non-activated sample three weight lost steps and four endothermic act having peaks at 66°C, 378°C, 496°C and 577°C were determined. Steps occurring intervals are 25-180°C, 298-400°C and 400-600°C. For 15 min activated sample two weight lost steps occurred between 25-230°C and 300-550°C and one detectable endothermic act at 356°C. Both mechanically activated for 60 and 120 min malachite samples haven't multi step correspond to weight lost and endotherm. Size of particles can be decreased to some critical values, further energy supply cause energy accumulation in the volume or at the surface of crystals (Balaz, 2008, p.121). For these samples it can be said that reactions start at the beginning of the process because of the stored energy that accumulate in the structure sufficient for these reactions.

Related weight losses for intervals are 3.7%, 3.14%, 2.48% respectively for non-activated sample. For 15 min activated sample the weigh losses are, 4.66% for first step and 2.78% for second. For 60 and 120 min mechanically activated samples weight losses were determined as 8.28% and 8.42% respectively.

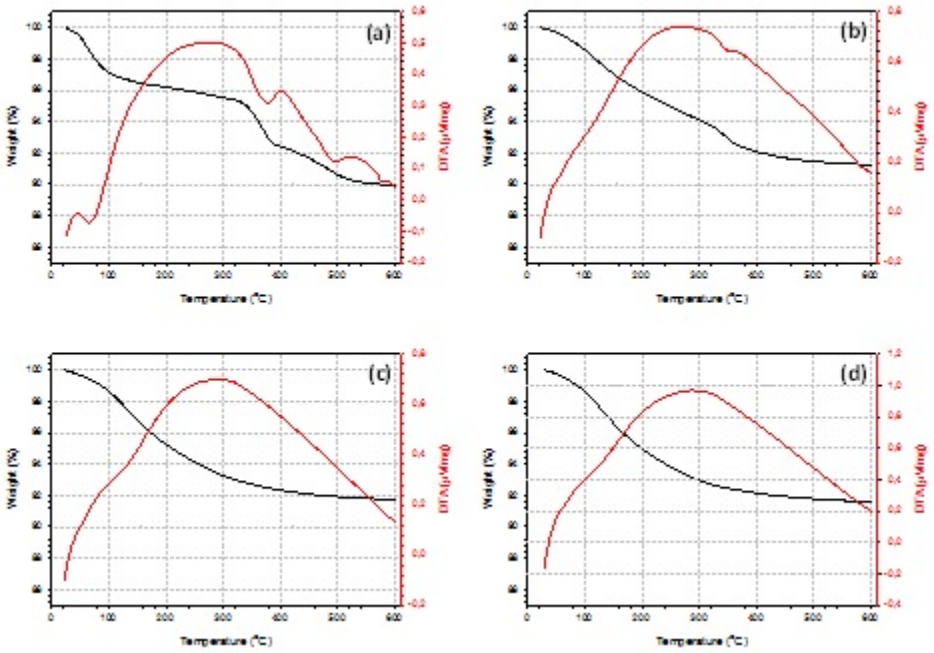

Figure 2: DTA and TG analysis of (a) non-activated, activated for (b) 15 min. (c) 60 min. and (d) 120 min. malachite samples

First endothermic act for non-activated malachite that found at 66°C corresponds to physical water liberation. For activated samples there is no peak were detected for this temperature. Endothermic peak at 378°C may be

attributed to dehydroxylation for non-activated malachite and this peak shifted to 356°C for 15 min mechanically activated sample. For other durations there is no endotherm for this event. As stated by study of Wieczorek et al. (2002), alteration of the crystal structure and formation of the new surface and stored energy (Balaz, 2008, p.121) caused this phenomenon. At 496°C CO_2 liberation takes place for original sample. This phenomenon couldn't be seen for mechanically activated samples. Seguin (1975) stated that dissociation of malachite starts at 310°C and finish at 420°C and between 95°C and 210°C depending on the particle size stability changes metastable to unstable in air and nitrogen. Finer malachite particles have higher surface energy and let the diffusion of large polar CO_2 molecule. At 577°C, transformation of α-β quartz takes place. For high grade SiO_2 powders, Mikhail et al. (1993) submitted an endotherm at 573°C for this transformation. Like other endotherms this occurrence haven't been detected for mechanically activated samples.

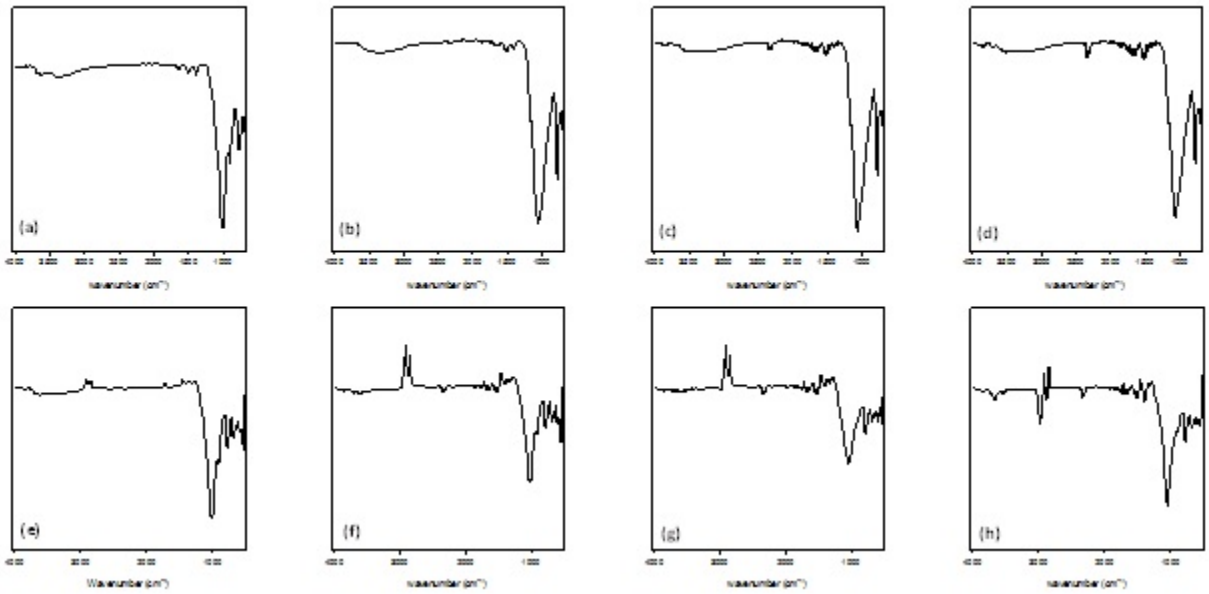

Figure 3: FT-IR analysis of (a) original, mechanically activated for (b) 15 min, (c) 60 min, (d) 120 min and calcined sample at 400°C for (e) 2 hours, (f) 5 hours and 600°C for (g) 2 hours, (h) 5 hours samples.

In Figure 3(a)-(h), Fourier transform infrared spectroscopy analysis of mechanically activated and calcined samples are given. Related wavenumbers are given as a separate table. Table 1 is for original and activated samples and Table 2 is for calcined malachite samples. For original sample the area between 3400 and 3700cm^{-1} compose of three bands. Ruan et al. (2002) stated that 2700-3700cm^{-1} interval is representative for hydroxyl stretching and sensitive for dehydroxylation temperature. Frost et al. (2007) determined this act for minerals belong to rosasite group at 3486, 3401, 3311 and 3139 cm^{-1}. With mechanical activation, three bands belong to original sample tend to become one broad band that means activated sample still contain OH units. This phenomenon somewhat different for calcined samples. With increasing temperature and dwell time, OH stretching vibrations appear with higher intensity. Frost et al. (2007) stated that for different minerals bands of hydroxyl stretching vibrations occur in various positions and explain this with variation in hydrogen band distance between OH units and oxygen of adjacent carbonate unit. Other reason may be attributed to surface energy and hygroscopic water. As seen from 60 and 120 min mechanically activated samples some bands realize low in intensity within this area. After prolonged mechanical activation durations, high temperature and long dwell time make sample capable to adsorb water molecule from the environment. Frost et al. (2007) reported v_3 asymmetric $(CO_3)^{2-}$ stretching modes of malachite at 1500 and 1400 cm^{-1}. For original sample this mode occurred at 1392.61 and 1504.48 cm^{-1}. For mechanically activated samples characteristic of these bands changed. For calcined samples while OH stretching vibrations decreased, deformation of $(CO_3)^{2-}$ bands accompanied this situation that means dehydroxylation and liberation of carbon dioxide take place simultaneously. For original sample the band at 1006.84 cm^{-1} attributed to Si-O stretching mode according to study of Belver et al. (2002) With prolonged mechanical activation duration this band shifts as

seen from Table 1. For calcined samples this peak shift takes place not the same ratio as the mechanical activated ones as seen from the Table 2. According to study of Madejova (2003) 1120-1000cm^{-1} region attributes to Si-O stretching vibrations. In their study, located at 1030 cm^{-1} band shifted to 1100cm^{-1} accompanied with increased in intensity after chemical treatment and they concluded that this band is enunciative for amorphous silica. This phenomenon occurred our activated sample but calcined samples hadn't shown the same change. It can be said that with mechanical activation the amorphization of the structure achieved and with calcination structure was altered.

Table 1: Wavenumbers of FT-IR of the mechanically activated samples and original sample

Samples	**Original**	**15 min**	**60 min**	**120 min**
Wavenumber (cm^{-1})	779.24	779.24	779.24	779.24
	794.67	794.67	798.53	798.53
	910.40	-	-	-
	1006.84	1056.99	1060.85	1064.71
	1026.13	1080.14	-	-
	1161.15	1161.15	1161.15	1161.15
	1392.61	1396.46	-	-
	1504.48	1519.91	1519.91	1508.33
	1647.21	1651.07	1651.07	1651.07
	3402.43	3390.86	3390.86	3390.86
	3622.32	-	-	-
	3695.61	-	-	-
	-	-	-	3722
	-	-	3849	3846.06

Table 2: Wavenumbers of FT-IR of calcined samples

Samples	**400°C-2h**	**400°C-5h**	**600°C-2h**	**600°C-5h**
Wavenumber(cm^{-1})	532.35	547.75	532.35	570.93
	563.21	563.21	597.93	601.79
	597.93	605.65		667.37
	690.52	690.52	690.52	690.52
	779.24	779.24	779.24	779.24
	794.67	794.67	794.67	794.67
	914.26	914.26	-	-
	1006.84	1010.70	1045.42	1053.13
	1029.99	1033.85	-	-
	1161.15	1161.15	-	-
	-	1338.60	1338.60	-
	1396.46	1396.46	1396.46	1396.46
	1519.91	1519.91	1519.91	1508.33
	1647.21	1651.07	1651.07	1651.07
	2877.79	2877.79	2877.79	2881.65
	-	-	-	2985.81
	3622.31	3618.46	-	3668.61
	3695.61	3695.61	-	-
	-	-	3722.62	3838.34
	-	-	3849.92	-

Doublet at 779.24 cm^{-1} and 794.67cm^{-1} are indicative for SiO_2 mode (Madejova, 2003). 15 min activated and calcined samples have same vibration at these wavenumbers except 60 and 120 min mechanically activated samples.

As seen from the Table 1, peak shift occurred. Sagadevan et al. (2012) specified 603.3cm^{-1} as Cu-O stretching mode. For calcined at 600°C for 5 hours this peak appears confirming the XRD results.

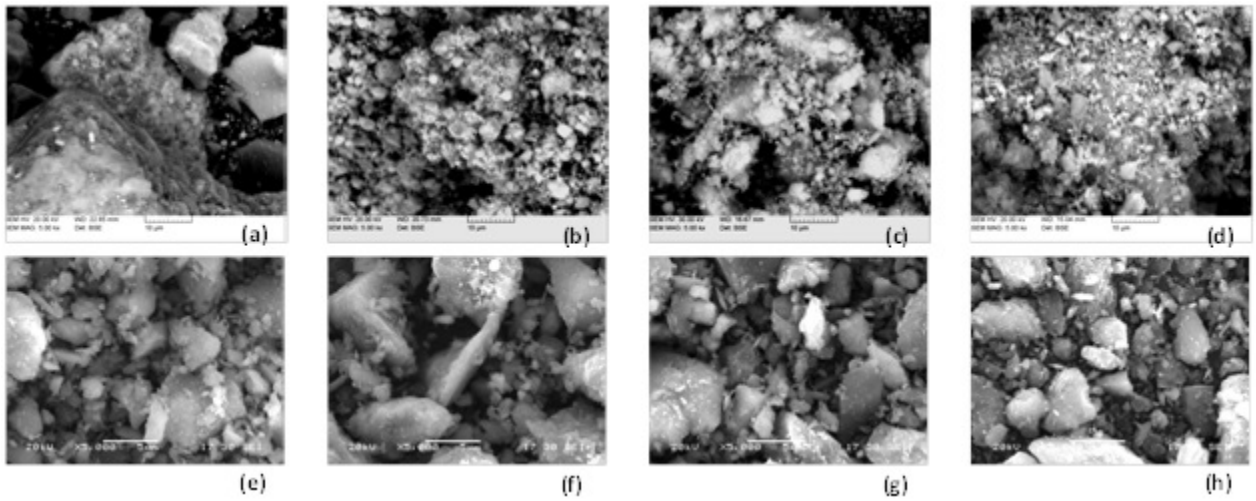

Figure 4: SEM analysis of (a) original, mechanically activated for (b) 15 min, (c) 60 min, (d) 120 min and calcined sample at 400°C for (e) 2 hours, (f) 5 hours and 600°C for (g) 2 hours, (h) 5 hours samples

SEM analyses of the samples are given in Figure 4. With mechanical activation the size of particles decreased and round particles occurred instead of angled particle.

Conclusion

In this study effects of mechanical activation and calcination process had been compared. XRD results showed that with mechanical activation the phase of malachite disappeared after 60 min and quartz peaks shifted in degree and decreased in intensity that means amorphization is proceed. This observation confirmed with calculation of amorphization and 32.68% amorphization was achieved for quartz after 120 min. At 400°C calcined samples formation of CuO identified. But calcined at 600°C for 5h samples have intense CuO peaks than the other calcined ones. DTA-TG results showed that with mechanical activation deformation of bonds that determined with FT-IR realized and stored energy that provided from accumulation of energy into the crystal due to the limited reduction of size of particles caused one step reaction including liberation of both hydroxides and carbon dioxides.

References

Arzatug, M. E., Kocakerim, M. M., Copur, M. (2004). Leaching of Malachite Ore in NH_3-Saturated Water, *Ind. Eng. Chem. Res.*43, (pp. 4118-4123).

Balaz, P. (2008), *Mechanochemistry in Nanoscience and Minerals Engineering*, Berlin, Springer-Verlag.

Belver, C., Muñoz, M. A. B., Vicente, M. A.(2002). Chemical Activation of a Kaolinite under Acid and Alkaline Conditions, *Chem. Mater.* 14 (5) (pp 2033–2043).

Bingöl, D., Canbazoğlu, M., Aydoğan, S. (2005). Dissolution Kinetics of Malachite in Ammonia/Ammonium Carbonate Leaching, *Hydrometallurgy* 76 (pp. 55-62).

Ciurowa, K. W., Shirokv, J. G., Parylo, M. (2000). The Use of Thermogravimetry to Assess the Effect of

Mechanical Activation of Selected Inorganic Salts, *Journal of Thermal Analysis and Calorimetry* Vol.60 (pp. 59-65).

Frost, R. L., Ding, Z., Kloprogge, J. T. Martens, W. N. (2002). Thermal Stability of Azurite and Malachite in Relation to the Formation of Mediaeval Glass and Glazes, *Thermochimica Acta* 390 (pp. 133-144).

Frost, R. L., Wain, D. L., Martens W. N., Reddy B. J. (2007). Vibrational Spectroscopy of Selected Minerals of the Rosasite Group, *Spectrochimica Acta Part A* 66 (pp. 1068–1074).

Liu, Z., Yin, Z., Hu, H., Chen, Q. (2012). Leaching Kinetics of Low-grade Copper Ore Containing Calcium-Magnesium Carbonate in Ammonia-ammonium Sulfate Solution with Persulfate, *Trans. Nonferrous Met. Soc. China* 22 (pp. 2822−2830).

Madejova, J. (2003). FTIR Techniques in Clay Mineral Studies, *Vibrational Spectroscopy* 31 (pp. 1–10).

Mikhail, S. A., King, P. E. (1993). High-Temperature Thermal Analysis Study of The Reaction Between Magnesium Oxide and Silica, *Journal of Thermal Analysis*, Vol. 40 (pp.79-84).

Molchan, I.S., Thompson, G.E., Skeldon, P., Andriessen, R. (2008). Synthesis of Malachite Nanoparticles and Their Evolution During Transmission Electron Microscopy, *Journal of Colloid and Interface Science* 323 (pp. 282–285).

Moskalyk, R. R., Alfantazi, A.M. (2003). Review of Copper Pyrometallurgical Practice: Today and Tomorrow, *Minerals Engineering* 16 (pp. 893–919).

Pourghahramani, P., Forssberg, E. (2007a). Effects of Mechanical Activation on the Reduction Behavior of Hematite Concentrate, *Int. J. Miner. Process*. 82 (pp. 96–105).

Pourghahramani, P., Forssberg, E. (2007b). Reduction Kinetics of Mechanically Activated Hematite Concentrate with Hydrogen Gas Using Nonisothermal Methods, *Thermochimica Acta* 454 (pp. 69–77).

Ruan, H. D., Frost, R. L., Kloprogge, J. D., Duong, L. (2002). Infrared Spectroscopy of Goethite Dehydroxylation. II. Effect of Aluminium Substitution on the Behaviour of Hydroxyl Units, *Spectrochimica Acta Part A* 58 (pp. 479 - 491).

Ethiraj, A. S., Kang, D. J. (2012). Synthesis and Characterization of CuO Nanowires by a Simple Wet Chemical Method, *Nanoscale Research Letters, a SpringerOpen Journal,* 7:70.

Samouhos, M., Hutcheon, R., Paspaliaris, I. (2011). Microwave Reduction of Copper(II) Oxide and Malachite Concentrate, *Minerals Engineering* 24, (pp. 903-913).

Seguin, M. K. (1975). Thermogravimetric and Differantial Thermal analysis of Malachite and Azurite in Inert Atmospheres and in Air, *Canadian Minealogist* Vol. 13 (pp. 127-132).

Stoilova, D., Koleva, V., Vassileva, V. (2002). Infrared Study of Some Synthetic Phases of Malachite ($Cu_2(OH)_2CO_3$)–Hydrozincite ($Zn_5(OH)_6(CO_3)_2$) Series, *Spectrochimica Acta Part A* 58 (pp. 2051–2059).

Watling, H.R. (2006). The Bioleaching of Sulphide Minerals with Emphasis on Copper Sulphides — A review, *Hydrometallurgy* 84 (pp. 81–108).

Xu, J., Xue, D. (2005). Fabrication of Malachite with a Hierarchical Sphere-like Architecture, *J. Phys. Chem. B* 109 (pp. 17157-17161).

Sustainable Production of Bioethanol using Augmented Bacterial Cellulases

Mariyam Zameer, Maham Tabbasum, Maham Ali

College of Earth and Environmental Sciences, University of the Punjab, Lahore, Pakistan

e-mail: mariyambukhari@gmail.com

Abstract: Due to over-dependence on fossil fuels, Pakistan is undergoing a serious energy crisis. Cellulosic ethanol appears to be a promising renewable fuel in light of the country's current economic and environmental conditions. However, in order to produce ethanol from cellulose, the latter must first be broken down into glucose by cellulases. The objective of this work was to amplify bacterial cellulase production via chemical mutagenesis. Five cellulase-producing bacterial strains were isolated from cow dung as well as effluent from local textile and pharmaceutical industries. Each of these strains was subjected to five different concentrations of two separate chemical mutagens viz. Ethyl methanesulfonate (EMS) and Ethidium bromide. Of the 50 mutants obtained, five best strains were screened out by using Carboxy methyl cellulose (CMC) plate assays, and their isozymes were studying via Native PolyAcrylamide Gel Electrophoresis (PAGE). Of these five, the most efficient cellulase producer (RB200) was selected for further studies. Using pre-treated wheat straw (which is abundantly available in Pakistan) as a substrate in shake flask cultures, cellulase extract was collected for partial characterization (i.e. to determine enzyme stability at various pH and temperatures). CMCase and FPase assays were used to monitor enzyme activity. The mutant RB200 was further used to perform saccharification in shake flasks, and glucose, reducing sugars as well as total sugars were periodically analyzed to examine the reaction progress. Finally, the glucose produced was utilized in shake flask fermentation by the yeast Saccharomyces cerevisiae G-1, and the resultant ethanol concentration was estimated. From the results it can be concluded that for the purpose of enhancing cellulase production in the chosen bacteria, Ethidium bromide was a better mutagen than EMS. Native PAGE revealed two important findings: first, that mutant CE150 produced an isozyme of 34kDa in excessive amounts; second, that RB300 produced a unique isozyme not found in any other mutant. Enzyme assays showed that FPase activity in the selected mutant RB200 was almost 7 times that of CMCase. From saccharification and subsequent fermentation, bioethanol was successfully produced at a concentration of 1.523%. The study demonstrates that mutated bacterial strains can be effective cellulase producers, and that wheat straw is a suitable substrate for making the production of cellulosic ethanol sustainable.

Keywords: cellulases, augmented bacterial strains, fossil fuels, bioethanol

Introduction

In a time when soaring petroleum prices and growing environmental problems are becoming major concerns, bioethanol presents an attractive option for fulfilling future energy demands. It is an alternative fuel derived from biomass (Demirbas, 2008).

Alcoholic fermentation, the process of anaerobic respiration by which microorganism break down carbohydrates or polysaccharides (i.e. sugars) to produce ethanol (a type of alcohol), is the basic process responsible for production of bio-ethanol. According to U.S. Department of Energy studies, cellulosic ethanol is particularly advantageous because it releases 85% lesser greenhouse gases than gasoline. On the other hand, starch ethanol reduces greenhouse gas emissions by only 18-29% (Wagner, 2007). It is also known that cellulose is the most abundant renewable resource in the world (Vu et al., 2010). In light of these environmental benefits, the current study has been designed to focus on cellulosic ethanol, in which the cellulosic parts of a plant are broken down to produce ethanol.

One reason for the skepticism surrounding cellulosic ethanol is that it requires an additional step before fermentation can occur: cellulolysis (Wagner, 2007). Cellulolysis is the hydrolysis of cellulose, i.e. breaking down cellulose into simpler polysaccharides (such as glucose) by reaction with water. This process depends on cellulases, i.e. the enzymes that catalyze celluolysis. In other words, the cellulases are enzymes capable of breaking down cellulosic compounds into fermentable sugars which can be used for the production of bioethanol (Maki et al., 2009).
Bacteria, owing to their diversity and rapid growth, can produce both alkali-stable and temperature-stable enzymes which can be very important from an industrial point of view (Deka et al., 2011). In this paper, an attempt has been made to enhance cellulase activity in a group of locally-isolated bacteria.
Mutagenesis plays an imperative role in enhancing cellulase production. Essentially, mutagenesis is the process by which an organism is subjected to mutagen(s) to bring about genetic mutation. It can be carried out by using chemical mutagens (e.g. EMS, Ethidium bromide, Nitrous acid etc) and/or physical mutagens (e.g. X-rays, UV radiations, and particle radiations).
EMS, when applied individually to a wild strain of Saccharomyces cerevisiae, caused bioethanol production to increase by 17.3% (Mobini-Dehkordi et al., 2008).
In this research, certain bacterial strains were isolated from local textile and pharmaceutical industry waste water. These strains were exposed to two chemical mutagens i.e. EMS and Ethidium bromide, to boost their cellulase activity. Also, to compare the effectiveness of enzyme production when using untreated and pre-treated wheat straw as a substrateand to determine the optimum temperature and pH for cellulose activity. This improved activity can amplify the amount of bioethanol produced from fermentation. This cheap source of alternative energy can then be promoted on an industrial scale, to replace the more expensive fossil fuels such as coal and furnace oil.

Materials and methods

2.1 Isolation of bacterial strains

Bacterial strains were randomly isolated from three sources viz. cow dung, textile industry effluent and pharmaceutical wastewater. After an initial screening, five strains exhibiting cellulase activity were cultured in Lysogeny Broth (LB). The test tubes were incubated at 37°C for 24 hours. Using a sterile inoculation needle, colonies were picked from each tube and streaked on to separate agar plates under sterile conditions. These plates were tightly sealed and stored at a temperature of 4°C.

2.2 Maintenance of cultures

The selected bacterial strains, i.e. 1, 2, 3 (from textile industry wastewater); C (from cow dung); and R (from pharmaceutical wastewater) were revived. Using a sterile loop, respective colonies were picked from the initially streaked plates. These were inoculated in freshly prepared LB medium under sterile conditions, and incubated at 37°C for 24 hours.

2.3 Mutation of bacteria

2.3.1 Mutagenesis

Using the method adopted by Shafique et al. (2009), the selected strains were subjected to chemical mutation by using two accepted chemical mutagens: Ethidium Bromide and Ethyl-Methanesulfonate (EMS). Five different concentrations of each mutagen were prepared: 100, 150, 200, 250, and 300µL/mL. For both mutagens, 0.5mL of each strain was added to 0.5mL of the prepared concentrations. This gave 50 specimens containing 1mL of the mutagen-bacteria mixture, which were incubated at 37°C for 30 minutes.

2.3.2 Centrifugation, washing and storage

In order to separate mutants from the mutagen-bacteria mixture, the 50 vials were centrifuged at 7000 revolutions per minute (rpm) for 15 minutes. The supernatant was discarded. In order to protect bacteria from mutagen over-exposure, the vials were washed. For this purpose, 1% sterile saline solution was prepared. To each vial, 0.75mL of this solution was added and the pellets were completely dissolved via manual shaking. The vials were again centrifuged at 7000 rpm for 15 minutes, and the supernatant was discarded. This process of washing was repeated thrice. In the end, 0.5mL distilled water was added to the vials, and these were refrigerated at 4°C.

2.4 Plate screening for cellulase enzyme

2.4.1 Preparation of cellulase activity evaluation medium

In order to observe the amount of cellulases produced by each mutant strain, Carboxymethylellulose (CMC) medium was prepared. Under sterile conditions, this medium was poured into ten sterilized petri plates, and the medium was allowed to solidify at room temperature.

2.4.2 Inoculation of mutant strains

The plates were divided into five equal zones. On five prepared plates, five EMS-mutants of each strain were applied, using a sterilized inoculation needle. On each of the other five plates, five Ethidium Bromide-mutants of each strain were inoculated. The plates were incubated at 37°C for 16 hours.

2.4.3 Washing of plates

CTAB (Cetyl Trimethyl Ammonium Bromide) solution of concentration 0.1% was prepared for washing the plates (Namasivayam et al., 2011). In each plate, 10mL of the solution was poured and allowed to stand for 15 minutes. The liquid was carefully removed using a micropipette and sterile blue tips. This process was repeated to expose clear zones.

2.4.4 Selection of mutants

Using a simple millimeter scale, diameter of the zone formed by each mutant was measured and noted. These readings were used to calculate percentage cellulase activity exhibited by each mutant, by using the following formula:

$$\text{Cellulase activity (\%)} = \frac{\text{degraded zone's diameter} - \text{colony diameter}}{\text{diameter of colony}} \times 100$$

The resultant values were used to plot a graph for cellulase activity. After applying ANOVA with 5% standard error, five best strains (i.e. those showing highest cellulase activities) were selected for further studies. These were stored in five separate falcon tubes by using LB cultures.

2.5 Cellulase isozymes study using native Poly-Acrylamide Gel Electrophoresis (PAGE)

For identifying cellulase isozymes produced by the five chosen mutant species, Native PAGE was performed by adapting the method of Mateos et al. (1992). First the required gels (resolving + stacking) were prepared in the prescribed manner and poured into the glass plates (already fixed in the casting frame) using a micropipette and sterile blue tips. The comb was inserted and gels were allowed to solidify. After about 30 minutes, the comb was removed and the prepared samples were carefully injected in the wells. The electrodes were connected to a 150 V power supply, allowing the process of electrophoresis to commence. When the tracking dye had reached the bottom, the glass plates were removed and the gel was studied using a gel documentation system connected with a computer.

2.6 Slant culturing

Out of the five selected mutants, the one showing highest cellulose-degrading ability was selected, i.e. the mutant labelled RB200 (Strain R, treated with Ethidium Bromide applied at a concentration of 200µL/mL). In order to store this mutant for future use, it was streaked on slant cultures under sterile conditions. The slants were incubated at 37°C for 24 hours, and were later refrigerated at 4°C.

2.7 Shaking flask culture

In a conical flask, 25mL of sterilized LB medium was prepared. A few colonies of RB200 were transferred from one of the prepared slants to the broth by using a sterilized inoculating loop in laminar flow. This flask was incubated at 37°C for 24 hours in a shaking incubator.

2.8 Flask-level cellulase production to determine optimum reaction duration

Wheat straw was used as the carbon source for testing cellulose-degrading capability of RB200, by monitoring the production of cellulase enzyme. Nutrient medium was prepared in a volume of 600mL, and 100mL was poured into each of the six experimental flasks. In three of these, 1g pre-treated wheat straw was added, while in the other three 1g of untreated wheat straw was added. From the fresh shaking flask, 3mL of RB200 culture was added into each of the six flasks. All of these were incubated at 37°C in a shaking incubator. After five days, two of the flasks (one containing treated and one containing untreated substrate) were removed and studied. Similar studies were carried out on the pair of flasks removed on the 6^{th} and 7^{th} day of incubation.

2.9 Enzyme assays

From the cellulases produced by RB200, the activity of endogluconase and exogluconase was tested via CMCase and FPase assays respectively.

2.9.1 CMCase assay

On the 5^{th} day of incubation, mixture from each of the two flasks (one containing treated and one containing untreated substrate) was separately centrifuged at 7000 rpm for 20 minutes, with the temperature maintained at 10°C. The supernatant (containing extracellular cellulases) was transferred from the centrifuge tubes into fresh test tubes, while the pellet was discarded. CMCase was tested by using prescribed method of Ghose, 1987.

2.9.2 FPase assay

For determining exogluconase activity prescribed method of Ghose, 1987 was used.

2.10 Enzyme production at flask level using pre-treated wheat straw

4 large flasks were again prepared with the same nutrient medium, using treated wheat straw. The mixture volume in each flask was raised to 250mL and 0.001% glucose was added as an inducer (to further stimulate enzyme production). Under sterile conditions, 15mL of inoculum was added to each flask. After 6 days of simultaneous shaking and incubation at 37°C, the mixture from all the flasks was filtered using muslin cloth. A few milliliters of the filtrate were used to perform CMCase and FPase assay. Enzyme stability at various temperatures (30°C, 37°C and 40°C) and pH (5, 5.5, 6, 6.5, 7, 7.5, 8, 8.5, 9, 9.5 and 10) was measured.

2.10.1 Partial characterization of enzyme at various temperatures

Enzymes are temperature-sensitive (Jones et al., 2007). In order to check cellulase stability at various temperatures and time periods, further experiments were conducted. Filtrate obtained from the flask incubated at 37°C was further divided into 4 equal portions. Each part was submerged in separate water baths set at 40°C, 50°C, 60°C and 70°C

Samples were drawn from the solution in each beaker at four time intervals i.e.: 20, 40 and 60 min. In this manner, 12 samples were obtained. CMCase and FPase assays were performed for each sample.

2.11 Saccharification

The collected filtrate (approximately 700mL in volume) was transferred into a 1L conical flask. In this flask, 0.5% treated wheat straw was added and was kept at 37°C in a shaking incubator. Samples were drawn at three different time intervals, i.e. 2, 4 and 6 hours. The drawn sample was first given heat shock and then centrifuged to estimate Glucose content, Reducing sugars and Total sugars. At the end of 6 hours, all of the remaining mixture was filtered using muslin cloth, and the filtrate was given heat shock before being stored (at 4°C) for future use.

2.11.1 Glucose estimation

The mixture drawn from the flask was boiled at 100°C. Then, it was centrifuged at 7000 RPM for 20 minutes at a temperature of 10°C. The sample, standard and blank was prepared according to the prescribed method (using the PSCIR Diagnostica glucose kit). Readings were taken at 546nm in a spectrophotometer to measure the optical density (OD) of each solution. (PCSIR Dignostica kit Cat No. 0018)

2.11.2 Test for reducing sugars

Sample, standard and blank were prepared and boiled as required. All three were run in a spectrophotometer at 540nm (Miller 1959).

2.11.3 Test for total sugars

Sample, standard and blank were prepared and boiled as required. All three were run in a spectrophotometer at 470nm (Dubois et al., 1957).

2.12 Fermentation

In a conical flask, 50ml yeast peptone dextrose (YPD) broth was prepared. Under sterile conditions, dried yeast culture of Saccharomyces cerevisiae G-1 was inoculated in the medium. This flask was incubated at 30°C in a shaking incubator for 24 hours.

In 500ml of the stored filtrate, nutrients were added to facilitate future yeast growth. 15ml of molasses was further added, and a pH of 5.0-5.5 was maintained by adding a few drops of 1N Hydrochloric acid. This mixture was poured into 2 fermentation flasks (250ml mixture in each) which were autoclaved. Under sterile conditions, 25ml of the prepared yeast culture was added into each flask. The fermentation flasks were then placed in a shaking incubator at 35°C. Each day, approximately 7mL of the mixture was drawn. Of this sample, 5mL was saved for measuring ethanol concentration, while the remaining volume was used for estimating glucose, reducing sugars and total sugar units.

2.13 Ethanol estimation

The saved sample (5mL) was transferred into a round bottom flask, and distilled water was added to it. The mixture was distilled at 78°C, till 20mL distillate was obtained. This was allowed to drop into a measuring cylinder containing 25mL Potassium Dichromate solution. The obtained mixture was kept in a water bath (set at 60°C) for 20 minutes, after which spectrophotometer reading was taken at 600nm.

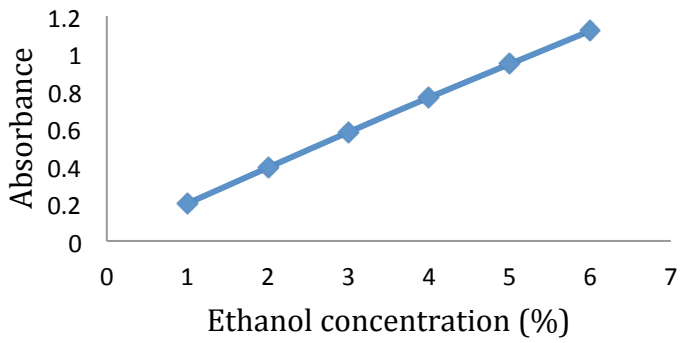

Fig.1: Ethanol standard curve

Results and Discussion

3.1 Plate screening for cellulase enzyme

After washing each of the ten plates with CTAB, zones of various diameters were obtained for each strain at different concentrations of EMS and Ethidium bromide. The results of these zones are displayed in Fig. 2.

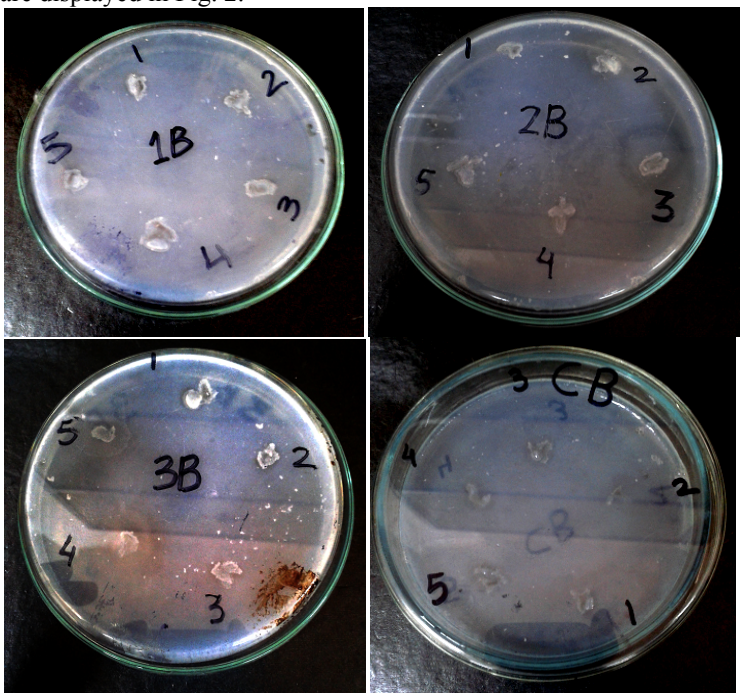

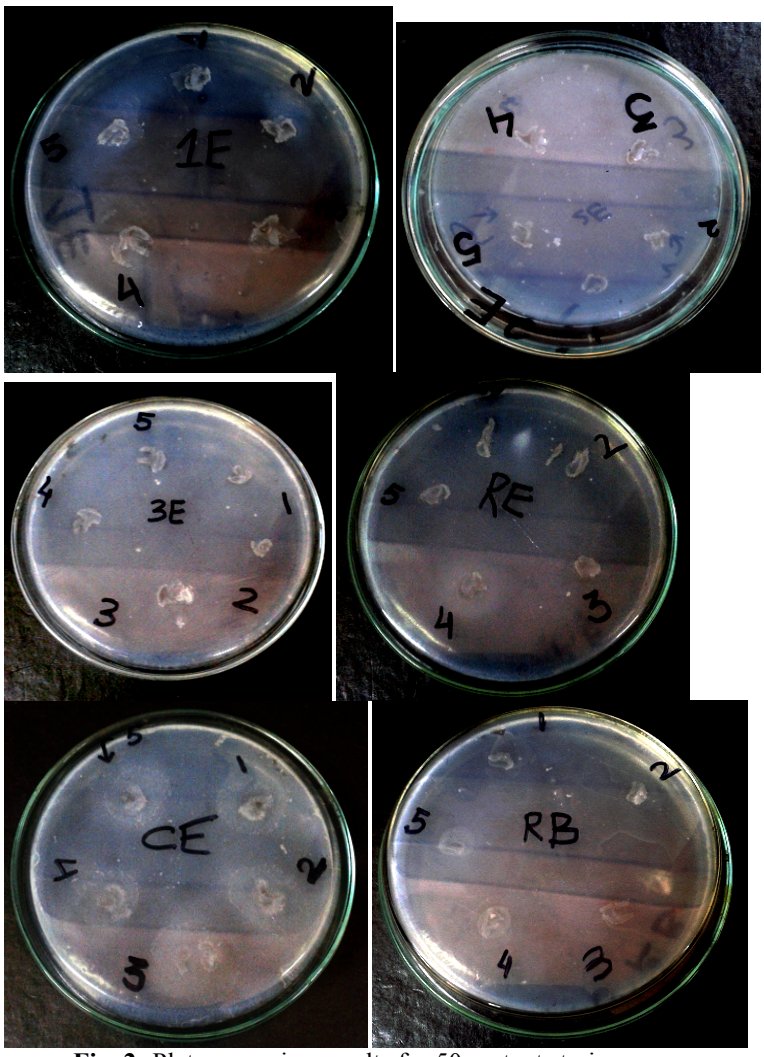

Fig. 2: Plate screening results for 50 mutant strains

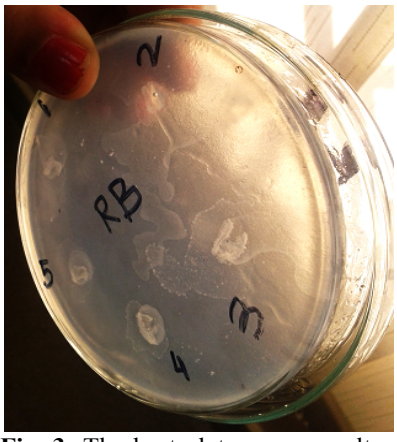

Fig. 3: The best plate assay result was shown by strain R, treated with Ethidium Bromide (B) at five concentrations (1=100µg/mL, 2=150 µg/mL, 3=200 µg/mL, 4=250µg/mL, 5=300µg/mL)

The formation of zones indicated that the mutants contain cellulases which effectively degrade CMC. The mutants CE300, CE150, RB300, RB200, and 3B300 formed wider zones than other mutated bacterial strains. The best zone was formed by RB 200 showing 385.71% cellulase activity. A statistical method ANOVA was applied to choose the best mutant (i.e. the most efficient cellulase-producer) for further studies. The results of this test are displayed in Fig. 3.

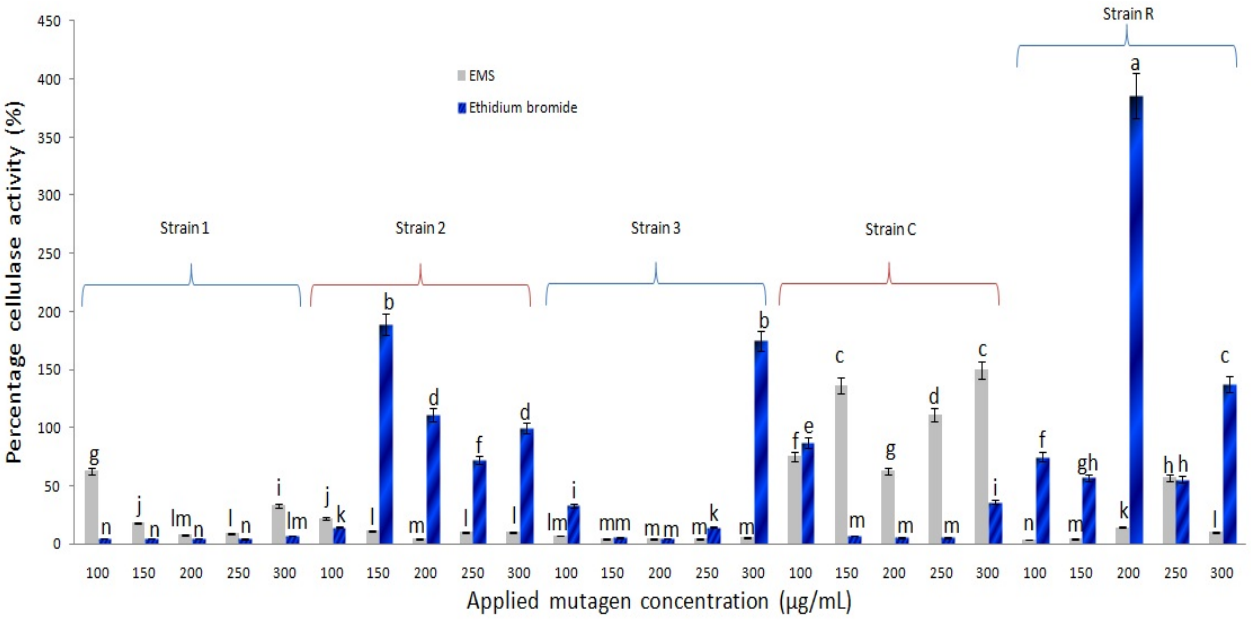

Fig. 4: Results of plate assays after applying ANOVA

The calculated percentage cellulase activities were plotted against applied mutagen concentrations to obtain the graph shown in fig. 4. ANOVA was applied to these results at a probable 5% standard error. Five mutants showing the highest cellulase activities were selected viz. CE300, CE150, RB300, RB200 and 3B300. Of these, the mutant labelled "a" (RB200) showed an exceedingly high activity, because of which it was chosen for the forthcoming saccharification and fermentation studies. ANOVA was applied to ensure that the selected species would always show the highest cellulase activities (out of the 50 mutants) even if the experiment was repeated multiple times.

3.2 Study of cellulase isozymes through Native PAGE

Cellulase is an enzyme complex, consisting of various sub-enzymes (which have similar functions but different structure and size, i.e. isozymes) such as exogluconase, endogluconse, and β-glucosidase. These isozymes can be segregated on the basis of the difference in their sizes. After applying ANOVA, five best mutants (3B300, CE150, CE300, RB200, and RB300) were screened out. The isozymes of these mutants were studied using Native PAGE. The results of the isozyme study are displayed in Fig. 5.

CE300 CE150 RB300 RB200 3B300

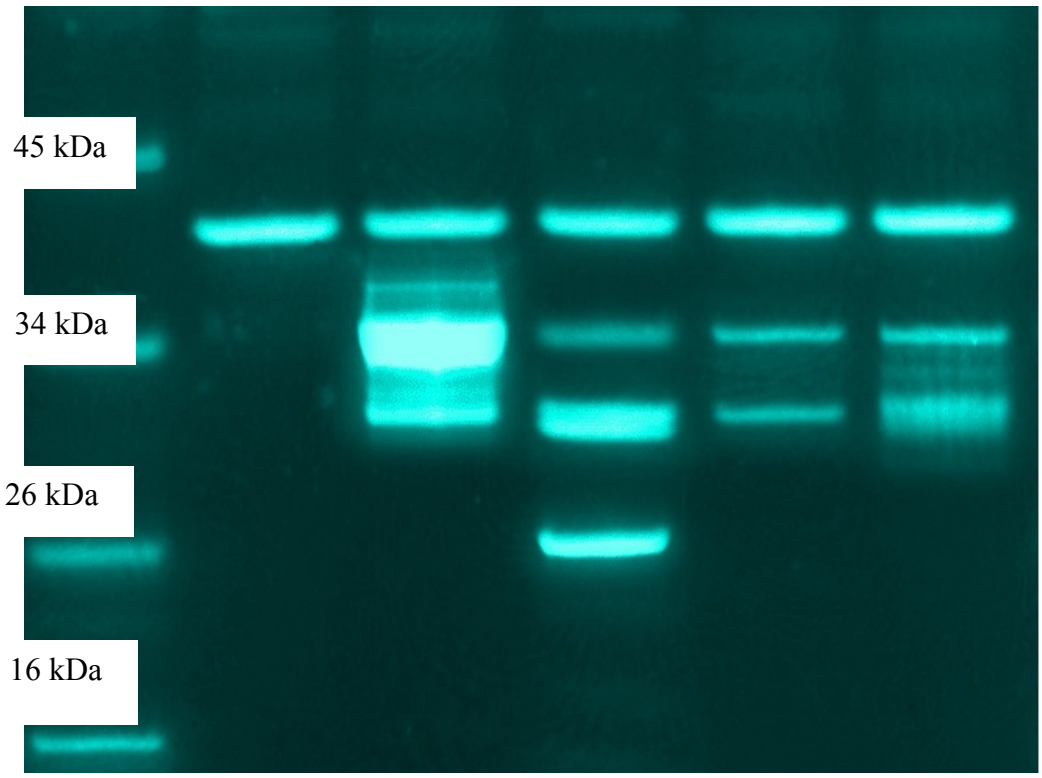

Fig. 5: Results of isozyme study (using Native PAGE)

Moving down, the number of bands indicates the number of isozymes in each mutant, while the thickness of each band represents the quantity of isozyme produced by a particular strain. It can be seen that in CE300 only one isozyme (42kDa) is present, and this isozyme is also present in all of the selected mutants. The second isozyme (occuring at 34kDa) is present in all of the mutant strains except CE300. CE150, in particular, produces this isozyme in copious amounts. The last four mutants also have another isozyme (31kDa) in common, RB300 being the richest source of it. RB300 is also special because it produces a fourth, unique type of isozyme (26kDa), not found in any of the other selected mutants.
A similar study was conducted on the nitrogen-fixing bacterium Rhizobium leguminosarum, and it was seen that the cellulases produced by it are composed of 3 isozymes (Mateos et al., 1992). Their results seem to resemble the pattern shown by CE150, however the size of R. leguminosarum's isozymes was almost double that of isozymes produced by CE150.

3.3 Flask-level cellulase production to determine optimum reaction duration

The activities of CMCase and FPase were separately monitored for pre-treated and untreated wheat straw, at eight time intervals.

3.3.1 Using pre-treated wheat straw as substrate

The results in Fig. 6 show that when the substrate was pre-treated wheat straw, CMCase and FPase activities increased over time. Maximum CMCase activity (67.823µmol/ml/min) occurred at 192 hours, while maximum activity for FPase (1215.987µmol/ml/min) was achieved at 144 hours.

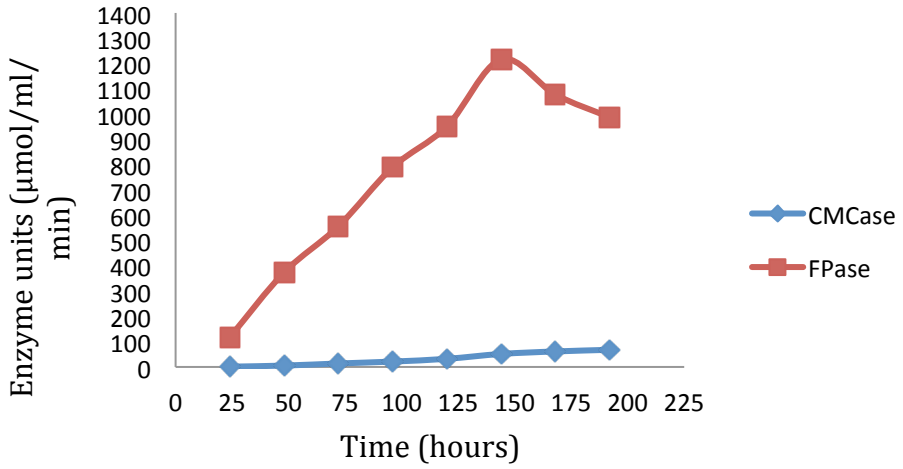

Fig. 6: Study of cellulolytic activity of RB200 on pre-treated wheat straw at various time periods

Ariffin et al. used CMC as a carbon source and found that their bacteria gave maximum CMCase and FPase activities at 24 hours. Purwardia et al. (2004) found that when 2% pre-treated wheat pollard was used as substrate, highest CMCase activity occurred at 72 hours, while highest FPase activity occurred at an interval of 120 hours. Owing to the variation in microorganisms and substrates used, the recorded observations are quite different.

3.3.2 Using untreated wheat straw as substrate

From Fig. 7 it can be seen that maximum activity of both CMCase and FPase (111.588µmol/ml/min and 1163.795µmol/ml/min respectively) was achieved at a time interval of 144 hours when using untreated wheat straw. After this, their cellulolytic activity declined.

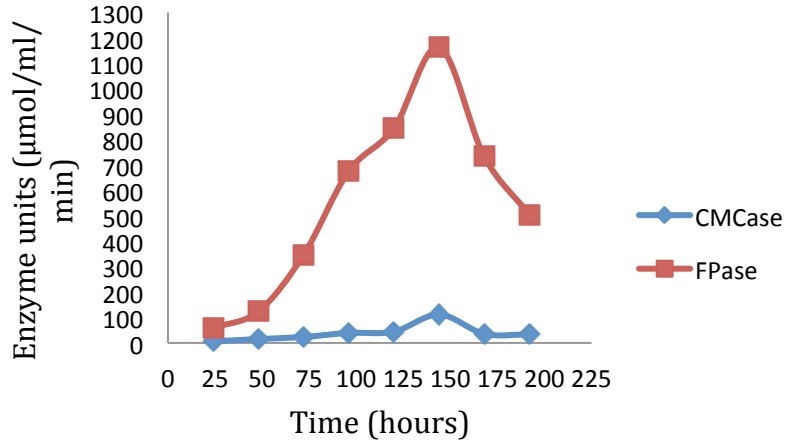

Fig. 7: Study of cellulolytic activity of RB200 on untreated wheat straw at various time periods

The study revealed surprising results, because CMCase activity using untreated wheat straw was almost twice that of the activity found when using pre-treated wheat straw (111.588µmol/ml/min and 67.823µmol/ml/min respectively). Results opposite to these were obtained by Sridevi et al. in 2006. They observed that CMCase activity in pre-treated wheat straw (6.6µmol/ml/min) was thrice that of untreated wheat straw (2.6µmol/ml/min). FPase activity in the current work

increased only slightly due to pre-treatment (from 1163.795µmol/ml/min to 1215.987µmol/ml/min), while Sridevi et al. reported FPase activity to have increased from 2.8 to 5.8µmol/ml/min.

3.4 Enzyme production at flask level using pre-treated wheat straw

The enzyme extract obtained from filtration of the flask mixture was tested for CMCase and FPase activities, as displayed in Fig. 8.

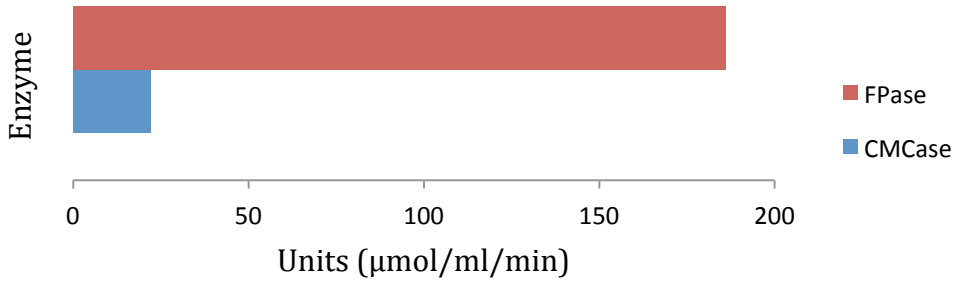

Fig. 8: Enzyme activity exhibited by mutant RB200 using 1% pre-treated wheat straw as carbon source

It was seen that the bacterial strain under study produces FPase (186.176µmol/ml/min) almost 8 times the amount of CMCase (22.201µmol/ml/min). On the other hand Ahmed et al. (2012) observed that when using pre-treated sugarcane bagasse as a substrate, the CMCase activity (0.3µmol/ml/min) was thrice of FPase (0.1µmol/ml/min).

3.5 Saccharification

Sachharification of 0.5% pre-treated wheat straw, containing 70% delignified cellulose, was performed by using the cellulases produced by mutant RB200. This step was performed in order to hydrolyze complex sugars into simple ones (i.e. glucose). The results in Fig. 9 indicate that total sugars in the reaction mixture were exceedingly higher than both glucose and total reducing sugars. Maximum total sugars (78696.43µmol/mL) and glucose (266.212µmol/mL) occurred at the 6th hour, showing an obvious linear trend. Reducing sugars, however, peaked at the 4th hour (1963.029µmol/mL), declining thereafter.

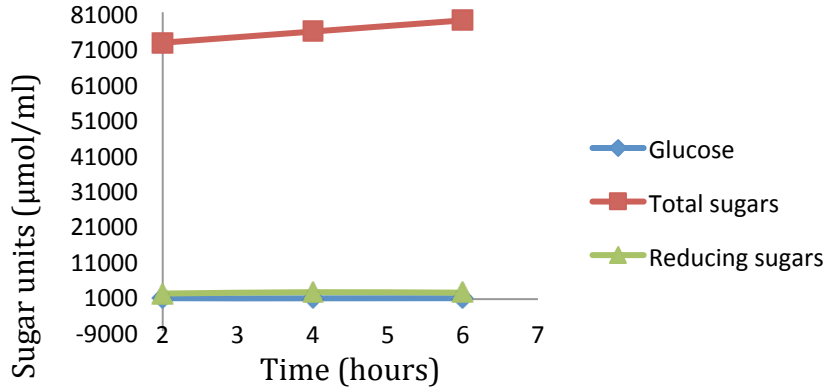

Fig. 9: Saccharification of treated wheat straw by indigenous cellulase enzyme

Since the quantity of glucose and total reducing sugars was much lower than total sugars, a separate graph was drawn for them to study their trends in detail, using the same results. Fig. 10 clearly shows how the glucose level rises as sachharification proceeds. A study conducted by the Food and Agricultural Organization of the United Nations (FAO, 1997) on sachharification of bagasse reported similar results. Total sugars, evidently, were of highest quantity. Both total sugars and glucose showed an upward trend, with the rate of increase eventually dwindling. Reducing sugars, on the other hand, showed a dip after reaching a peak, just as observed in the current study.

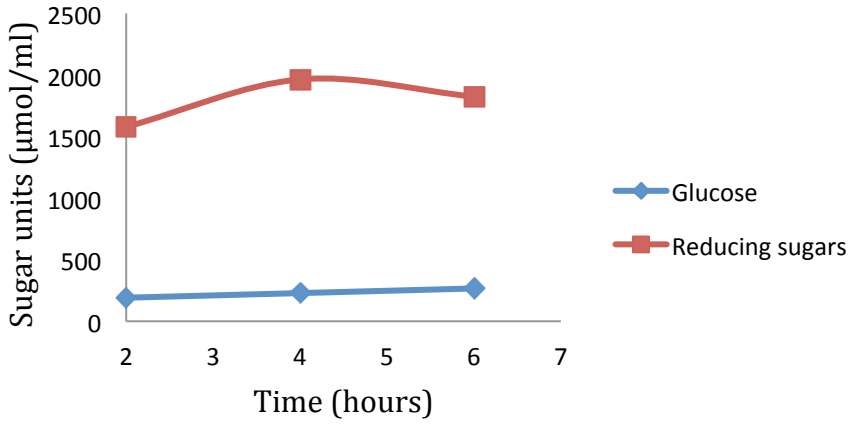

Fig. 10: Variation in the units of glucose and total reducing sugars during sachharification

3.6 Fermentation

Saccharified biomass was subjected to fermentation by the yeast Saccharomyces cerevisiae G-1 in order to convert the sugars into bioethanol.

3.6.1 Variation in sugar levels

The variation of sugar contents during this process can be viewed in Fig. 11. There is a fluctuating decrease in the level of reducing sugars with increase in time. As shown in Fig. 12 glucose units exhibit a similar pattern. However, according to Fig. 11 total sugars demonstrate an extremely unusual pattern. An erratic trend can be observed, in which the total sugar units increase until they reach a peak (99518.53µmol/mL) at 144 hours. Only after this do the units of total sugars begin to decrease.

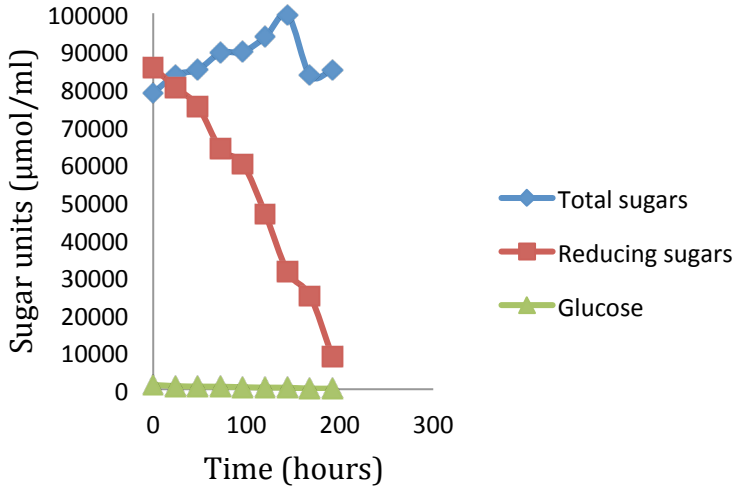

Fig.11: Sugar configuration during fermentation with Saccharomyces cerevisiae G-1.

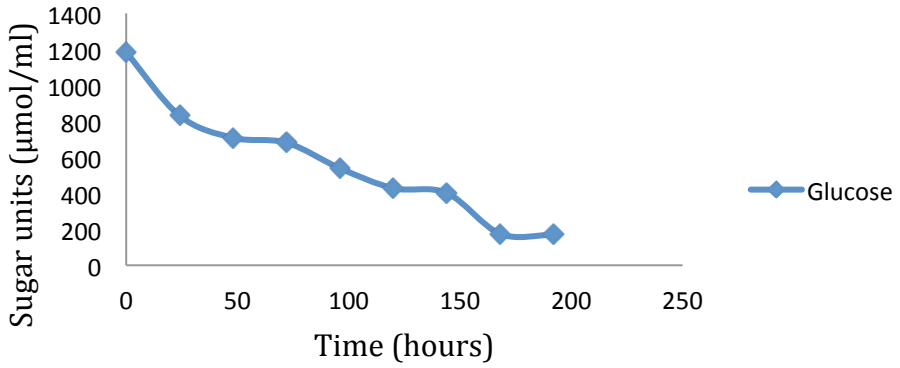

Fig.12: Decrease in glucose units during fermentation with Saccharomyces cerevisiae G-1.

All experiments were repeated and averages were calculated in order to minimize probable human error. Yet, the displayed results for total sugars completely contradict those observed by Wilson et al. (2012), in which the sugars declined at a steady rate. It is known that as ethanolic fermentation proceeds, various compounds (other than ethanol itself) may be produced as a result of the yeast's metabolic activities (Viegas, 1988). One probable reason for the odd pattern recorded above could be that initially, the yeast may have produced certain by-products that maximally absorbed the same wavelength of light as the sugars, i.e. 470nm. This could have caused the spectrophotometer to give very high absorbance readings. Therefore, these results represent areas that could become the focus of future research.

3.6.2 Variation in the level of ethanol

The fermentation results shown in Fig. 13 reveal that maximum ethanol yield (1.523%) was achieved at a time interval of 120 hours and a temperature of 35ºC under anaerobic conditions. After this peak, an evident decline is visible.

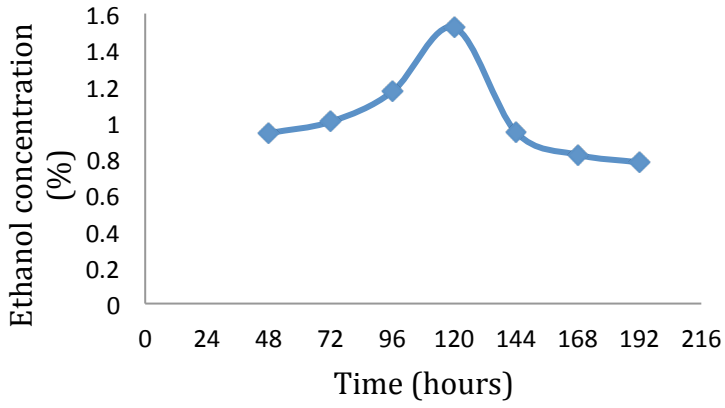

Fig.13: Ethanol production from sachharified biomass with Saccharomyces cerevisiae G-1

Several reasons may be responsible for the eventual decrease in ethanol yield. It has been reported that certain fermentation by-products slow down the growth of Saccharomyces cerevisiae, causing the ethanol yield to drop. Research has also demonstrated that presence of octanoic and decanoic acids can stop the process of fermentation early on (Viegas et al., 1988). Another research showed results similar to those displayed above. Using wheat straw as a substrate in sachharification, Saha

et al. (2005) used recombinant Escherichia coli to produce ethanol via fermentation. They also recorded highest ethanol yield at 120 hours.

3.7 Cellulase activity at various temperatures

Filtrate from the three flasks was used to estimate CMCase and FPase activities at three different temperatures. Fig. 14 shows that the cellulolytic activities of both CMCase and FPase increased until they reached a peak, after which there was a gradual decline. Peak CMCase activity (167.091µmol/ml/min) was achieved at a temperature of 37ºC whereas peak FPase activity (207.987µmol/ml/min) occurred at 40ºC.

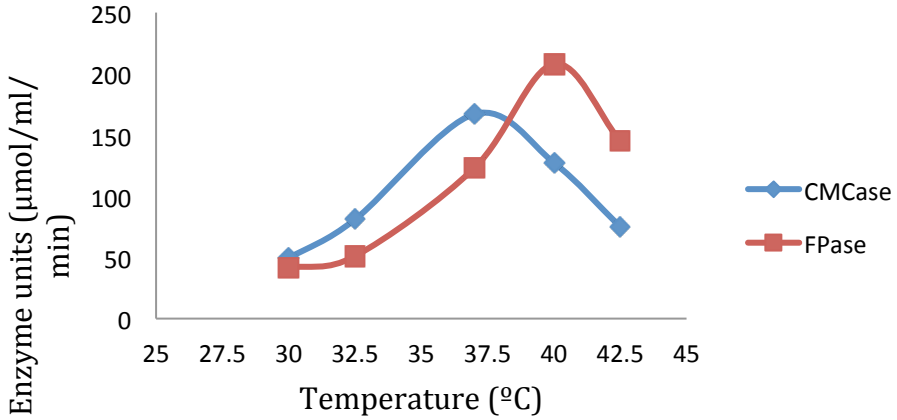

Fig.14: Study of cellulase activity on treated wheat straw at various temperatures by using mutant bacterial strain RB200.

The results indicate that FPase produced by the mutant strain RB200 is more efficient at higher temperatures as compared to CMCase. An opposite trend was recorded by Lowe et al. (1987) i.e. CMCase activity was highest at a temperature of 50ºC while FPase activity reached a maximum at 45ºC, showing that CMCase activity was better as the temperature increased. The fact that the latter research was conducted on fungi rather than bacteria could be one of the primary reasons for the difference in results.

3.8 Partial characterization of cellulase enzyme produced by RB200

Partial characterization was performed for cellulase enzyme produced by RB200 in order to check its stability at various time intervals, temperatures and pH. The objective of these lab studies was to evaluate the optimum time period, temperature and pH for enzyme stability.

3.8.1 Study of thermostability of cellulase enzyme

3.8.1.1 Thermostability of CMCase

Samples drawn from each of the four beakers were tested for CMCase and FPase activity at various time intervals. Fig.15 shows CMCase activity at four different incubation temperatures. The trends observed at 40 and 70 degrees Celsius were somewhat similar: As the duration of incubation increased, so did the activity of CMCase. After reaching a peak, the activity then fell. For the incubation temperature of 40ºC, CMCase was stable between 40 and 60 minutes, and its peak units (248.88µmol/ml/min) occurred at 60 minutes. As for the enzyme incubated at 70ºC, it appeared to be stable between 20 and 55 minutes, and its activity peak (212.66µmol/ml/min) was achieved at the 40-minute time interval.
Enzymes incubated at 50 and 60 degrees Celsius showed highest activities initially (285.106 and 98.151µmol/ml/min respectively), stayed stable till the 40-minute interval, and then declined.

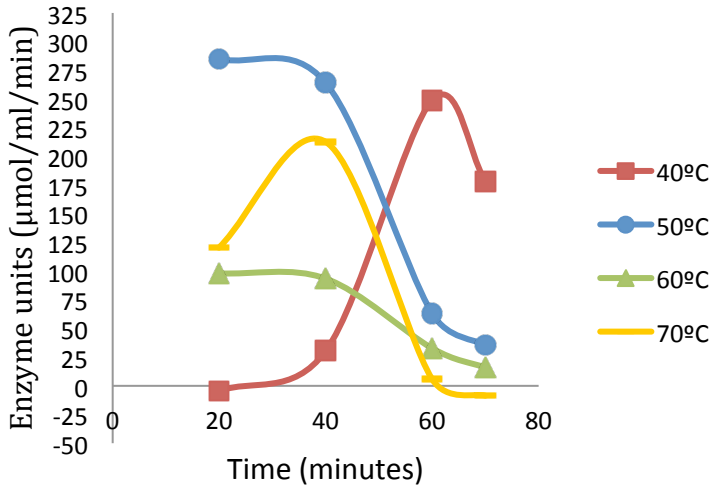

Fig.15: Thermostability study of CMCase at various time intervals

Wang et al. (2005) monitored CMCase activity in Trichoderma reesei with respect to time and temperature separately. Peak CMCase activity occurred at a time interval of 96 hours and a temperature of 28ºC. This indicates that their enzyme worked more efficiently at cooler temperatures and so could remain stable for longer time periods (higher temperatures can rapidly cause enzyme denaturation).

3.8.1.2 Thermostability of FPase

Fig. 16 shows the stability of FPase produced by RB200 at varying temperatures and time intervals. In this case as well, the pattern shown by enzymes incubated at 40 and 70 degrees Celsius was similar. Peak enzyme units occured at the very beginning, i.e. at 20 minutes for both 40ºC and 70ºC incubations (105.941 and 234.473µmol/ml/min). With increasing incubation time, FPase activity fell until it reached a minimum at 70 minutes. The stability duration lied between 20 and 60 minutes for both.

In the case of enzymes incubated at 50 and 60 degrees Celsius, FPase activity increased with increasing incubation time, reached a peak and then decreased. For the 50ºC incubation, FPase was stable between 30 and 60 minutes, attaining a peak of 170.596µmol/ml/min at 60 minutes. For the 60ºC incubation, the enzyme appeared to be stable between 20 and 55 minutes, and peak units (172.155µmol/ml/min) were achieved at 40 minutes.

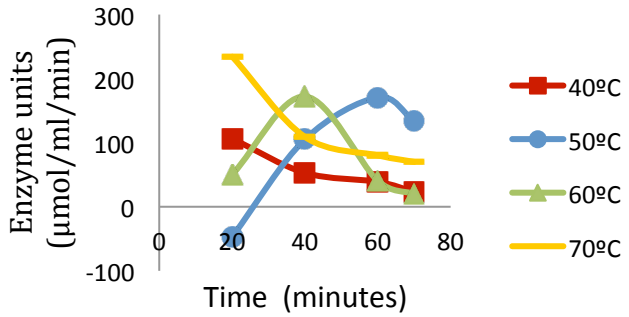

Fig.16: Thermostability study of FPase at various time intervals

Wang et al. (2005) also studied FPase activity at various time intervals and temperatures, and from their results it can be seen that maximum FPase activity occurred at the 72nd hour, and a temperature of 28ºC. Among their enzymes, both CMCase and FPase were most active at 28ºC

and their fungus was a more efficient CMCase producer. On the other hand, the current results show that maximum activities for the two isozymes occurred at different temperatures, and the chosen mutant bacterium RB200 was a more efficient FPase producer.

3.8.2 Study of pH stability of cellulase enzyme

Fig. 17 shows that maximum CMCase (283.938µmol/mL/min) and FPase (448.692µmol/mL/min) activity was obtained at pH 8 and 6 respectively, and that at these pH both isozymes are most active and stable. CMCase, between pH 4 – 7, is less active and a similar trend can be seen for pH above 8. FPase activity is much greater than CMCase at almost every pH, thus revealing that it is more stable and active than CMCase.

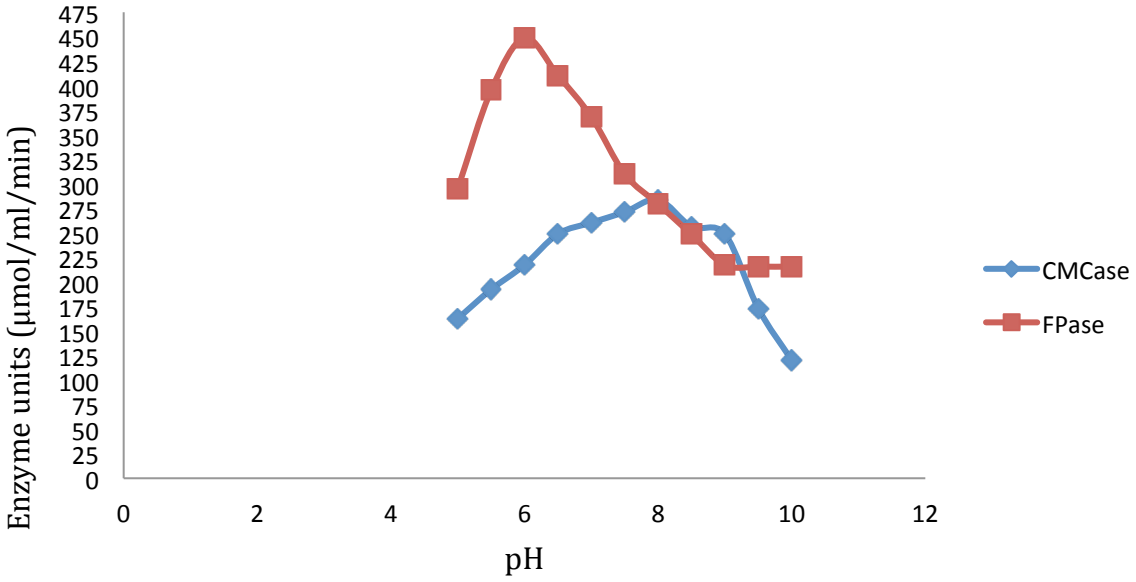

Fig.17: pH stability of cellulase at various pH for different time intervals

Wang et al., (2005) found that the maximum CMCase and FPase activity is obtained at pH 5.0, while in the current work peaks of CMCase and FPase were obtained at different pH values. Since CMCase and FPase are two different isozymes of cellulase, they are likely to show different activities with variation in pH, as apparent in the displayed in Fig.17.

Conclusion

In this work, bioethanol was successfully produced from cellulase degraded by mutant bacteria. At every step, from application of mutagens to bioethanol synthesis, interesting findings were obtained through the conduction of detailed analyses. Comparisons were drawn between, the efficiency of EMS and Ethidium bromide as mutagens, isozymes produced by five best mutant strains, Pre-treated and untreated wheat straw as substrates, selected mutant's FPase and CMCase activities and variation in the quantity of glucose, reducing sugars, and total sugars during saccharification and fermentation.

Keeping the rising global need for alternative energy in mind, the results presented in the current research may be utilized in the future to make the process of bioethanol production even more economically and environmentally sustainable.

Refrences

Adsul, M.G., Bastawde, K.B., Varma, A.J. and Gokhale, D.V. (2007) Strain improvement of Penicillium janthinellum NCIM 1171 for increased cellulase production. Bioresource Technology, 98, 1467-1473.

Ahmed, F.M., Rahman, S.R. and Gomes, D.J. (2012) Saccharification of Sugarcane Bagasse by Enzymatic Treatment for Bioethanol production. Malaysian Journal of Microbiology, 8, 97-103.

Ariffin, H., Abdullah, N., Kalsom, M.S.U., Shirai, Y. and Hassan, M.A. (2006) Production and Characterization of Cellulase by Bacillus Pumilus EB3. International Journal of Engineering and Technology, 3, 47-53.

Asad, W., Asif, M. and Rasool, S.A. (2011) Extracellular Enzyme Production by Indigenous Thermophillic Bacteria: Partial Purification and Characterization of α-Amylase by Bacillus Sp. WA21. Pakistan Journal of Botany, 43, 1045-1052.

Borzani, W. and Jurkiewicz, C.H. (1998) Variation of the ethanol yield during very rapid batch fermentation of sugar-cane blckstrap molasses. Brazilian Journal of Chemical Engineering, 15, 225-233.

Chand, P., Aruna, A., Maqsood, A.M. and Rao, L.V. (2005) Novel mutation method for increased cellulase production. Journal of Applied Microbiology, 98, 318-323.

Dashtban, M., Buchkowski, R. and Qin, W. (2011) Effect of different carbon sources on cellulase production by Hypocrea jecorina (Trichoderma reesei) strains. International Journal of Biochemistry and Molecular Biology, 2, 274-286.

Deka, D., Bhargavi, P., Sharma, A., Goyal, D. and Goyal, M.J. (2011) Enhancement of Cellulase Activity from a New Strain of Bacillus subtilis by Medium Optimization and Analysis with Various Cellulosic Substrates. Enzyme Research, 2011.

Deka, D., Bhargavi, P., Sharma, A., Goyal, D., Jawed, M. and Goyal, A. Enhancement of Cellulase Activity from a New Strain of Bacillus subtilis by Medium Optimization and Analysis with Various Cellulosic Substrates. Enzyme research, 2011, 151656.

DemÄ°RbaÅž, A. (2005) Bioethanol from Cellulosic Materials: A Renewable Motor Fuel from Biomass. Energy Sources, 27, 327-337.

Demirbas, A. (2008) The Importance of Bioethanol and Biodiesel from Biomass. Energy Sources, Part B: Economics, Planning, and Policy, 3, 177-185.

Dexter, J. and Fu, P. (2009) Metabolic engineering of cyanobacteria for ethanol production. Energy & Environmental Science, 2, 857-864.

Dhaliwal, S.S., Oberoi, H.S., Sandhu, S.K., Nanda, D., Kumar, D. and Uppal, S.K. Enhanced ethanol production from sugarcane juice by galactose adaptation of a newly isolated thermotolerant strain of Pichia kudriavzevii. Bioresource Technology, 102, 5968-5975.

Dombek, K.M. and Ingram, L.O. (1988) Intracellular accumulation of AMP as a cause for the decline in rate of ethanol production by Saccharomyces cerevisiae during batch fermentation. Applied and Environmental Microbiology, 54, 98-104.

Dubois, M.K., Gils, J.K., Hanniton, P.A., Robes and Smith, F. (1956) Use of phenol reagent for the determination of total sugar. Analytical Chemistry, 28, 350.

Elangovan, N., D, J.R., K, M., Akil, j., Mukash, K. and Richard, L.J. - Production of Extracellular Pectinase by Bacillus Cereus Isolated From Market Solid Waste.

Ghose, T.K. (1987) Measurement of cellulase activities. Pure Applied Chemistry, 59, 257-268.

Groleau, D. and Forsberg, C.W. (1983) Partial characterization of the extracellular carboxymethylcellulase activity produced by the rumen bacterium Bacteroides succinogenes. Canadian Journal of Microbiology, 29, 504-517.

Hemmati, N., Lightfoot, D.A. and Fakhoury, A. (2012) A Mutated Yeast Strain with Enhanced Ethanol Production Efficiency and Stress Tolerance. Atlas Journal of Biology, 2, 100-115.

Jones, M., Fosbery, R., Taylor, D. and Gregory, J. (2007) AS Level and A Level Biology. Cambridge University Press, Cambridge, UK.

Kotchoni, O.S., Shonukan, O.O. and Gachomo, W.E. (2003) Bacillus pumilus BpCRI 6, a promising candidate for cellulase production under conditions of catabolite repression. African Journal of Biotechnology, 2, 140-146.

Kurose, N., Kinoshita, S., Yagyu, J., Uchida, M., Hanai, S. and Obayashi, A. (1988) Improvement of ethanol production of themophilic Clostridium sp. by Mutation. Journal of Fermentation Technology, 66, 467-472.

Lowe, S.E., Theodorou, M.K. and Trinci, A.P. (1987) Cellulases and xylanase of an anaerobic rumen fungus grown on wheat straw, wheat straw holocellulose, cellulose, and xylan. Applied and Environmental Microbiology, 53, 1216-1223.

Maiorella, B., Blanch, H.W. and Wilke, C.R. (1983) By-product inhibition effects on ethanolic fermentation by Saccharomyces cerevisiae. Biotechnology and Bioengineering, 25, 103-121.

Maki, M., Leung, K.T. and Qin, W. (2009) The prospects of cellulase-producing bacteria for the bioconversion of lignocellulosic biomass. international Journal of Biological Sciences, 5, 500-516.

Manikandan, K., Saravanan, V. and Viruthagiri, T. (2008) Kinetics studies on ethanol production from banana peel waste using mutant strain of Saccharomyces cerevisiae. Indian Journal of Biotechnology (IJBT) 7, 83-88.

Mateos, P.F., Jimenez-Zurdo, J.I., Chen, J., Squartini, A.S., Haack, S.K., Martinez-Molina, E., Hubbell, D.H. and Dazzo, F.B. (1992) Cell-associated pectinolytic and cellulolytic enzymes in Rhizobium leguminosarum biovar trifolii. Applied and Environmental Microbiology, 58, 1816-1822.

Miller, G.L. (1959) Use of dinitrosalicylic acid reagent for determination of reducing sugars. Biotechnology and Bioengineering Symposium, 5, 193.

Miyamoto, K. (1997) Renewable biological systems for alternative sustainable energy production. FAO Agricultural Services Bulletin - 128. Food and Agriculture Organization of United Nations - Agriculture and Consumer Protection Department, Online.

MK, B. (2000) - Cellulases and related enzymes in biotechnology. Biotechnol Adv, 18, 355-383.

Mobini-Dehkordi, M., Nahvi, I., Zarkesh-Esfahani, H., Ghaedi, K., Tavassoli, M. and Akada, R. (2008) Isolation of a novel mutant strain of Saccharomyces cerevisiae by an ethyl methane sulfonate-induced mutagenesis approach as a high producer of bioethanol. Journal of Bioscience and Bioengineering, 105, 403-408.

Narasimha, D.G. (2012) Enhanced Production of Cellulase by Mutant Fungal strain Aspergillus Niger on Pretreated Lignocelluloses. World Congress on Biotechnology. Bright International Conferences & Events, Hyderabad, India.

Neelakandan, T. and Usharani, G. (2009) Optimization and production of bioethanol from cashew apple juice using immobilized yeast cells by Saccharomyces cerevisiae. American-Eurasian Journal of Scientific Research 2009, 4, 85-88.

Osman, Y.A., Conway, T., Bonetti, S.J. and Ingram, L.O. (1987) Glycolytic flux in Zymomonas mobilis: enzyme and metabolite levels during batch fermentation. Journal of Bacteriology, 169, 3726-3736.

Pradeep, M.R. and Narasimha, G. (2011) Utilization of Pea Seed Husk as a Substrate for Cellulase Production by a Mutant Aspergillus Niger. Insight Biotechnology, 1, 17-22.

Purwadaria, T., Kumalasari, A.T., Tutiharyat, Ketaren', P.P. and Arnold P, S. (2004) Optimization of Cellulase Production with Penicillium Nalgiovense S11 Grown on Pretreated Wheat Pollard. Biotropia, 23, 1-12.

Rajoka, M., Bashir, A., Hussain, S. and Malik, K. (1998) γ-ray induced mutagenesis of<i>Cellulomonas biazotea</i> for improved production of cellulases. Folia Microbiologica, 43, 15-22.

Saha, B.C., Iten, L.B., Cotta, M.A. and Wu, Y.V. (2005) Dilute acid pretreatment, enzymatic saccharification and fermentation of wheat straw to ethanol. Process Biochemistry, 40, 3693-3700.

Sridevi, A., Narasimha, G. and Reddy, B.R. (2009) Production of Cellulase by Aspergillus niger on natural and pretreated lignocellulosic wastes. The Internet Journal of Microbiology, 7.

Tangnu, S.K., Blanch, H.W. and Wilke, C.R. (1981) Enhanced production of cellulase, hemicellulase, and β-glucosidase by Trichoderma reesei (Rut C-30). Biotechnology and Bioengineering, 23, 1837-1849.

Viegas, C.A., Rosa, M.F., SÃ-Correia, I. and Novais, J.l.M. (1989) Inhibition of Yeast Growth by Octanoic and Decanoic Acids Produced during Ethanolic Fermentation. Applied and Environmental Microbiology, 55, 21-28.

Vu, V.H., Pham, T.A. and Kim, K. Improvement of Fungal Cellulase Production by Mutation and Optimization of Solid State Fermentation. Mycobiology, 39, 20-25.

Wagner, L. (2007) Cellulosic Ethanol. Mora Associates, pp. 1-2.

Wang, J.S., Wang, J. and Gulfraz, M. (2005) Efficient Cellulase Production from Corn Straw by Trichoderma Reesei LW1 Through Solid State Fermentation Process. Ethnobotanical Leaflets, 2005.

Xu, F., Wang, J., Chen, S., Qin, W., Yu, Z., Zhao, H., Xing, X. and Li, H. Strain improvement for enhanced production of cellulase in Trichoderma viride. Prikl Biokhim Mikrobiol, 47, 61-65.

Yazdi, M.T., Woodward, J.R. and Radford, A. (1990) The cellulase complex of Neurospora crassa: activity, stability and release. Journal of General Microbiology, 136, 1313-1319.

Zhou, X., Chen, H. and Li, Z. (2004) CMCase activity assay as a method for cellulase adsorption analysis. Enzyme and Microbial Technology, 35, 455-459.

MODELING AND RHEOLOGICAL CHARACTERIZATION OF SLUDGE BASED DRILLING OIL

Abderrahmane MELLAK, Khaled BENYOUNES

Engineering Physics Laboratory Hydrocarbons – Dept. of Petroleum and Mineral deposits.
Faculty of Hydrocarbons and Chemistry, University of Boumerdes- 35000 - Algeria.

E-mail: Mellakabder@yahoo.fr

Abstract: When the drilling mud is in contact with more or less permeable walls of the well, the liquid filter part in the formation by depositing on the walls of the solid part is called the cake (silty clay film). Among the main functions of drilling fluid include keeping the walls of the well due to the hydrostatic pressure exerted by the flowing fluid. Also, the mastery of the rheological properties of the mud used is required.
The rheological characterization focus on the drilling mud used for drilling the 121/4 phase in the well AY (Hassi Messaoud) is an invert emulsion mud with oil report / water 85/15 and its density is 2.04, consisting essentially of gas oil, organophilic clay, two emulsions, sodium chloride and barite. It would define the rheological model of drilling fluid used and seek the most suitable rheological model. The rheological tests were carried out using a Fann viscometer 6-speed (3, 6, 100, 200,300 and 600 rpm) to determine the rheological properties of the mud as the yield value or yield stress, the plastic viscosity and apparent viscosity. Other rheological parameters such as the consistency index (k) and the behavior index (n) of the mud were estimated. The results show that the Herschel-Bulkley model is a minimal deviation from other models (model Bingham and Ostwald de Waele or Power).

Keywords: drilling mud, rheology, plastic viscosity, yield value.

Introduction

Originally drilling "Rotary," the essential role of the mud was to evacuate cuttings (cuttings) from the bottom of the well to the surface. Today, the drilling mud is of paramount importance for the realization of a survey because it has important functions that can be grouped in three main functions, namely participation in the advancement of the tool, the hole cleaning and proper maintenance of the walls of the hole.

There are three types of sludge, sludge whose continuous phase is water, sludge whose continuous phase is oil and sludge air (rarely used because of the expensive equipment, security problems and inefficiency if rash of fluid from the formations traversed). Sludge from the oil, there are the direct and inverse sludge sludge direct (oil) contain 5 to 15% water and a maximum inverse sludge may contain up to 60% water. Sludge oil is complex fluids threshold (Osisanya, 2001; Coussot, 2009). The oil-based mud's are mainly used in all phases of drilling (except phase surface, shallow and where the land is poorly consolidated, the bentonite slurry is used). Sludge oil are mainly used for drilling and core producer levels to solve problems or swelling clays high dispersant, drilling deep wells and high temperature as well as the recovery and maintenance of producing wells (workover) (Thai-Son et al., 2009; Clain X et al., 2009) power.

This research is to characterize the most suitable for the drilling mud used rheological model, acting on the rheological parameters of the drilling mud (Fadairo et al., 2012; Maglione et al., 2000) while keeping the optimal characteristics of the drilling mud used so that it plays its role. The determination of the rheological model of the mud is made, according to the test program described in the experimental part of study.

Formulation of the drilling mud used

Mud used: The mud used to drill the $12^{1/4}$ phase in the slurry is well HY invert emulsion with an oil/water (O/W) 85/15 and a relative Specific Gravity (SG) of 2.04. The formulation of a cubic meter of this mud is shown in Table 1.

Table 1. The formulation of drilling mud used

Produits	Quantité (l/m3 ou en Kg/m3)
Gas Oil	516.00
Saumure (NaCl)	108.00
Lime (fatty based emulsifier activor)	30.00
Primary emulsifier	12.00
Secondary emulsifier and wetting agent	12.00
Lignite based fluid loss additive	8.00
Wetting agent	2.00
Barite (BaSO4)	1420.00

Equipment used: Rheometer was used Fann 35 A 6-speed (Fig.1). Speeds were 600, 300, 100, 6 and 3 rpm (rotation per minute). The measured parameters are the plastic viscosity and yield value.

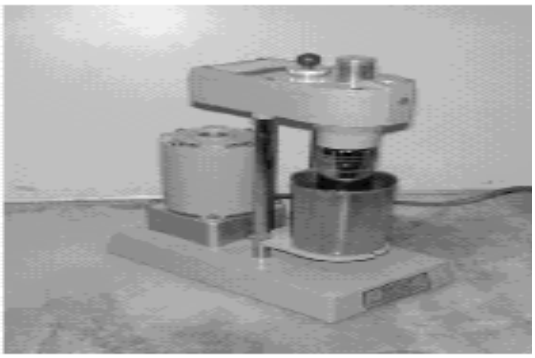

Fig. 1. Fann viscosimeter 35A.

The principle of determination of these parameters is to take readings at rotational speeds of 600 to 300 rpm.

The Fann viscometer is calibrated to give directly:

- The plastic viscosity (PV) PV = L 600 - L 300
- The apparent viscosity (AV) AV = L 600/2
- Yield value (YV) YV = (L300 – PV) = 2 (AV-PV).

Experimental Protocol

The determination of the rheological model of the mud was as follows:

- Using a Fann viscometer was performed four tests and took the arithmetic mean of a sample of the mud used;
- Using the readings obtained, the actual curve $\tau = f(\gamma)$ is plotted;
- Draw on the same graph the curve $\tau = f(\gamma)$ following the approach of Bingham;
- On the same graph Tracer the curve $\tau = f(\gamma)$ according to Ostwald approach;
- Make a comparative interpretation to define the rheological model is best used with mud.

The results obtained during tests conducted with the Fann viscometer shown in table2.

Table 2. The results obtained during tests conducted with the Fann viscometer.

Rate of rotation Ω (tr/min)	600	300	200	100	6	3
Rate of deformation γ (sec^{-1})	1021.8	510.9	340.6	170.3	10.218	5.109
lectures θ (cadran)	86	50	37	23	13	11
	86	50	37	23	13	11
	85	49	35	21	12	10
	88	52	37	22	13	11
the average (cadran)	86.25	50.25	36.5	22.25	12.75	10.75
Shear stress τ ($dynes/cm^2$)	440.73	256.77	186.515	113.69	65.15	54.93
Shear stress τ ($Lb/100ft^2$)	92.08	53.64	38.96	23.75	13.66	11.47

Rheological modeling mud

To set the rheological model of the mud used, it assimilates every time a known rheological model, namely, the Bingham model, the Ostwald model and Herschel Bulkley model and is subsequently a comparative interpretation.

Approach following the Bingham model

Bingham model is given by the following equation:

$$\tau = \tau_0 + \mu_P * \gamma \qquad (1)$$

where :
τ: Shear stress (Pa)
γ : Gradient de vitesse de cisaillement (sec^{-1})
τ_0: Yield value ($lb/100ft^2$)
μ_P: plastic viscosity (Pa. s).
Was obtained :
$\mu_P = \theta_{600} - \theta_{300}$ =86.25-50.25

$$\mu_P = 36\ cp$$

$\tau_0 = 2\theta_{300} - \theta_{600}$ = (2*50.25)-86.25

$$\tau_0 = 14.25\ \text{lb/100 ft}^2$$

For different values of "γ" are the values of "τ", the results are shown in table 3.

Table 3. Approximate results following the approach of Bingham.

Rate of rotation Ω (tr/min)	600	300	200	100	6	3
Rate of deformation γ (sec^{-1})	1021.8	510.9	340.6	170.3	10.218	5.109
Shear stress τ ($lb/100ft^2$)	91.20	52.72	39.90	27.07	17.92	14.63

Approach following the model of Ostwald Weall:

This model power is characterized by the following equation:

$$\tau = k * \gamma^n \qquad (2)$$

Where:

k and n: rheology factors
k = consistance indice et n = Comportment indice.

Was obtained :

$$n = 3.32 * log\left[\frac{\theta_{600}}{\theta_{300}}\right] = 3.32 * log\left[\frac{440.73}{256.77}\right]$$

$$n = 0.78$$

$$k = \frac{\theta_{300}}{511^n} \quad \text{d'où :} \quad k = \frac{50.25}{511^{0.78}}$$

$$k = 0.38\ lb.sec^{-n}/100ft^2$$

For different values of "γ" are the values of "τ", the results are shown in Table 4.

Table 4. Results obtained using the approach of Ostwald.

Rate of rotation Ω (tr/min)	600	300	200	100	6	3
Rate of deformation γ (sec^{-1})	1021.8	510.9	340.6	170.3	10.218	5.109
Shear stress τ ($lb/100ft^2$)	84.54	49.23	35.88	20.89	2.32	1.35

Comparative study:

Is plotted on the same graph of the rheogram curve τ = f (γ) of each model 02 provided with the real curve (Fig. 2).

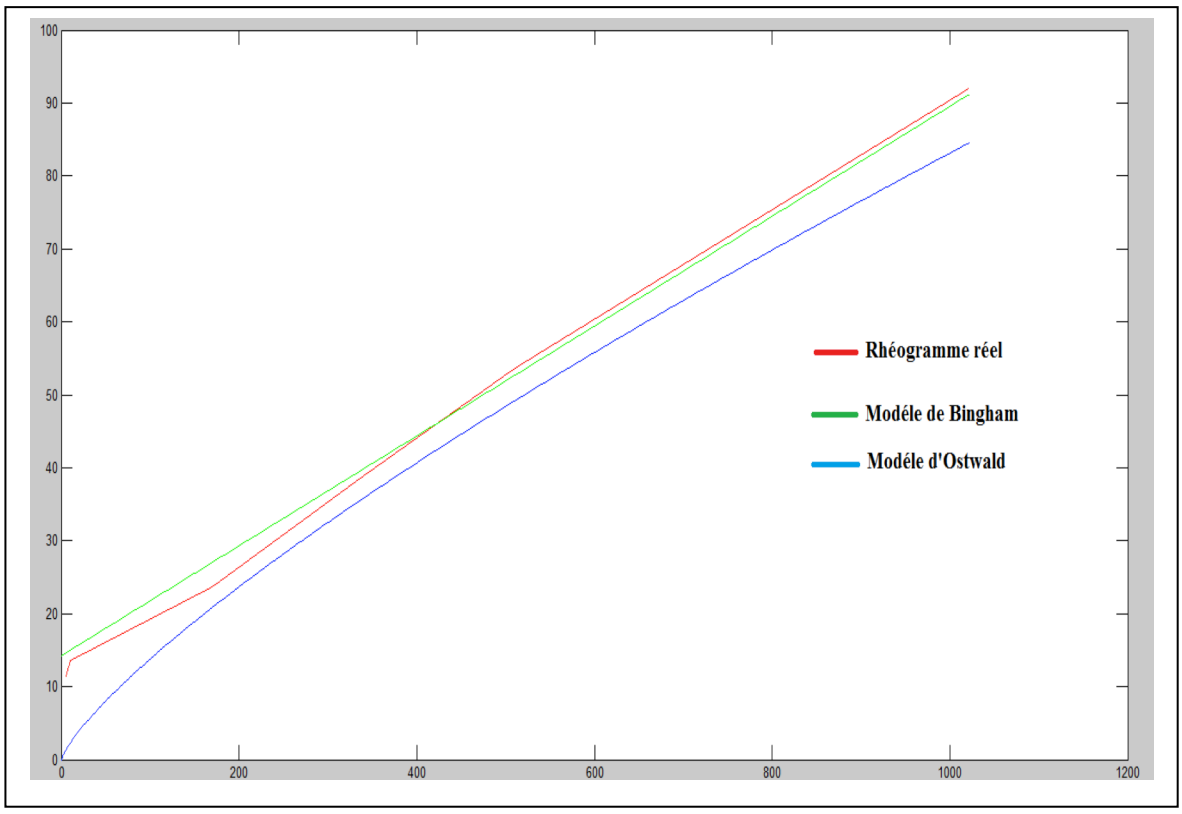

Fig. 2. Rheologicals models and the actual flow chart of drilling mud used.

The graph above shows the curves rheograms 02 rheologicals models and the actual flow chart of drilling mud used. According to the graph, we see that for the model of Ostwald, there is a large gap between the curve and the real flow chart, which to exclude this model to be the most suitable model drilling mud used. Regarding the Bingham model, we see that is a very small gap for large values of strain rate "γ" by against a standard that can not be neglected for small values of "γ ". For this we propose a different model is the Herschel-Bulkley model.

Approach following the Herschel-Bulkley model:

This model is most common in the case of drilling muds, it is characterized by the equation:

$$\tau = \tau_0 + k * \gamma^n \qquad (3)$$

With: $\tau_0 = \theta_3 = 10.75$

$$\tau_0 = 10.75 \ \ lb/100ft^2$$

$$n = 3.32 * log\left[\frac{\theta_{600}-\tau_0}{\theta_{300}-\tau_0}\right] = 3.32 * log\left[\frac{86.25-10.75}{50.25-10.75}\right]$$

$$k = \frac{\theta_{300}}{511^n} = \frac{50.25}{511^{0.91}}$$

$$n = 0.91$$

$$k = 0.15 \ \ lb.sec^{-n}/100ft^2$$

For different values of "γ" are the values of "τ", the results are shown in table 6.

Table 6. Results obtained using the approach of Herschel-Bulkley.

Rate of rotation Ω (tr/min)	600	300	200	100	6	3
Rate of deformation γ (sec^{-1})	1021.8	510.9	340.6	170.3	10.218	5.109
Shear stress τ ($lb/100ft^2$)	92.90	54.46	30.22	26.83	11.99	11.41

The results are shown in Figure 3.

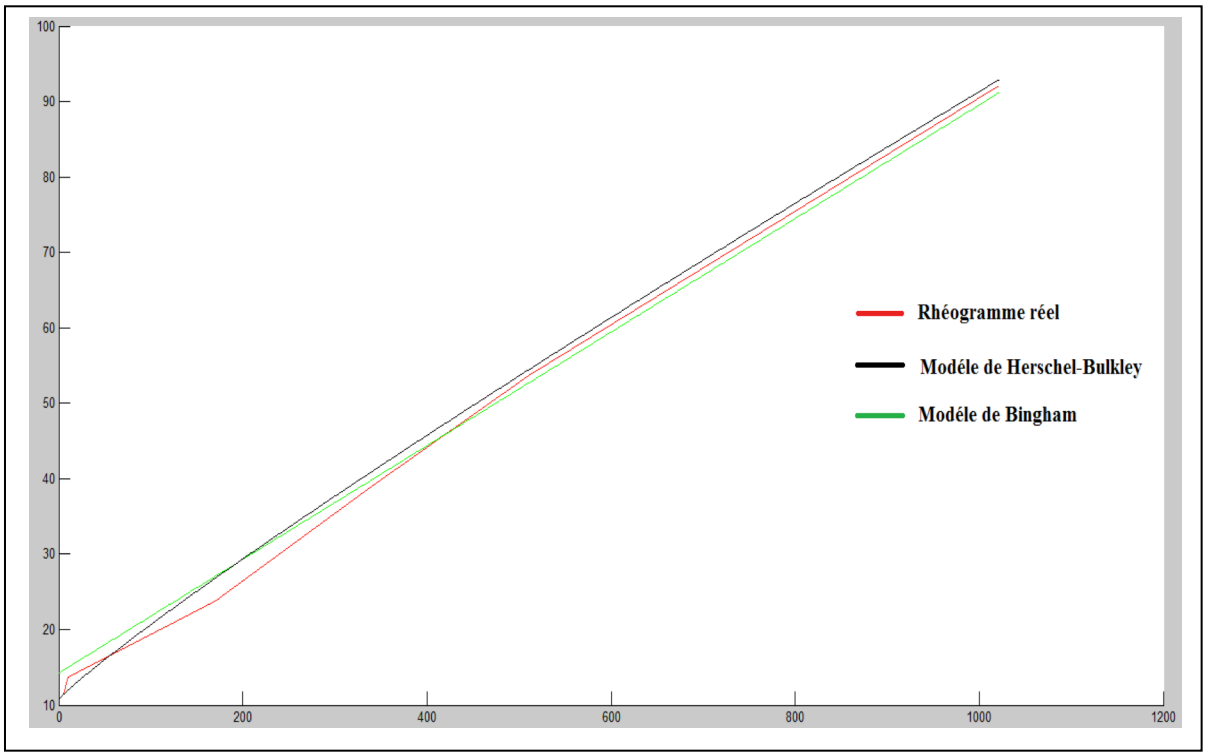

Fig. 3. Approach of Rheologicals models Herschel-Bulkley's and Bingham's

The graph above shows the curves of the flow chart of drilling mud used following the approach of Herschel-Bulkley and Bingham's approach with that of real rheogram. On notes that the Herschel-Bulkley model, represented in this case, by the state equation:

$$\tau = 10.75 + 0.15 * [\gamma]^{0.91}$$

According to the flow chart layout, we see a gap between the model and the Herschel Bulkly real rheogram for small values of strain rate "γ", but represent a minimum standard for large values of strain rate.

Conclusion

Modeling of complex fluid flows threshold is a field of research in its own right, particularly because of the difficulties in the coexistence of a solid diet and liquid diet. On the complex as drilling mud's used in oil well fluids, it is noteworthy that whatever the geometry (mud flow into a well and often in a porous medium) force or pressure gradient to provide according to the mean flow velocity follows a similar law in Herschel-Bulkley model (with the distinction of having a τ_0 threshold flow and a change of shear rate γ as a function of stress τ imposed).

The results thus show that the Herschel-Bulkley model is a minimum distance in relation to the mud studied (and compared to other models, namely the Bingham model or the Ostwald model), which confirms that the Herschel-Bulkley model best characterizes the drilling mud used.

References

Bingham, E.C., (1922). Fluidity and plasticity Mc Graw.

Coussot P., Nguyen Q. D. et al.(2002), "Viscosity bifurcation in thixotropic, yielding fluids" in journal Rheology. 46 pp. 573-589.

Coussot P. (2009). La vie secrète des fluides à seuil, in 44ème colloque annuel du groupe français de Rhéologie, Strasbourg, France.

Clain X, Chevalier C, Canou J, Dupla J-C, Coussot P. (2009). Injection de fluide d'Herschel-Bulkley en milieu poreux in 44ème colloque annuel du groupe français de Rhéologie, Strasbourg, France.

Fadairo A. S., Tozunku K., S., Kadiri T., M., Solarin T., Falode O., A., (2012), Investigating the Effect of Electrolytes and Temperature on Rheological Properties of Jatropha Oil Based Mud, Nigeria Annual International Conference and Exhibition, 6-8 August 2012, Lagos, Nigeria, p:11.

Herschel, W.H. abs Bulkley 1926). Konsistenzmessungen von Gummi-Benzollosungen. Kolloid Z. 39: 290-300.

Krieger I. M. (1989), "L'écoulement plastique et le rhéomètre rotatif à plateaux parallèles", Cahiers de Rhéologie, VIII, 61- France.

Maglione R., Robotti G., Romagnoli R., (2000) In-Situ Rheological Characterization of Drilling Mud, SPE Journal, Volume 5, Number 4, p 377-386

Mellak A. ; Baudeau Ph. (1994). "Etudes physico-chimiques sur des coulis de ciment saumurés et microsilicés appropriés aux formations salifères", Annales de l'ITBTP, 526, Paris.
Mellak A. (2004). Caractérisation d'un ciment destiné aux zones à pertes et modélisation de son caractère thixotrope in 39ème Colloque du Groupe Français de Rhéologie (GFR), A15 (2004), Mulhouse, France.

Mellak A. (2007). Caractérisations rhéologiques des coulis de ciment spécifiques aux formations salifères in Lebanese Science Journal (CNRS), vol. 8, n°2, pp115-120.

Quemada D, (1977). Rheol. Acta, 16, 82.

Nguyen V. H. (2006). Flow of Hershel-Bulkley fluids through the Marsh cone in Journal Non Newtonian Fluid Mechanics, 139, 128 -134

Osisanya S.O. (2001). Non Newtonian fluid mechanics, Lecture notes, School of petroleum and geological engineering, Algerian Graduate program Spring, the University Oklahoma USA.

Son T., Ovarlez G., Château X., (2009). Comportement rhéologique de suspension bidisperses de particules dans un fluide à seuil in 44ème colloque annuel du groupe français de Rhéologie, Strasbourg, France.

Disaster Management and Disaster Preparedness: Examples of Practices in California and Turkey

Hilal Kaya[1], Abdullah Çavuşoğlu[2], Baha Şen[2], Elif Çalık[3]

[1] Ministry of National Education, Ankara, TURKEY
hilalkaya@meb.gov.tr
[2] Yıldırım Beyazıt University, Department of Computer Engineering, Ankara, TURKEY
abdullah.cavusoglu@ybu.edu.tr bsen@ybu.edu.tr
[3] Karabük University, School of Health Sciences, Karabük, TURKEY
elifcalik@karabuk.edu.tr

Abstract: Disaster is the result of natural and human-induced events that community can't be able to overcome by their own facilities and that causes economic and social losses by interrupting or stopping the social life. Nowadays, causes of the transformation of the disasters to catastrophes appear to be the results of incorrect risk management methods. Most effective way of preventing the losses resulting from disasters is applying a good disaster plan. In order to ensure this, it's necessary to increase the awareness of community members about the disasters and on which task they will be responsible in case of disaster.

In this study, practices in the California State are examined as a sample of disaster preparedness and disaster management applications due to its similarity to our country because of its location in the area that has high probability rate of natural and technological disasters and on the major fault outlines. Also results and recommendations achieved in this area are given as illustrating best practices in our country in terms of raising awareness.

Key words: Disaster, disaster management, incident command system, Great Shakeout Drill.

Introduction

Disaster is a natural or human-induced impact that adversely affects a society or the environment. Nowadays, disasters appear as the results of the wrong risk management practices. These risks are the products of hazards and vulnerabilities. Developing countries are much affected by natural disasters. Financial losses of developing countries access 20 times more than the developed countries while 95% of death events occur in developing countries as the results of disasters (http://www.ahder.org).

Disasters are divided into two groups as natural disasters and human-induced and technological disasters. Natural disasters occur as the results of natural hazards as earthquake, flood and volcanic eruptions that affect people. Vulnerability caused by lack of emergency management, leads to financial and moral losses. On the other hand, technological and human-induced disasters are the results of the human impact, negligence, error and system failure. These disasters can be classified into two groups as technological and sociological disasters. Technological disasters are caused by technological failures such as traffic accidents and engineering errors. Nuclear and chemical accidents, major fires and environmental pollution are some examples of technological disasters. In sociological disasters, there are powerful human impulses as the events of crime, riots, wars and panics.

The main task of disaster management is to reduce loss of life and property, and protect the nation against natural, technological and human-induced disasters. In doing so, a risk-based comprehensive disaster and emergency management system including items such preparedness, protection, response, recovery and mitigation should lead

and support the public. Recently modern disaster management systems also emphasize the importance of preventing disasters before occurrence in addition to the disaster preparedness issue (Kadıoğlu, 2008).

The State of California, USA, is similar to our country due to its place in a region that people intensely experiences disasters and must always be ready to cope with these hazardous incidents. The largest earthquake in the history of California occurred in 18 April 1906. After this 7.9-magnitude earthquake in San Francisco, three thousand people died and 200 thousand people became homeless and San Andreas Fault was broken along the 500 km distance. Experts have detected underground vibrations on incomprehensible reasons when examining the San Andreas Fault along the Pacific in California in the centenary of the massive earthquake. For a while, new movements of the earth's crust have expressed suspicions after 100 years passed over the San Francisco Earthquake, one of the most powerful earthquakes in history. San Bernardino Fault that most recently caused an earthquake of magnitude of 7.7 in 1690 is expected to break again in the near future. According to experts' estimates, in the next 30 years, a devastating earthquake in San Francisco is likely to be expressed as 62 percent.

This area is also under the threat of storms, hurricanes, floods and tsunami as well as earthquakes. Not only natural disasters but also technological disasters affect this area adversely. Latest in April of 2012, San Onofre nuclear power plant, in the south of the province, was closed indefinitely due to problems of radioactive gas leak. Because the geography is always vulnerable to disasters and these disaster and emergency situations lead to casualties, a systematic disaster and emergency system is established.

In 2001, the United States Federal Emergency Management Agency (FEMA - Federal Emergency Management Agency) working group indicated the greatest third disaster scenario listed below and the risk map of the region is shown in Figure 1 (Carter, 1992):

- Terrorist attack in New York,
- Hurricane in New Orleans,
- Earthquake in California.

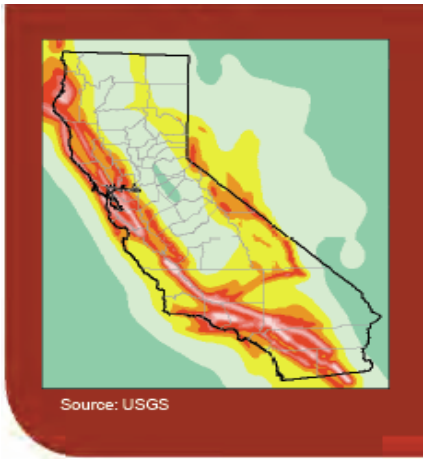

Figure 1. FEMA 2001 report

In the first part of this study, an introduction to the concept of disaster, disaster types and disaster management systems is presented and it’s focused on elements of integrated disaster management systems in the second part. In the third part, plans of creating disaster awareness and disaster preparedness implemented in California is examined, in the fourth part, best practices from our country are sampled and finally conclusions and recommendations are given in the fifth part.

Integrated Disaster Management System

Integrated Disaster Management System consists of disaster management and incident command system.

A. Disaster Management

Disaster management is the task of managing whole of the resources and institutions of the society together in order to plan and implement activities to be done before, during and after the disaster intended to prevent these events or mitigate the damages. On the conversion of a natural event to a disaster, what is done in the previous and subsequent periods has a very important role. Those made after the realization of the danger has an influence on preventing the next danger from becoming a disaster or reducing the losses that may be caused by a disaster.

With dealing the periods before and after the disaster within a process:

- Hazards can be defined correctly,
- Risks of hazards can be analyzed,
- Communities can be informed about the risks and can be informed in required level about the potential disaster risks,
- Activities can be planned to reduce the risks,
- When danger comes true, intervention measures can be intaken in order to prevent the danger from turning into disaster and deal with the disaster in a controlled manner.
- By taking disaster-development relationship into consideration, development can be achieved in a way that it reduces rather than increase the existing risks.

Approaching this process in a detailed and a holistic manner allows the development of more systematic approaches in order to increase community's resistance to disasters and minimize the adverse impacts (Erkan, 2010).

During disaster management loop, as taking into consideration the activities carried out before and after the disaster can be expressed as in Figure 2 (Erkan, 2010):

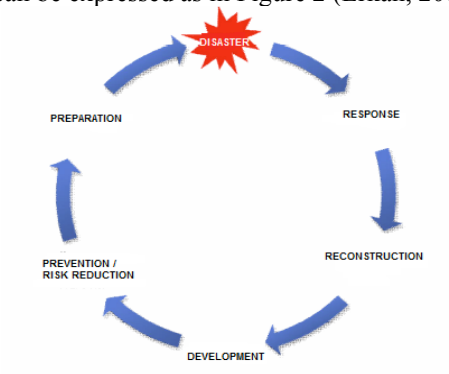

Figure 2. Schematic diagram of disaster management loop

In our country, progress of disaster management has begun after 1939 and what to be done before and after the disaster was identified with the law 4623. The first building code and seismic zones map were prepared according to this law. Ministry of Development and Housing was established in 1958 and with the law numbered 7269 which came into force in 1958, disaster services are counted among the tasks of this ministry. Then, the Directorate of Disaster Affairs was established in 1964, converted in 1965 to the Directorate General of disaster search and rescue process, except for safety and health services are authorized in almost all the central level. Search and rescue services are conducted by the Ministry of Interior, General Directorate of Civil Defence with the Law 7126; other than this, Red Crescent has very important tasks as providing especially tents, blankets, food, clothing, domestic and foreign aid, including medical services, including the collection and distribution of blood supply. At the central level, General Directorate of Turkey Emergency Management under Turkish Prime Ministry, Mineral Research and Exploration, Universities, the Scientific and Technological Research Council of Turkey and Turkish Armed Forces are the major institutions involved in this process. At local level, Provincial Governor and Provincial Rescue and Aid Committee attached to it has the full authority (http://www.afet.gov.tr).

B.Incident Command System

Search and rescue operations, such as other all emergency interventions, require fast, efficient and continuous action plan. Most efficient assessment of time and conditions can be ensured through a well-designed and planned operation. Incident Command System (ICS) is a system developed for the purpose of ensuring the functioning of the planned action in order to ensure the continuity of the intervention independent of individuals. Which is ideal is development of such a system in the national level and ensuring the system working in coordination with other services.

This system is configured with an expandable five functional sections:

- Responsible People of Incident Command Systems and Command Staff,
- Intervention / Operations Service Supervisor,
- Information and Planning Service Supervisor,
- Logistics and Maintenance Services Supervisor,
- Head of Finance and Administration Services.

The main condition of activating incident command system is to create an emergency plan. To do this, the following sequence must be enabled (http://www.biltek.tubitak.gov.tr):

Sensation

Receipt and delivery of sensation mechanisms must be created in advance. What should the first sense information include, how to categorize the sensations and which areas of expertise should start-up must be clearly planned.

Organization

Immediately after the completion of the sensation process, ICS should be organized. Neither should this process fast, nor should be slow. It's necessary to establish ICS in the right place and the time, with the right content and qualification.

Intervention

A well-organized ICS is not enough alone. The intervention phase that implements this system should renew the steady state analysis, assess the possibilities and change the strategies if it's necessary.

Example of Practices from California

It is the State's responsibility to take all appropriate measures on the safety of life and property of the citizens. At the state level, to cope with the adverse effects before and after the disasters, local authorities have the great responsibility. State administration has the guiding role of being a model for mitigating the local hazards measures and entering the inputs to national disaster reduction programs in the future (Koçak, 2004).

There are many laws on disaster management such as California Earthquake Education Law, California Emergency Services Act and California Earthquake Mitigation Law etc.

The coordinating institution responsible for emergency and disaster management in the United States is Federal Emergency Management Agency (FEMA). FEMA is an independent organization which manages disaster management system and prepares reports for the President. In state level, FEMA and other institutions implement and fund the mitigation of disaster measures. The head of FEMA serves as a consultant for the National Security Council on national security preparedness (Şengezer, 2002).

Although "Emergency" passes in the term "FEMA", its law and practices are based fully on the tasks and phases of "Integrated Disaster Management System" (Kadıoğlu, 2008).

National Level Policies and programs are guiding the states. Each state has different regulations. However, these legal regulations at the federal level integrate with the upper scale system.

As it is an example of the functioning of the Incident Command System, the School District Administration that connects the school incident command systems across the region exemplified below. School District Administration is a systematic structure that connects the police and the fire brigade, hospitals, radio, television and communication networks as newspapers with the schools.

A. School Incident Command Systems and Their School District Administration

In California, each school has its own incident command system and everyone is trained to know what to do in emergency situations. School District Administration Emergency Management Center provides education in all areas and is the unit that will help in an emergency situation. There are 13 units of School Police Department across the United States. In the State of California, it's indicated that there are 7 regions; from these regions only in Los Angeles there are 1100 schools, in week days with the elders there are over 1.000.000 students and the number of teachers and the staff is 95000 (MONE-Study Visit Report, 2010).

There are many devices with their backups used for communication in this region. 88 different agencies are studied with for the communication. Radio and wireless communications are very important. In this center, there is a system that allows communication with all the regions. Schools, police departments and hospitals are essential communication units. On monitors, police cars, fire brigades and student services are displayed. Thus, referrals can be made. To do this, electronic maps are used and there are 3 different projection systems. The main objective is monitoring the schools on the host system (MONE-Study Visit Report, 2010).

In the School District Administration Center for Emergency Management, people are trained about the National Incident Management System. Central Steering Committee of Emergency Management Board is trained here, too.

Trainees of this unit come together under certain groups to do their duties in case of disaster and emergency situations. These groups are Operations, Planning&Intelligence, Finance&Administration, Liason, Logistics, Personal Information Office (PIO) and Management. Each group is represented in a different color; members of the groups wear waistcoats in the colours of their groups during their extraordinary tasks. Managers are represented by black color, Command group by orange, Planning&Intelligence group by blue and Finance&Administration group by green (MONE-Study Visit Report, 2010).

In these centers, software system of ShakeCast- Background provided by American Geological Center, is used. In these software system, Decision Support System that will be used after an earthquake and Shake Map System are also available. ShakeCast software provides a Geographical Information System including all schools. Schools are monitored by the help of this software and a message is sent to all staff by this system in the situation of an earthquake (LAUSD-Executive Briefing, 2010).

ShakeCast system structure and operation flow are shown in Figure 3 (U.S. Geological Survey, 2004):

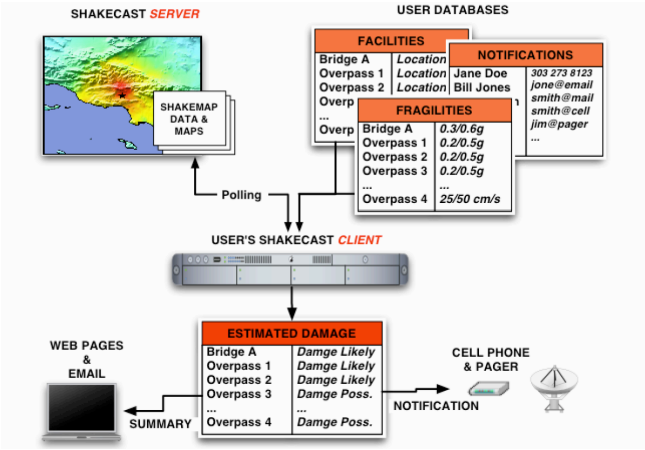

Figure 3. Summarized ShakeCast flowchart

B. Great ShakeOut Drill

ShakeOut Drill is a coordinated organization that has started to be implemented in California, but increasingly spread to other states and countries. This is a very important initiative on creation of disaster awareness. Participation to official ShakeOut organization requires a significant local or regional coordination that is carried out

by an institution responsible for emergency situation management or an alliance of many organizations. Total of 8.6 million people worldwide consisting of individuals, schools, universities, governments, institutions and organizations participated to 2011 ShakeOut Drill. On October 18, for 2012 ShakeOut Drill, numbers of participants reached 14.6 million (http://www.shakeout.org)

Scenarios that will be followed in this great drill applied to a wide range are delivered to people in public areas and by the Internet before the drill date. This scenario is an earthquake scenario likely to occur in more than estimation and it's prepared by U.S. Geological Research Center experts. The aim is to present the preparedness awareness to a possible earthquake event as starting with a specific scenario.

Stages of the realization of a well applied ShakeOut scenario are as follows:

- Urban planning,
- Emergency response training,
- School, work, environment and public earthquake drills,
- Prioritization of preparation efforts,
- Understanding the potential impact on the financial and social systems,
- Identifying vulnerabilities of the system infrastructure caused by interactions of the separate systems (Southern California Fall, 2008).

People are invited to this exercise carried out on the 3rd Thursday of October, days or even months before the incident. It's aimed to raise the awareness of people that can cope with any moment turn into a major catastrophe of an earthquake. People are earned to protect themselves from the damages of the buildings and the furniture as a reflex with the aid of DROP-COVER-HOLD ON exercise carried out in schools, universities, all institutions and organizations. It's highlighted that it's not the earthquake that kills people, buildings, furnishings and the negligence are more threatening. In the next stage of this exercise, an exercise on how can the building evacuated healthily and with least damage after the event is applied. "DROP-COVER-HOLD ON" and "Building Evacuation Drill" are drill applications in the 1st level as "Simple".

Figure 4. Representation of "DROP-COVER-HOLD ON" exercise

"Basic" drill exercise at the 2nd level of the practice is the "Safety of Life Drill". This drill ensures participated students, teachers and other staff to think over the actions of their emergency response during the drill and provides discussions about reducing risk and reaction time in order to make changes on later exercises [14].

3rd level "Intermediate" work is "Desktop Exercise to Decide". In this application, by the help of a comprehensive overview and additional regulations made with teachers, parents, staff and administrators after the drill, contribution to the next exercise is performed (The Great ShakeOut Drill Manual).

In the 4th level practice, as considering applications in schools, it represents "School Standard Emergency Management Simulation Drill". This exercise involves the implementation of the whole school and the school's emergency plan. It targets all of the response system. All staff in schools is as well as employees in the event of an emergency. For this reason, all of the staff previously trained or untrained, would have applied in an emergency duties with this application (The Great ShakeOut Drill Manual).

C. Other Best Practices

In schools and other public buildings, there are double entrances and doors have no risk of being locked and damaging people at the time of panic and can be opened outward by pushing manner. Heavy objects are fixed

against the danger of falling. Attention is paid to maintaining smoke and fire sensors. Also there are small water jets in the roof to repel water in case of fire.

Buildings are built considering the geographical characteristics of the region. Fire fighting cocks are kept in the beginnings of the streets. Ramps are set to make life easier for people with disabilities.

Receiving basic first aid training is widespread because its importance is understood by people. Even people who will be employed as a teacher in the United States are required to have first aid certificate. People carry cards involving their personal information and their critical health status with themselves. Students' emergency cards are also kept in schools and also their earthquake bags are kept ready for them.

In California, everyone who is working as a staff in the local region must take disaster and emergency trainings. All public officials do not go to their homes in case of disaster, work as disaster workers and perform their duties in an extraordinary situation defined for them.

In written and visual media, books and publications are available to increase the awareness of people about disasters. Also documents for small children's level are prepared. Science Centers give information about disasters as illustrating the state. As an example, purpose of California Science Center is to train students and inform people who comes to visit California.

Disaster Preparedness Practices in Turkey

Our country Turkey is also frequently facing natural disasters especially earthquakes and floods due to its geographical conditions. To increase awareness of our people on this issue, it's important to inform them on the issue at early ages. In addition, to ensure the sustainability of these training programs, it's essential to inform especially teachers and administrators about the importance of the issue.

For this purpose, Turkish Ministry of National Education signed a protocol with Japan International Cooperation Agency (JICA) on 18th October 2010 for collaboration on "School-Based Disaster Education Project" on account of the similarity between two countries in terms of disasters and benefitting from Japan's experiences on disaster management and mitigation. Overall purpose of the project being carried out by Turkish Ministry of National Education -General Directorate of Teacher Training- and Japan International Cooperation Agency (JICA) is strengthening the capacity of disaster management in order to promote awareness of risk management throughout elementary and secondary schools in Turkey. In this context, during implementation of 3-year duration of the project, it was started with 8 cities in the Marmara region and in the provinces of Bolu and Düzce involving 80 pilot schools. By the help of training programs throughout primary school students, school managers and parents, raising awareness of disaster and trying to create a culture of disaster preparedness is targeted. Thus, school-based education will be strengthened in the target area. Following the dissemination of the project is also aimed at training and practice throughout the country. In this context, established model classrooms in 10 demonstration schools selected from 80 pilot schools, when extension of the project across the country actualized, pilot schools will serve as a model for other schools (http://www.meb.gov.tr/duyurular).

"Disaster Preparedness Training Programme" carried out by Bogazici University Kandilli Observatory and Earthquake Research Institute since 2000, with the financial support by the United States Agency for International Development Office of Foreign Countries Disaster Support (USAID / OFDA), on the issues of "the basic disaster awareness", "earthquake against the structural consciousness", "non-structural hazards reduction"," governmental disaster volunteer skills" by public education and teacher training programs, training materials, have been developed and successfully implemented. The most striking and significant success in extending the program, has been provided in cooperation with the Ministry of National Education. In this context, 4,000 teachers in provinces i.e. Istanbul, Bursa, Canakkale, Istanbul, Izmir and Yalova and their districts attended "Basic Disaster Awareness Training of Trainers" program and completed in success and transferred these information to more than 30,000 teachers and school employees, more than 1.5 million students and tens of thousands parents (http://www.meb.gov.tr/duyurular/duyurular/TemelAfetEgitimiProjesi).

However, DREAMS project (Disaster Reduction Education Learning Support System) carried out in collaboration of Ministry of National Education and the American Red Cross and Risk Red was completed at the end of 2011. Under the distance education system offered within the scope of this project, there are two courses and 19 lessons. By the help of these course materials, through all teachers and administrators works in 30.000 schools in

Turkey, Disaster Preparedness Training for Individuals and Families (DPTIF) and School Emergency and Disaster Management (SEDM) Training is provided (http://www.riskred.org).

Viewing rates of these training courses data queried in November 2012 is taken from the Ministry of National Education is seen in Table 1 and Table 2:

Table 1: **Teachers-**Viewing rates of courses on disaster issues in Distance Education System of Ministry of National Education **(November-2012)**

School Emergency and Disaster Management (SEDM)		Total Number of Teachers	703776	
CONTENT NAME	Teachers_ Viewed	Teachers_Not_Viewed	Teachers_ Viewed_%	Teachers_Not_ Viewed_%
01. Comprehensive School Safety	109.612	594.164	16%	84%
02Disaster and Emergency Management Committee and Plans	73.739	630.037	11%	89%
03. Assessment and Planning	66.480	637.296	10%	90%
04. Physical Protection for Schools	64.141	639.635	9%	91%
05. Basic Disaster and Emergency Response Procedures	62.586	641.190	9%	91%
06. Hazard-Specific Procedures	61.735	642.041	9%	91%
07. An Overview of the School Event Management System	61.118	642.658	9%	91%
08. School Disaster Response Materials	60.898	642.878	9%	91%
09. School Disaster Drills	63.795	639.981	9%	91%
Disaster Preparedness Training for Individuals and Families (DPTIF)				
CONTENT NAME	Teachers_ Viewed	Teachers_Not_Viewed	Teachers_ Viewed_%	Teachers_Not_Viewed_%
01.Scope of Disaster Preparedness	100.016	603.760	14%	86%
02.Earthquake Risks in Turkey	64.164	639.612	9%	91%
03 Structural Awareness Against Disasters	55.997	647.779	8%	92%
04.Reducing Non-Structural Hazards	51.562	652.214	7%	93%
05. Fire Protection and Prevention	49.513	654.263	7%	93%
06 Other Hazards	48.035	655.741	7%	93%
07. During the Disaster	47.254	656.522	7%	93%
08. Psychological Support	46.436	657.340	7%	93%
09. Disaster Response Skills	45.744	658.032	7%	93%
10. Personal Needs	45.571	658.205	7%	93%

Table 2: **Managers-**Viewing rates of courses on disaster issues in Distance Education System of Ministry of National Education **(November-2012)**

School Emergency and Disaster Management (SEDM)		Total Number of Managers	77027	
CONTENT NAME	Managers_Viewed	Managers_Not_Viewed	Managers_Viewed_%	Managers_Not_Viewed_%
01. Comprehensive School Safety	11.857	65.170	15%	85%
02.Disaster and emergency management committee and plans	7.191	69.836	9%	91%
03. Assessment and Planning	6.445	70.582	8%	92%
04. Physical Protection for Schools	6.221	70.806	8%	92%
05. Basic Disaster and Emergency Response Procedures	6.060	70.967	8%	92%
06. Hazard-Specific Procedures	5.953	71.074	8%	92%
07. An Overview of the School Event Management System	5.901	71.126	8%	92%
08. School Disaster Response Materials	5.883	71.144	8%	92%
09. School Disaster Drills	6.267	70.760	8%	92%
Disaster Preparedness Training for Individuals and Families (DPTIF)				
CONTENT NAME	Managers_Viewed	Managers_Not_Viewed	Managers_Viewed_%	Managers_Not_Viewed_%
01. Scope of Disaster Preparedness	10.441	66.586	14%	86%
02. Earthquake Risks in Turkey	5.846	71.181	8%	92%
03. Structural Awareness Against Disasters	4.982	72.045	7%	93%
04. Reducing the Non-Structural Hazards	4.573	72.454	6%	94%
05. Fire Protection and Prevention	4.407	72.620	6%	94%
06. Other Hazards	4.259	72.768	6%	94%
07. During Disaster	4.177	72.850	6%	94%
08. Psychological Support	4.103	72.924	5%	95%
09. Disaster Response Skills	4.029	72.998	5%	95%
10. Personal Needs	4.002	73.025	5%	95%

Numbers and proportions seen in Table 1 belongs to teachers that had disaster education by the method of distance education and Table 2 indicates the number and proportions of viewing rates of the managers in the schools. Percentages seen in both tables are calculated by proportioning the numbers to the total numbers of teachers (703776) and managers (77027). In the project, as of 2013, at least 40%-50% of teachers and managers are targeted to be taken these courses. In order to achieve the targeted rates, follow-up of the usage of the system, the necessary announcements and disclosures made by the relevant units. On 30th March 2010, under the coordination of the Prime Ministry - Disaster and Emergency Management Presidency, "Disaster Education Accreditation Principles Determination of the Workshop" was organized.

Conducting studies on the different branches within the scope of this workshop, especially the Red Crescent, non-governmental organizations, universities, municipalities, representatives of public institutions and organizations came together. The workshop has been beneficial in terms of gathering different stakeholders carrying out independent studies within the topic of disasters and take joint decisions on the subsequent activities in the future. As a result of this workshop on disaster awareness and risk management decisions were taken for as follows:

- National Disaster Education Strategy should have been prepared together with all stakeholders.
- Through close cooperation with the Ministry of Education, disaster education curriculum should be taken.
- A common terminology should be determined in the process of disaster management.
- Voluntary system in disaster education should be developed.
- Training exercises should be used and should be consolidated and made mandatory.
- Education certification must be provided and certificates should be updated.
- Disaster training should be taken at all levels of the public with all relevant stakeholders.
- Repeats in projects should be avoided and waste of time and sources should be prevented.
- A standard in disaster training materials should be developed and these materials should be designed according to the target audience.
- Screening and case studies should be made for the serving institutions / organizations in "Disaster and Emergency Situations", NGOs and volunteers.
- Indicators of minimum service standards of institutions/organizations that provide disaster education should be identified.
- Cooperation with the Council of Higher Education shall be provided with the aim of putting compulsory and/or elective courses for training about disasters in the universities.
- Trainings for on-site manager that takes part in disaster response phase should be provided.

- People must become an integral part of disaster education.
- A digital library on the issue of disaster should be designed.
- Phychosocial aid training should be considered as the basic component of disaster trainings.
- Training should be planned with a focus on harm reduction.
- Feedback of the training should be followed.
- Disaster trainings should have leveling/grading system.
- Accredited institutions and organizations should be inspected.
- Accredited studies with other institutions / organizations made together, a large contribution in this regard should be provided.
- Realities of the country should be made on the basis of studies to determine the standards of disaster education.
- Trainings should be classified as basic disaster training, training of volunteers, training of experts and training of trainers.
- Trainings in schools should be provided by Ministry of National Education, other trainings by Turkish Red Crescent, universities, NGOs, Provincial Disaster Emergency Directorate and the President coordinate all of the training activities. Principles, standards, should be made in a coordinated manner by the Presidency.
- Expression of "informing" should be used instead of training people.
- Disaster trainings should not be only considered in the concept of the earthquake and intervention.
- Disaster coordination in the education has the priority (http://www.afetacildurum.com)

Conclusions

According to experiences acquired as a result of disasters, most damaging effects are that the negligence and insufficient disaster awareness was experienced. Considering the structural hazards is very important on construction of buildings and structures. Non-structural hazards must be eliminated as fixing all the utensils that can damage by falling. It'll minimize the loss of life that even the smallest individuals in our society, rather than to escape by running during the earthquake they protect themselves until shaking will have stopped. Because the experts clearly stated, earthquakes do not kill, unfixed goods and panic kills.

Training on disaster and risk management, and individual, family, neighborhood, school, institution and country-level action plans to be prepared for emergency will decrease the incidence of disasters caught unprepared. As mentioned in the example practice, regular and large-scale exercises will facilitate the conversion of the information received by training programs into behavior. Also by increasing the awareness of the community, support and solidarity will be placed.

In the situation of disaster, if staying alive is possible, people will need to sustain life, a bag containing materials readily available is very important. Public education about life after the disaster is of great importance too. The purpose of public awareness about life after the disaster is to prepare people to continue living in spite of the losses and damages. Protection and backup of personal and corporate information on the policies and values are determined and applied to make the point to continue living in the post-disaster is an important detail.

It is very important for the countries in disaster risk, to generalize the disaster awareness practices. Strict building codes, the buildings to have two outputs, the doors to be opened to the outside, the buildings kept in fire and smoke sensors, educational environment and other buildings to be free from structural and non-structural hazards, disaster education programs that increase awareness, exercises, written and visual elements preparing of a person's identity information will intervene in an emergency situation and keep in contact cards that contain critical information related to the health status; earthquake kit application; disaster management chain of command to be created and that this coordination is tested every year, a large-scale exercises and so on are examples of best practice applications that need to be taken.

Awareness about disasters in our country come into prominence and is being carried out by several studies on this subject. Teacher and administrator training projects were delivered to a certain extent. By the distance

education method of Ministry of National Education, summary of each lesson taken by teachers and administrators is displayed in Table 1 and Table 2, the participation rate in later times to reach the level of the 40%-50%, will make much closer to the objectives of awareness about disasters. In order to increase this ratio, the provision of certification at the end of education is considered to be effective.

A number of practices on disaster management and education are carried out in our country, independent from each other. On March 30, 2010 under the coordination of the Prime Ministry - Disaster and Emergency Management Presidency of the "Workshop on Disaster Education Accreditation Principles Determination" on this issue with all stakeholders in the joint decisions were taken. In this context, it has great importance that the Prime Ministry chairs a full coordination on disaster education and nationwide implementation of a National Disaster Education Strategy. All attempts to get ready for the point of disaster and awareness of people in a holistic manner should always be based on the national strategy at the top.

Acknowledgement

We would like to thank the authority of Ministry of National Education for their sharing the results of DREAMS project (Disaster Reduction Education Learning Support System) with our study team.

References

Carter, W.N.(1992). *Disaster management – A disaster manager's handbook*, Asian Development Bank.

Erkan, E.A.(2010*). Afet yönetiminde risk azaltma ve Türkiye'de yaşanan sorunlar*, SPO Expertise Thesis, Ankara.

Internet: http://www.afet.gov.tr/AIGM/DataSource/TeskilatDetay.aspx? SayfaID=36 (Official web site of the General Directorate of Disaster Affairs) Date of Access: 30.10.2012

Internet: http://www.afetacildurum.com/index.php?topic=290.0 (Platform for Disaster and Emergency Personnel) Date of Access: 10.11.2012

Internet: http://www.ahder.org/afete-hazirlik/afet-nedir (Earthquake Disaster Preparedness and Education Association) Date of Access: 30.10.2012

Internet: http://www.biltek.tubitak.gov.tr/sandik/aramakurtarma/olaykomuta.ppt Date of Access: 01.11.2012

Internet: http://www.meb.gov.tr/duyurular/duyuruayrinti.asp?ID=8262 (Official web site of the Ministry of Education) Date of Access: 05.11.2012

Internet:http://www.meb.gov.tr/duyurular/duyurular/TemelAfetEgitimiProjesi/TemelAfetEgitimiProjesi.htm (Official web site of the Ministry of Education) Date of Access: 05.11.2012

Internet: http://www.riskred.org/newsletter/annual2011.pdf (Risk Red Annual Report 2011) Date of Access: 08.11.2012

Internet: http://www.shakeout.org/california/# (The Great ShakeOut Web site) Date of Access: 03.11.2012

Kadıoğlu, M.(2008). *Modern, bütünleşik afet yönetimin temel ilkeleri*, JICA Türkiye Ofisi Yayınları, 2: (pp.1-34), Ankara.

Koçak, H.(2004*). Bir doğal afet olarak depreme hazırlıklı olma bilinci ve katılım: ABD, Japonya ve Türkiye (Afyon İli Örneği)*, PhD Thesis, Ankara.

Los Angeles Unified School District (LAUSD) Facilities Information Systems, *LAUSD earthquake preparedness: Using ShakeCast in emergency response – Executive Briefing (2010*), California.

Ministry of National Education- *School Disaster and Emergency Management Project (e-Disaster) California-Los Angeles Joint Report of Study Visit (2010)*, Ankara.

Southern California Fall 2008 Edition, *Putting down roots in earthquake country* (2008), California.

Şengezer, B.(2002). *Japonya ve ABD'de afet yönetimi, kentlerin depreme karşı hazırlanması*, TMMOB Mimarlar Odası İstanbul Büyükkent Şubesi Yayını, (pp. 37-56), İstanbul.

The Earthquake Country Alliance, The California Emergency Management Agency, *The Great ShakeOut Drill manual*.

U.S. Geological Survey's ShakeMap and ShakeCast: Improving Utilization within the American Lifelines Alliance (ALA) Community (2004), USA.

Emissions trading in financial statements: new Italian accounting standards

Giovanna Centorrino

Università di Messina, Dipartimento di Scienze Economiche, Aziendali, Ambientali e Metodologie Quantitative, Italy

e-mail:gcentorrino@unime.it

Abstract: Interest in the topic of sustainable business derives from the realization of the scale of the detrimental environmental effects provoked by industrial activity. Consequently, a growing sense of responsibility, at both a political and corporate level, regarding environmental protection, is developing. This paper examines the issues surrounding the recent publication by the Italian accounting association (Organismo Italiano di Contabilità: OIC) of two new accounting standards concerning environmental protection: OIC 7 - energy from renewable sources[1], and OIC 8 on the emission of greenhouse gases.
After a brief introduction on the role of international accounting standards and their relationship with national principles, we shall explore the devices employed in Italy for the control of emissions regarding sources of renewable energy and greenhouse gases, including how they are treated in accounting procedures.

Keywords: Sustainable Business, Environmental Cost Management, Environmental Management Accounting

Introduction

The topic of environmental sustainability involves various disciplinary areas and should be seen as an indispensable value in the model of modern development, no longer measurable just in terms of wealth, but in the wider, long term regarding respect for nature. Thus, also public and private institutions are, directly or indirectly, increasingly involved, and are responsible for the result of their actions on the environment.

Even from a business management perspective, attention and protection of the natural environment are widely accepted values by companies of all types and sizes. Modern business interacts with the external environment using new dynamics, mostly unknown in the past; it is projected in an increasingly extended manner, defining its impact on sustainable development as being of prime importance.

The still ongoing process of development, started back in 1900, has determined today's business reality as totally involved in a coherent action in the field of environmental protection. Even then, the issues to be addressed concerned political and social fields, as well as economic (RH Coase, 1960), which needed to be examined both at a theoretical and conceptual level, as well as practical. Today, although the debate continues, we are in a phase which greatly needs more operational actions. Some instruments have been developed on the basis of social and economic

[1] Green Certificates were first introduced in Europe, in Holland, in 1997, as a method of obliging companies to use energy produced from renewable sources. The innovative system came from Dutch electric energy producers who, through their EnergieNed association, voluntarily set emission allowances. This agreement was later made public through a law called "Environmental Action Plan 2000". On the basis of this agreement, a green labels market was created, parallel to a market where the corresponding physical quantity of renewable energy was exchanged. Following implementation of Directive 96/92/EC the green certificate market system became obligatory, with the Government attributing emission allowances and the contemporary halt of the voluntary system, from 2001.

theories and empirical research, helping to correctly determine, monitor and control the scale of the impact that companies have on sustainability.

Ongoing debate in the EU on environmental responsibility of companies also has "approached the point where emphasis should be shifted from 'processes' to 'outcomes', resulting in a measurable and transparent contribution from business in the fight against environmental degradation in Europe and around the world"[2].

We are now seeing the widespread diffusion of information tools designed to support the activities of government and improve standards of disclosure. Also with regard to mandatory disclosure regarding financial statements, it is clear that there is more receptiveness to requests coming from the economic environment and, therefore, not so far from the new development model based on environmental protection. Various initiatives that the European Union has implemented in accounting derive from this change. Civil law relating to financial statements unfolds on different perspectives which mainly concern protection of the various stakeholders and the establishment of the legal situation concerning accounting rules, seen as the main element regarding the evolution of the role of business in modern society.

This path explains both the legislative and jurisprudential evolution, and the modified doctrinal thinking on the relationship companies have with the environment. Therefore, the many EU initiatives on accounting are flanked by several interventions, often of remarkable relevance, from different countries, including also Italy. In the context of the conceptual framework just outlined, which will be further analyzed, the objective of this paper is to clarify the content and purpose of the recent standards issued by the Italian Accounting Association (Organismo Italiano di Contabilità: OIC) OIC[3] on the so-called "green certificates" (OIC 7)[4] and "gray certificates" (OIC 8). The choice to focus on these issues was inspired by lively debate on the need to define adjustments relating to international agreements on climate change, in particular, related to the link between the system of trading emissions of the European Union and renewable energy in accordance with the guidelines of the Kyoto Protocol[5].

After dealing briefly with the evolution of the dynamics of financial statements, in order to highlight the action of national and international accounting principles, this paper focuses on issues related to the production of energy from renewable sources and emissions of gas from companies and the related OIC standards, OIC 7 and 8. Finally some concluding remarks have been formulated.

1. Financial statements and the main Italian and international accounting standards

In the early 2000s, new interests with regard to the dynamics of financial statements were the subject of numerous measures for the implementation of EU directives aimed at improving the quality of information. Initially, the process implemented by the European Union to reduce the differences between financial statements of the different nations was based on the issuance of Directives[6] within a program of harmonization of company law. The Directives, however, did not bring about a good level of comparison, and effective solutions were not forthcoming concerning preparation and use of financial statements of European companies. Instead, a simple 'formal equivalence' of national accounting norms was obtained. During the debate between the European Commission and

[2]EUROPEAN PARLIAMENT, 2004-2009, Session Document A6 0471/200620.12.2006, Report on Corporate Social Responsibility: a new partnership (2006/2133 (INI)), Committee on Employment and Social Affairs. Rapporteur: Richard Howitt, n.7.

[3] OIC (Organismo Italiano di Contabilità – Italian Accounting Association) arose/was born from the keenly felt need of both the private and public sector in Italy for a national standard setter, endowed with wide representation attributes, able to express national issues in accounting, in a coherent way. The OIC was set up as a foundation on 27 November, 2001. (www.fondazioneoic.eu)

[4] These principles were approved by the OIC Foundation on 7 February 2013.

[5] The Kyoto protocol is an international environmental treaty regarding global warming, signed in Kyoto, 11 December 1997, by more than 180 countries, during the COP3 Conference of the United Nations Framework Convention on Climate Change. The treaty was implemented on 16 February 2005, after also being ratified by Russia.

[6] The status of Directive, usually implemented by national jurisdictions and also approved by law, makes it suitable for accounting normalization, by nature inclined to promptness, uniformity and legal certainly. The modification or issuing of new directives, which is inevitably necessary, involves long activation times, requiring political intervention (approval of laws proceeded by analysis and implementation). This often means that accounting regulations being dealt with have been superseded by more widespread regulations or even in contrast with more accredited International techniques.

Member States, it became increasingly clear that the process of harmonization, based on simultaneous compliance with accounting traditions of the various European countries and the acceptance of minimum requirements imposed by the Directives, did not allow for the delivery of results expected. In addition, we witnessed the increasing need for comparability that could only be satisfied by the use of a corpus of accepted accounting standards at a broader level. Therefore, a strategy was launched for application of internationally accepted accounting standards: IAS, now IFRS. Thus, since 1 January 2005, financial reporting requirements in accordance with these standards, initially issued by the IASC[7] became mandatory for companies trading on regulated markets in any of the member states. The institutional purpose of IASC was: "To develop a single set of high quality, understandable and enforceable accounting standards to help participants in the world's capital markets, and other users, make economic decisions"[8]. From 1999, a strategy was implemented to amend the IASC and, from 1st April 2001, the task of preparing the accounting standards was entrusted to a Board called IASB.
The acceptance of international accounting standards in our legal system triggered a series of problems related to the huge difference between them and those envisaged by Italian civil law. The problem has been tackled at a technical level by the OIC, which has the task to draw up Italian accounting standards for the preparation of financial statements and consolidated financial statements in compliance with the law, by coordinating its activities with those carried out by other European bodies, and assisting the national legislature in accounting matters, in order to incorporate the principles of international accounting standards. The OIC has prepared a series of national accounting standards and guidelines[9] in order to lay the groundwork for the current civil law approach to EU directives and international accounting standards, with clear benefit for comparability of financial statements. With regard to the implementation of European and international policies to protect the environment, the Italian Accounting Board, upon approval of specific accounting principles for environmental protection, has introduced accounting criteria for market mechanisms aimed at boosting environmental protection measures, so as to reduce harmful emissions and increase energy efficiency of industrial processes, and the application of new technologies with low environmental impact[10].

Green certificates and energy production

The production and use of energy from renewable non-traditional sources and the resulting level of environmental impact, have made it necessary to resort to a series of interventions aimed at the use of alternative sources of renewable energy that lower the effects of environmental pollution. These are sources the use of which does not affect natural resources, as they typically regenerate and are considered inexhaustible. Usually, the following sources are considered as renewable:

- Wind (often further divided into onshore and offshore)
- Solar (often further divided into photovoltaic and thermal)
- Wave (often further divided into onshore and offshore) and tidal (often further divided into onshore and offshore)
- Geothermal
- Hydro (often further divided into small - microhydro - and large)
- Biomass (mainly biofuels, often further divided by actual fuel used).

At the same time, there has been an increase in economic instruments suitable for the control of emissions[11] such as Green Certificates - terminology used in Europe - also known as Renewable Energy Certificates (RECs) in the USA, that represent the environmental value of renewable energy generated. They represent a novelty, in line with the international commitments made at Kyoto and with the guidelines contained in the White Paper on

[7] IAS principles were originally formulated and published by the International Accounting Standard Committee (IASC), created in 1973 on the basis of an agreement between the main professional world organizations.
[8] Site: www.iasb.org.
[9] See "Statuto di Costituzione dell'Organismo Italiano di Contabilità" art. 3, (www.fondazioneoic.eu)
[10] "*Presently, there is no authoritative accounting literature in either IFRS or U.S. GAAP that addresses these issues. Both the IFRIC and the EITF have previously considered the accounting for emissions trading schemes, but neither issued guidance that was implemented in practice"*. International Accounting Standard Board, Information for Observers, 20 May 2008, London.
[11] Today, the principal quantitative instruments in use for controlling emissions are "base line and credit" and "cap and trade".

renewable energy, resulting in an action of incentive-based market rules that minimize the burden on the community and are more suitable in a liberalized context.

Their own mechanism is based on the obligation, through legislation, for producers and importers of electricity produced from non-renewable sources, to put annually, a minimum share of electricity produced by plants using renewable sources, into the national electric grid. In other words, the producers of fossil fuels are required to transform an annual percentage of their production from fossil fuels to renewable; if they do not, or can only do so partially, they must purchase green certificates in amounts corresponding to the non-transformed quota and forward them to the GSE (Gestore Servizi Energetici)[12] (Manager of Energy Services). Instead, those who produce from renewable sources are granted a Green Certificate for each MWh produced, every year, which they may trade, that is, grant to producers from fossil fuels that have not reached the required quota. The Green Certificate in bearer form can then be traded freely both through the platform of the Manager of the energy markets, and with bilateral contracts between the parties. Their use aims at the creation of demand for energy from renewable sources based on a legal requirement that increases a corresponding energy offer from renewable sources. Accordingly, anyone who produces or imports energy from non-renewable sources is obliged to include a specific percentage of energy from renewable sources in his production or importation, calculated on the amount of non-renewable energy produced in the previous year. Alternatively, as seen, green certificates equivalent to the amount of the obligation can be bought on the market. They are valid for three years and must be pertinent to the output obligation of that year of production or the following two years.

OIC 7: accounting treatment of the production of electrical energy from renewable energy sources

We shall now address the accounting treatment required by OIC 7 for green certificates in financial statements. As seen, green certificates certify that an amount of energy was produced from renewable sources. Each certificate covers the output of the reference year and the following year it is used, and forwarded to the Network Manager, in order to be canceled as proof of compliance with the green portfolio relative to the operator concerned. It can also be requested with reference to expected production for the following year. The mechanism foresees that GSE may issue preventive or consumptive certificates.

Preventive certificates are related to expected production and may be issued in the current year or in the year preceding production. Also green certificates issued on the basis of monthly measurements of generated energy are part of this type. If actual production is lower than expected production (production deficit) the producer must return the green certificates issued in excess. Alternatively, the GSE can compensate for the difference by holding certificates which apply to other installations for the same year or by using the certificates for the year following the one which produced a deficit. Instead, if actual production is higher than expected (over-production), the GSE will issue a number of green certificates for the excess amount.

With regard to green certificates issued in consumptive, emission takes place in the year following the one in which the production was realized in a quantity equivalent to the same production. Producers and importers of electricity from non-renewable sources must deliver green certificates to the GSE equal to their requirement by 31 March of the year following the reference year.

The mechanism of green certificates is an incentive for companies that produce energy from renewable energy sources and penalizes those that produce from non-renewable sources. For the former, the certificates can be considered as a supplement to income for the period which offsets the higher costs associated with the production of energy from renewable sources. For producers from non-renewable sources, however, the mechanism involves an increase in production costs related to the purchase, on the market, of certificates which are necessary to comply with legal obligations.

Accounting treatment for companies that produce energy from renewable sources.

[12] Green certificates are issued by the Manager of Energy Services (GSE) and each of them contains evidence regarding the production of 1 MWh of renewable energy.

In the case of companies that produce energy from renewable energy sources, certificates can be sold on the market or recalled from the GSE at a price established by the reference standard. In preparing the annual financial statements, the company registers the amount due the GSE under assets, and the related income in the income statement under accruals. The revenues of the certificates received are recognized in the period in which production took place, and in proportion to the production itself. Their sale generates income that has to be recorded in the income statement and a credit to be shown under assets.

If the sale of preventive green certificates occurs during the period of competence, the entire revenue is shown. However, if a part of the amount is not accrued at the year end due to a production deficit, a deferred income for the share of revenues is recorded, to be dealt with in the future. In the case of over-production, it is necessary to integrate the revenues concerning the release of other green certificates by the GSE. If the company carries out a sale after the end of the year, the difference between the book value and net realizable value is calculated and any profit or loss is shown. The company must highlight the issuance of preventive green certificates received in the memo accounts in relation to the commitment to produce a proportional amount of green energy certificates received. The commitment is written for the expected value of the withdrawal guaranteed by the GSE. At year end, the actual energy production determines the total or partial cancellation of the memo accounts.

Accounting treatment for companies that produce energy from non-renewable sources.

For companies producing/importing electricity from non-renewable sources, there is the opportunity to purchase green certificates up to the time that the relevant legislation foresees delivery of the certificates to the GSE. Costs concerning the obligation of delivery of certificates are calculated in relation to the relevant time period.

Purchase of the certificates is recorded in the income statement as a cost and in the balance sheet as a debt.

If the purchase is made within year-end the full cost is recorded. If the quantity of green certificates acquired before year end is lower than the quantity needed for compliance with the law, the company records the burden as a debt due to GSE. If, instead, the quantity purchased is higher, a prepaid asset to future cost must be recorded. If buying occurs after year end, the difference must be calculated between the value of the liability recorded in the balance sheet and the market price and any profit or loss be shown.

Greenhouse gases and the European community

It is well known that greenhouse gases occur naturally in the atmosphere and while being transparent to incoming solar radiation on the earth, they hold back outgoing infrared radiation emitted by the Earth's surface and human activities, thereby helping to increase the so-called greenhouse effect, the phenomenon of global warming.

The European Union has recently set up a system (European Emission Trading System EU ETS)[13] which aims to reduce these gas emissions in a cost-efficient way, in order to meet its commitments under the Kyoto Protocol. However, it should be noted, that since the Kyoto Protocol only regulated the emissions for the period 2008-2012, it was considered necessary to initiate negotiations at an international level towards the adoption of a legally binding instrument for the reduction of greenhouse gases for the period after 2012.

In this perspective, today, companies that carry out their activities in the fields of energy and the production and processing of ferrous metals, mining sector, and manufacturing of paper and paperboard are compulsorily subject to the system known as "exchange of emission allowances". Each operator has an ‘emission allowance’, which gives him the right to release a metric ton of carbon dioxide (CO2), or an amount of any other greenhouse gas with an equivalent global warming potential, freely into the atmosphere[14]. At the beginning of each year, the National Authority issues part of the emission allowances free of charge which they have identified on the basis of a national allocation plan approved by the European Commission to the relevant companies. Quotas have long-term

[13] “The EU emissions trading system (EU ETS) is a cornerstone of the European Union's policy to combat climate change and its key tool for reducing industrial greenhouse gas emissions cost-effectively. The first - and still by far the biggest - international system for trading greenhouse gas emission allowances, the EU ETS covers more than 11,000 power stations and industrial plants in 31 countries, as well as airlines”. www. ec.europa.**eu**/clima/policies/**ets**/index_en.htm.

[14] Art. 3 Directive 2003/87/EC, European Parliament and Council, 13 October 2003.

validity, and are therefore used not only in the current year, but also in subsequent years. The mechanism foresees the obligation on the part of the company to return their shares to the competent authority by 30 April of the year following the year of reference. This mechanism is therefore a strong incentive tool for the reduction of greenhouse gases, aimed at encouraging improvements in the technology used in energy production and industrial processes, as well as the most efficient use of energy[15].

OIC 8: accounting treatment of greenhouse gases

According to Cook (2009) "The Emission Rights affair is worth studying because it illustrates the problems faced by standard setters as they explore the frontiers of accounting".

In this section, we will explore issues that relate to the recognition and successive inclusion in the budget of greenhouse gas emission allowances for companies that fall within the scope of the legislation, as established by OIC 8. This regulates accounting treatment both with respect to companies covered by the rules for reductions in emissions of greenhouse gases, and for company traders who do not perform industrial activities, but who acquire emission allowances for value with the intention of reselling them on the market[16].

At the time a company receives a free allocation of allowances from the National Authority, this operation is recorded with the use of memo accounts, according to the so-called "Commitment System" showing the total number of allowances allocated in the account "*Commitments for emission allowances allocated free of charge*" and a commitment to produce within set limits by the National Authority in the account "*Commitments to the Ministry of Environment for emission allowances allocated free of charge*". These amounts are recorded at market value, based on the interaction between supply and demand at the time the allocation takes place. At year-end in relation to actual gas emissions, the memo accounts are diverted and this commitment is canceled. However, in the case in which the relevant companies produce emissions in excess of the limits imposed, they can buy other allowances on the market. In the case of surplus allowances, these can be sold. Allowances are freely transferable and negotiable through special trading platforms or by contract (Article 19). Platforms for the exchange of emission allowances are private initiatives that assist users in finding and negotiating the transaction of sale of allowances[17].

At preparation of financial statements, when transactions have taken place entirely in the current year, these operations will generate costs or revenues to be recorded as profit or loss in payables and receivables, in the balance sheet. The costs are a "burden of the system" and will be recorded under item B14) *Other Operating Expenses*, revenues will be written in item A5) *Other Revenues*. Instead, in the case in which the relative values of the statutory requirement for the year must be shown in relation to the actual emission of gases, if at year-end the sum of the allowances owned (including those free of charge and those purchased) by the company is less than the quantity necessary for the fulfillment of legal obligations, the deficit can be covered by additional shares purchased on the market. This will be a residual charge incurred for emission allowances not yet purchased as off-set for liabilities to the National Authority. In the case in which the company has allowances that are greater than the legal requirements, these can be used in the following years or sold on the market. If this exceeding amount refers to allowances purchased, a prepaid expense will be recorded for the amount to be rectified for the next year. If the allowances in question were free allowances, these can be forwarded directly to the next year's statement. Emission allowances which are still available at year-end are recorded as inventory, under current assets on the balance sheet *Inventory of Finished Goods and Merchandise*. To record CO_2 allowances as inventory, the Accounting Principle indicates that it is preferable to allocate costs specifically incurred for the purchase of same to individual emission allowances. Changes in inventories of emission allowances are recognized in the income statement as *Changes in Inventories of Raw, Ancillary and Consumable Materials and Goods*.

Lastly, it should be noted that the delivery of emission allowances to the competent authority for the fulfillment of the obligation for the previous year does not involve any accounting registration, as all economic and financial considerations have already been taken into consideration on an accrual basis in the financial statements where the obligation arose.

---

[15] OIC 8, art. 5-6-8.

[16] Trader companies which are the subject of OIC8 are not dealt with here.

17 The first Italian platform for the Exchange of Greenhouse Gas Emission Allowances was set up by Gestore del Mercato Elettrico (GME).

Conclusions

The European system for allowances for energy produced from renewable sources and trading greenhouse gas emission allowances, aims at contributing to the solution of environmental policy issues through market mechanisms intent on reducing the level of environmental impact of companies. This paper briefly highlights the procedures by which, following accounting principles, allowances for energy produced from renewable sources and the emission of greenhouse gases are treated. Disclosure and evaluation of RECs in financial statements is discussed. The subject is particularly relevant, especially in relation to the support given by the Italian Accounting Association to promoting growth and that type of competitiveness in companies, in harmony with the pressing demands of environmental protection. The commitment of companies in this field must be supported by structures, laws and the business culture itself, all forces which, in their convergence, can contribute to a sustained and significant improvement of the current state of affairs. This paper also highlights another aspect that relates more closely to the economic-business perspective. The tension towards corporate social responsibility is the basis of a lively international debate which, involving multiple disciplines, is inevitably reflected also on the contents of the financial statements, stimulating legislative action inspired by the prevailing climate. The application of accounting principles OIC7 and OIC8 to financial statements contributes to the achievement of accounting information that also involves issues of social sustainability, amplifying and enhancing the contents, reunites ethical issues with those of a purely economic nature.

References

Alaimo S. (2005). *Protocollo di Kyoto, riduzione delle emissioni e mercati ambientali*. Phasar, UE. COM 629/3.

Azzali S., Allegrini M., Gaetano A., Pizzo M. & Quagli A. (2006). *Principi contabili internazionali*. Torino: Giappichelli.

Basosi R. & Verdesca D. (2006). *Emission Trading e piano assegnazione quote*. Ambiente e sicurezza, Il Sole 24 Ore.

Camfferman K. & Zeff S. A., (2000). *Financial Reporting and Global capital market. A history of the international Accounting Standards Committee*. Oxford University Press.

Capodaglio G.& Ricci A. (2008). *Le finalità conoscitive del bilancio d'esercizio: recenti modifiche normative e prospettive future*. Rivista italiana di ragioneria ed economia aziendale, novembre- dicembre.

Cicigoi E. & Fabbri P., (2007). *Mercato delle emissioni ad effetto serra: istituzioni ed imprese protagoniste dello sviluppo sostenibile*. Il Mulino.

Cook A., (2009). *Emission right: From costless activity to market operations*. Accounting Organizations and Society, 34, (pp.456-468).

D'Auria, M., (2005). *La direttiva europea "emissions trading" e la sua attuazione in Italia.* Giornale di diritto amministrativo, fasc. IV.

EPA (United States Environmental Protection Agency), (1995). *An Introduction to Environmental Accounting As A Business Management Tool: Key Concepts And Terms*. Erişim Adresi: http://www.epa.gov/gateway/learn/ (Erişim Tarihi: 07.09.2012).

Hall, J.K., Daneke G.A. & M. J. Lenox, (2010), *Sustainable Development and Entrepreneurship: Past Contributions and Future Directions,* Journal of Business Venturing, Article in Press. Vol. 25, Issue:5, 439–448.

Masanet, J. & Llodra M., (2006). *Environmental Management Accounting: A Case Study research on Innovative Strategy.* Journal of Business Ethics, Vol. 68, Issue:4, (pp.393-408).

Mei, L. (2011). *Full Cost Accounting in Solid Waste Management: The Gap in the Literature on Newly Industrialised Countries*. Journal Of Applied Management Accounting Research, Vol. 9, Issue:1, (pp.21-36).

OIC 8, (2013). *Le quote di emissione di gas ad effetto serra*. Organismo Italiano di Contabilità.

OIC 7, (2013). *I certificati verdi.* Organismo Italiano di Contabilità.

Potocan, V. & Mulej, M. (2003). *On Requisitely Holistic Understanding of Sustainable Development from Business Viewpoints*. Systemic Practice and Action Research, Vol: 16, (pp. 421-436).

Pulejo L., (2011). *La gender equality nell'economia dell'azienda. Strategie e strumenti di mainstreaming di genere per lo sviluppo sostenibile*. Milan: Franco Angeli.

Coase, R. H. (1960). *The problem of social cost*. The Journal of Law and Economics, vol. III.

Rupo D., (2001). *La variabile ambientale nella comunicazione d'impresa*. Torino: Giappichelli Editore.

Stanko, B. B., Brogan, E., Alexander, E. & Josephine Choy-Mee, C. (2006). *Environmental Accountin*. Business & Economic Review, Vol. 52, (pp.21-27).

UE (2007). *Comunicazione della Commissione al Consiglio e al Parlamento Europeo, Relazione sulla strategia di sviluppo sostenibile 2007*. COM (2007).

UE (2010). LIBRO VERDE. *La politica di sviluppo dell'Unione europea a sostegno della crescita inclusiva e dello sviluppo sostenibile. Potenziare l'impatto della politica di sviluppo*.

Vermiglio F. (2007). *Accounting Harmonization of SME lights and shadows over the Italian experience, in "Small and Medium- Size enterprises in the conditions of globalization: economic, social, legal and ecological problems of development,* Kyiv (Collected scientific reports of the international Ukrainian, Polish-Italian symposium, Yalta, 15-17 may).

Wilmshurst, T. D. & Frost, G. R. (2001). *The role of accounting and the accountant in the environmental management system*. Business Strategy & The Environment (John Wiley & Sons, Inc), Vol.10, (pp.135-147).

Xiaomei, L. (2004). *Theory and practice of environmental management accounting*. International Journal Of Technology Management & Sustainable Development, Vol.3, (pp.47-57).

Yakhou, M. & Dorweiler, P. V. (2004). *Environmental Accounting: An Essential Component Of Business Strategy*. Business Strategy and Environment, Vol.13, (pp.65-77).

Transverse Thermal Dispersion in Porous Media Under Oscillating Flow

Mehmet Turgay PAMUK[1], Mustafa ÖZDEMİR[2]

[1]Postane Mahallesi, Manastır Yolu Eflatun Sk. No:16, 34940 Tuzla/İSTANBUL-TURKEY
[2]Istanbul Technical University, İstanbul-TURKEY

[1]E-mail: mtpamuk@pirireis.edu.tr

Abstract: In this study, transverse dispersion thermal conductivity in a porous medium of mono-sized steel balls under oscillating flow has been investigated. Although mode of heat transfer is expected to be convection caused by fluid flow only, conduction and especially dispersion in porous media is very important depending on the solid material, structure and flow medium. The scope of this study is to obtain transverse thermal dispersion conductivity correlations to be used for oscillating flow. For this purpose, a total of 27 sets of heat transfer experiments, each representing a different frequency, flow displacement length and heat input, have been conducted for a porous medium of steel balls of 3 mm in diameters. Considering that the total thermal conductivity is a summation of dispersion conductivity and the medium's thermal conductivity, effective thermal conductivity is found to be a linear function of Peclet number. Thus, it has been possible to estimate effective thermal conductivity of the medium under oscillating flow by measuring heat flux, fluid velocity and calculating radial temperature gradients.

Keywords: Porous Media, Oscillating Flow, heat transfer, dispersion

Introduction

The porous media have been used widely in many engineering fields such as cryocoolers, solid matrix heat exchangers, cooling of electronic equipment and regenerators in order to enhance heat transfer. On the other hand, heat transfer in oscillating flow is a fundamental investigation field. Oscillation-induced heat transport processes maintain an effective heat enhancement comparable with heat pipes. It has many important applications in the compact heat exchangers, cooling processes of nuclear plants, design of Stirling heat machines and heat transport in internal combustion machines. There have been numerous theoretical, numerical and experimental studies on convection heat transfer in porous media and oscillatory flow, individually. Both fluid flow through porous medium and oscillatory flow inside a channel have an effect to enhance heat transfer, so that the investigators have been interested in oscillating flow inside porous medium in recent years.

Heat transfer formulation of porous media with continuum modeling based on a representative elementary volume was improved, and wide information can be found in the studies of Vafai (2005) (Authors referred to: Hsu, Nield and Kuznetsov, de Lemos), Kaviany (1995) and Nield and Bejan (2006).

Zhao and Cheng (1998) presented an extensive review of oscillatory duct flows including heat transfer characteristics. They introduced the similarity parameters of oscillating flow. Correlation equations for the space-cycle averaged Nusselt number in terms of A_o and Re_w have been obtained for oscillatory heat transfer in laminar and turbulent reciprocating internal flows.

Leong and Jin (2005) have investigated experimentally the heat transfer of the oscillating flow through a channel filled with aluminum foam subjected to a constant wall heat flux. They introduced a correlation equation for length averaged Nusselt number in term of A_o and Re_ω which was similar to that obtained by Zhao and Cheng for empty channels. They also pointed out that the length averaged Nusselt number for oscillating air flow in porous channel could be up to several times larger than that in empty channel.

Pamuk and Özdemir (2012) conducted heat transfer experiments using steel balls as porous media subjected to oscillating flow where flow medium is water as opposed to the previous studies that used gases. They obtained time and spaced averaged Nusselt numbers as the correlations of A_o Re_ω and Da valid to be a wide range of porous media. Experimental setup used in this study was the same as they used in the current study.

Byun et al. (2006) have investigated the transient behavior of porous media under oscillating flow condition. They presented an analytical characterization of the transient heat transfer in porous media under the oscillating flow condition in their work. They identified two important dimensionless parameters as the ratio of the thermal capacities between the solid and fluid phases and the ratio of the interstitial heat conductance between the phases to the fluid thermal capacity, based on a two-equation model. They obtained the analytic solutions for both the fluid and solid temperature variations, and they classified the heat transfer characteristics between phases into four regimes. They also suggested a criterion for the validity of the local thermal equilibrium in a simple form as the ratio of the two time scales. According this criterion set forth by the authors, the local thermal equilibrium can be achieved when the characteristic time of the porous media is much shorter than the time scale concerning the variation of the boundary condition ($t_p / t_o << 1$).

Dispersion is a complex phenomenon that the tortuosity within the pores cause. Tortuosity is the tendency that causes the fluid to move violently (circulations etc.) in a chatic manner due to the geometry of the porous medium. On the other hand thermal conductivities of both solid particles that constitute porous medium and the fluid decide the amount of heat transferred. An average, or weighted thermal conductivity to present both solid and fluid together which is the medium, is calculated using the porosity which is the volume fraction of the voids (or fluid displacing the voids) and the thermal conductivities of two separate phases. The total conduction heat transfer can be calculated by using the effective thermal conductivity that includes also the dispersion effect which is not easy to calculate since dispersion conductivity can be obtained empirically, or using the various correlations found in the literature. However, these correlations are all for steady flow and mostly for specific conditions. In this paper, we have intended to set forth a correlation for effective thermal conductivity for a porous medium of steel balls under oscillating flow. Following studies have been reviewed to cover literature consisting of stagnant thermal conductivity and dispersion thermal conductivity, thus effective thermal conductivity.

Kuznetsov (2000) investigated the effect of thermal dispersion on fully developed forced convection in a fluid-saturated porous-medium channel bounded by parallel plates. The author found that the effect of accounting for thermal dispersion strongly depends on the Darcy number. If $Da = 10^{-4}$, the effect of thermal dispersion on the Nusselt number becomes visible only for $Re_p > 10^{2.5}$. However, if $Da = 10^{-2}$, thermal dispersion has significant impact on the heat transfer already for $Re_p > 10^{0.5}$.

Hsieh and Lu (2000) performed a parametric study in their work regarding thermal conductivity within the porous media. Their results show that when the ratio of the thermal conductivity of the fluid to the solid increases, the Nusselt number distributions calculated from a one-equation model are getting closer to that from a two-equation model.

Özgümüş et al. (2011) have pointed out that the determination of transverse and axial thermal dispersion conductivities can be classified into three groups as a) Heat Addition/Removal at Lateral Boundaries, b) Uniform Temperature at Inlet Boundary, and c) Heat Addition Inside Bed. Generally, the procedure is almost the same for all these experimental approaches. A temperature gradient is generated in the bed. The temperature is measured at various locations in the packed bed. The equivalent thermal conductivity of the bed can be calculated by using thermal conductivity of fluid and solid and porosity. Thus, if one requires thermal dispersion conductivity, it can be found by subtracting of effective and equivalent thermal conductivities from each other.

Metzger et al. (2004) have found that excellent temperature residuals up to high Peclet numbers suggest that the one-temperature model may also be used in the case of local thermal nonequilibrium. Great attention was paid to the experimental estimation of a high number of parameters (dispersion coefficients, a velocity and six thermocouple positions): their estimated values do not only serve in a mathematical curve fitting exercise but also have to yield physically reasonable and intrinsic values. Three different experimental geometries could confirm the results for k_z.

Nield (1991) has stated that the medium's thermal conductivity can be taken as the geometric average of the thermal conductivities of fluid and solid which falls between those of the serial and parallel approaches, provided thermal conductivities of both phase are not too different from each other.

Yang and Nakayama (2010) have utilized a volume averaging theory to evaluate both stagnant thermal conductivity and thermal dispersion conductivity within porous media. For the stagnant thermal conductivity, a general unit cell model, consisting of rectangular solids with connecting arms in an in-line arrangement, was proposed to describe most homogeneous porous media. The resulting expression for the stagnant thermal

conductivity has been validated by comparing the present results with available experimental and theoretical data for packed beds, porous foams and wire screens. As for the thermal dispersion conductivity, a general expression has been derived with help of the two energy equations for solid and fluid phases. It has been revealed that the interfacial heat transfer at the local non-thermal equilibrium controls the spatial distribution of the macroscopic temperature and thus the thermal dispersion activities. The resulting expressions for the longitudinal and transverse thermal dispersion conductivities agree well with available experimental data and empirical correlations.

Experimental Setup

A schematic diagram of the experimental setup is shown in Figure 1. It is made up of a test section (porous medium) which is a stainless steel (AISI 304) pipe with 51.4 mm of inner diameter, 5 mm of wall thickness and 305 mm of length, 2 polyethylene pipes mounted at the each side of the test section where pressure values are collected via gauges and sensors installed in the taps drilled in them, 2 conical reduction fittings to reduce to 32 mm diameter, 2 concentric heat exchangers to absorb the heat applied on the outer surface of the test section, Keithley 2700 data acquisition system and a computer to analyze the collected data, an oscillation generator which consists of is a double-acting cylinder connected to an electrically driven moto-reductor by means of a flywheel and a crank-arm and some other components.

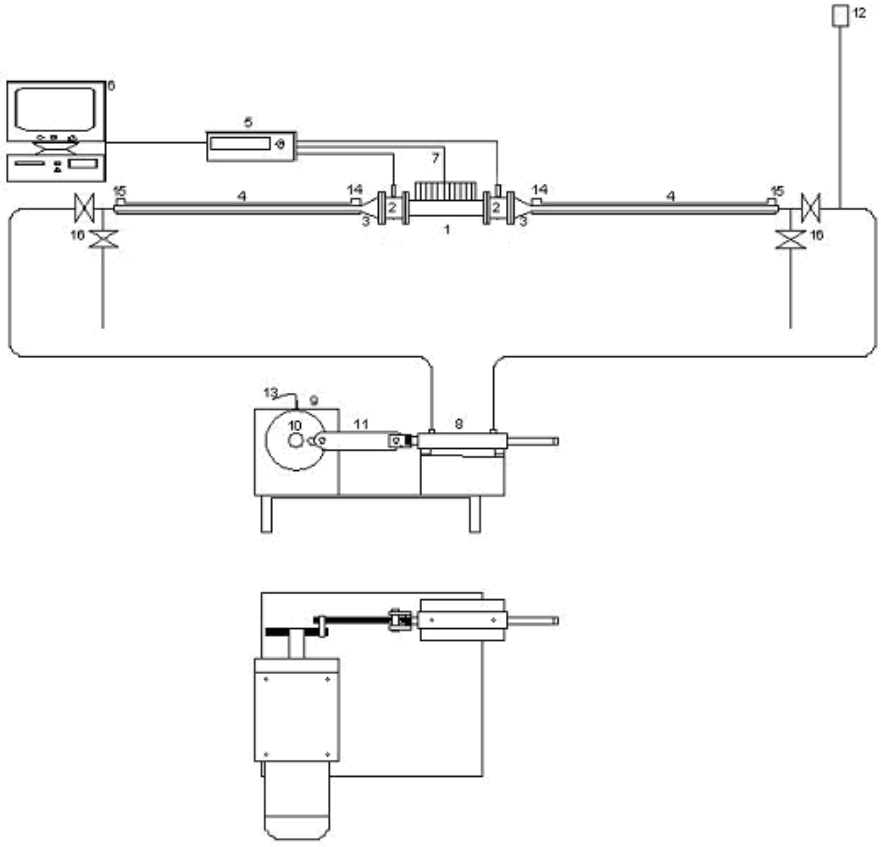

Figure 1 : Experimental Setup :1. Test Section (Porous Medium), 2. PE Pipe, 3. Reduction 4. Concentric Heat Exchanger 5. Keithley 2700, 6. PC 7. Signal Wiring 8. Oscillation Generator, 9. Motoreductor, 10. Flywheel, 11. Crank Arm, 12. Air Purger 13. Inductive Proximity Sensor 14. and 15. Connections to Circulator, 16. Separating Valves.

A custom-made temperature probe shown in Figure 2 is installed at the center of the test section. This probe contains three thermocouples to measure the temperatures at the channel axis (*D/2*) and halfway between the axis and the channel wall (*D/4*). All thermocouples are K-type (Ni-Cr/Ni-Al). Thermocouples attached on the surface and embedded in the pipe wall are utilized to estimate the wall temperature at the water side using Fourier law. Temperature data collected have been time averaged over the number of cycles each set of experiment was conducted. Thus, all the calculations have been performed using these time averaged temperature values.

A more detailed explanation of this experimental setup that also contains in-depth information regarding thermocouple allocations, energy supplying method and heat insulation can be found in the study of Pamuk and Özdemir. Heat inputs throughout this study are shown to be net amounts.

Water is used in this study as the working fluid unlike the majority of the experimental studies in literature. The compressibility of water is considerably affected due to air content, thus the flow rates of half cycles are different which drastically effects the symmetry of heat transfer. In order to overcome this problem a procedure to remove the air from the system is explained in detail in the study of Pamuk and Özdemir.

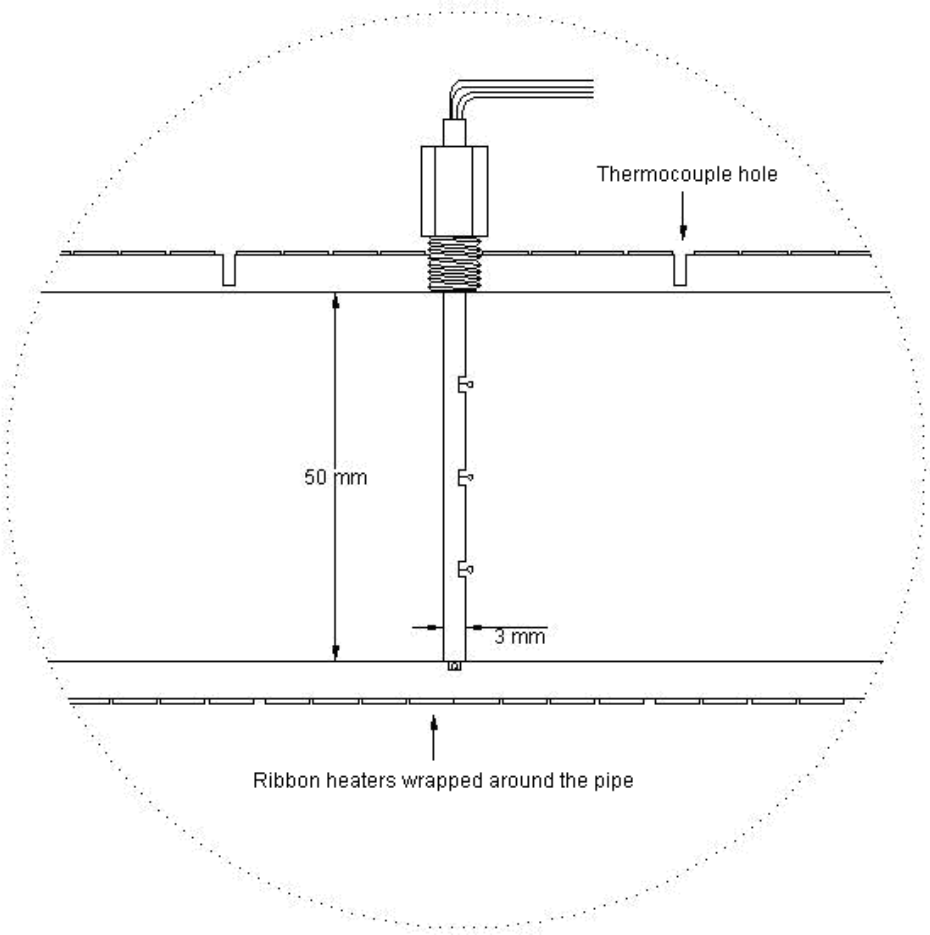

Figure 2 : Temperature probe.

Uncertainty analysis

Uncertainty in the experimental data is considered by identifying the main sources of errors in the primary measurements such as power supplied, dimensions of the test chamber and balls, volume, time and frequency. Then, an uncertainty analysis based on the method described by Figliola and Beasley (2006) is performed. The uncertainties of dimensions, power, temperature, and effective thermal conductivity are estimated to be 1.95%, 1.90%, 2.35%, and 3.58% respectively.

Results and Discussion

Heat transfer experiments for estimating the thermal dispersion conductivity in a porous medium subjected to oscillating flow have been conducted at three different power inputs q, by changing piston stroke, x_{pmax} and frequency output of A/C drive n for both porous media. This way 27 sets of experiments have been conducted. Rotational speed of moto-reductor at 50 Hz line frequency is nominally 70 rpm. Thus rotational speed and corresponding frequency are calculated by $N=(70/50)n$ and $f=N/60$ respectively for a given drive frequency n. Angular frequency is $\omega = 2\pi f$. Actual rotational speed of the moto-reductor determined is to be 69.9 rpm using fft. The displacement of the piston is taken as zero at the rear position inside the cylinder and it becomes a

maximum which is equal to the diameter of the flywheel at the forward position. The piston displacement will be equal to the fluid displacement due to the fact that the fluid is incompressible. Hence, at the entrance of the porous medium, the fluid displacement *xm* varies according to

$$x_m(t) = \frac{x_{\max}}{2}(1 - Cos\,\omega t) \tag{1}$$

where $x_{\max} = x_{p\max} A_p / A = 2RA_p / A$. Here, *R*, A_p and *A* are flywheel radius, cross sectional areas of double acting cylinder and test chamber, respectively. The cross-sectional mean fluid velocity in the channel is

$$u_m(t) = u_{\max} Sin\,\omega t \tag{2}$$

where $u_{\max} = \omega x_{\max} / 2$.

An inportant issue regarding the temperatures is whether solid and fluid temperatures can be taken equal which denotes the condition "Local thermal equilibrium (LTE)". The criterion set forth by Byun et al. [10] has been applied to find it out. It was found that for both medium, the value $t_p / t_o << 1$ for all conditions that guarantees that LTE exists. Thus, thermocouples at any given location read an average temperature of solid and fluid which are practically equal.
Temporal energy balance on the heated surface at time t can be written as follows:

$$\frac{q}{\pi DL} = q'' = (k_o + k_d)\frac{\partial T(t, r_o, z)}{\partial r} = h\left[T_w(t,z) - T_m(t,z)\right] \tag{3}$$

Here, dispersion coefficient and temporal heat convection coefficient are dependent on mean flow velocity. On the other hand, mean flow velocity varies harmonically with time. Heat balance on the surface can then be re-written using time averaged temperatures as follows:

$$q'' = (k_o + \bar{k}_d)\frac{\partial \bar{T}(r_o, z)}{\partial r} = \bar{h}(z)\left[\bar{T}_w(z) - \bar{T}_m(z)\right] = \text{constant} \tag{4}$$

Radial temperature data read out at the center of the porous channel where *z=L/2*, is utilized in estimating the radial temperature gradient $(\Delta T/\Delta r)$ and effective conductivity of the medium (k_e) by utilizing by applying Equation 4 in the form $q'' = -k_e(\Delta T/\Delta r)$. Temperatures used for calculating the radial temperature gradients are measured at wall and half the radius ($r_o/2$). The temperature measured at half the radius (12.85 mm from the wall) is within the channel region which is 5-6 ball diameter wide (17 mm). This facilitates the gradient equation of $\Delta T/\Delta r = \left[\bar{T}_w - \bar{T}_f(r_o/2)\right]/(r_o/2)$ to be used in calculations. Channel region where the highest flow velocity is attained has a higher porosity value than the average porosity of the medium. All the temperature data collected are in the vicinity of 43 ^{o}C. Therefore, considering Prandtl number is invariant within a small temperature change, kinetic Reynolds number, Re_ω together with non-dimensional fluid displacement, A_o have been used for calculations of effective thermal conductivity in order to account for fluid displacement and oscillation frequency, rather than Peclet number. Temperature data along with other parameters have been given in Table 1. Time averaging for temperature data has been made for 60 cycles. Space averaged Nusselt numbers are within the margin of 66-140. All these details and the way the experiments conducted have been explained in detail in the study of Pamuk and Özdemir.

Table 1 : Temperature data and other parameters.

n, Hz	*L=mm*	A_o	Re_ω	*q'', W/m²*	T_w	$T_f(r_o/2)$	$\Delta T/\Delta r$	k_e	k_e/k_f
5	130	1,413	1937	6.091	45,82	41,02	383,8	15,87	25,89
5	130	1,413	1937	8.122	51,99	42,81	734,5	11,06	18,04
5	130	1,413	1937	10.152	61,69	49,94	939,9	10,80	17,62
10	130	1,413	3873	6.091	43,15	37,69	437,0	13,94	22,74
10	130	1,413	3873	8.122	48,18	40,46	617,6	13,15	21,45
10	130	1,413	3873	10.152	53,18	45,04	651,5	15,58	25,42

15	130	1,413	5810	6.091	41,53	37,38	332,3	18,33	29,90
15	130	1,413	5810	8.122	45,17	39,74	435,0	18,67	30,46
15	130	1,413	5810	10.152	52,19	44,22	637,7	15,92	25,97
5	170	1,848	1937	6.091	45,10	39,46	451,3	13,50	22,02
5	170	1,848	1937	8.122	48,55	42,33	497,0	16,34	26,66
5	170	1,848	1937	10.152	54,64	46,36	662,3	15,33	25,01
10	170	1,848	3873	6.091	40,94	36,41	362,6	16,80	27,41
10	170	1,848	3873	8.122	43,74	38,85	391,8	20,73	33,82
10	170	1,848	3873	10.152	46,62	41,06	445,2	22,80	37,20
15	170	1,848	5810	6.091	38,98	35,75	258,4	23,57	38,45
15	170	1,848	5810	8.122	42,07	37,79	342,8	23,69	38,65
15	170	1,848	5810	10.152	45,45	39,57	469,8	21,61	35,25
5	195	2,119	1937	6.091	44,40	37,96	515,4	11,82	19,28
5	195	2,119	1937	8.122	47,12	39,90	576,9	14,08	22,97
5	195	2,119	1937	10.152	51,57	43,66	632,3	16,06	26,19
10	195	2,119	3873	6.091	37,54	34,37	253,6	24,02	39,19
10	195	2,119	3873	8.122	42,23	36,70	442,4	18,36	29,95
10	195	2,119	3873	10.152	46,22	38,49	618,2	16,42	26,79
15	195	2,119	5810	6.091	38,41	33,92	359,4	16,95	27,65
15	195	2,119	5810	8.122	40,92	36,04	390,7	20,79	33,91
15	195	2,119	5810	10.152	43,85	37,30	524,4	19,36	31,58

Figure 3 shows the variation of k_e/k_f with respect to A_oRe_ω, employing the equation $q'' = -k_e(\Delta T/\Delta r)$ where $k_e=k_d+k_o$. Using a linear curve fitting procedure, one obtains a correlation of k_e/k_f with A_oRe_ω. This correlation is in the form of $k_e/k_f = k_o/k_f + C\,(A_oRe_\omega)$ as defined by Yang and Nakayama where Peclet number is employed alternatively. By looking at the correlation carefully, it can be seen that k_o/k_f=18.072, or in other words k_o=11.078 W/m-^{o}C for no flow condition (Eq. 5). This value is very close to paralel model (~10.5 W/m-^{o}C) as given in Nield and Bejan. Therefore it is concluded that parallel model can be employed for estimating the stagnant thermal conductivity (k_o) of the porous medium under oscillating flow. Similarly, the second term in the correlation is $k_d/k_f=0.00145(A_oRe_\omega)$. Aside from a linear correlation, a non-linear curve fitting has been employed to see if data can be better represented (Eq. 6).

$$k_e/k_f = 18.072 + 0.00145(Re_\omega A_o) \tag{5}$$

$$k_e/k_f = -43.7 + 22.322(Re_\omega A_o)^{0.134} \tag{6}$$

However, as can be seen in Fig. 3, both linear and non-linear correlations has the same output for the margin experiments have been conducted. Therefore, for practical purposes, linear model has been adopted as the primary correlation for estimating the effective thermal conductivity in a porous medium of stainless steel balls of 3 mm in diameter under oscillating flow where flow medium is water. Both correlations are valid within the values shown in Table 1.

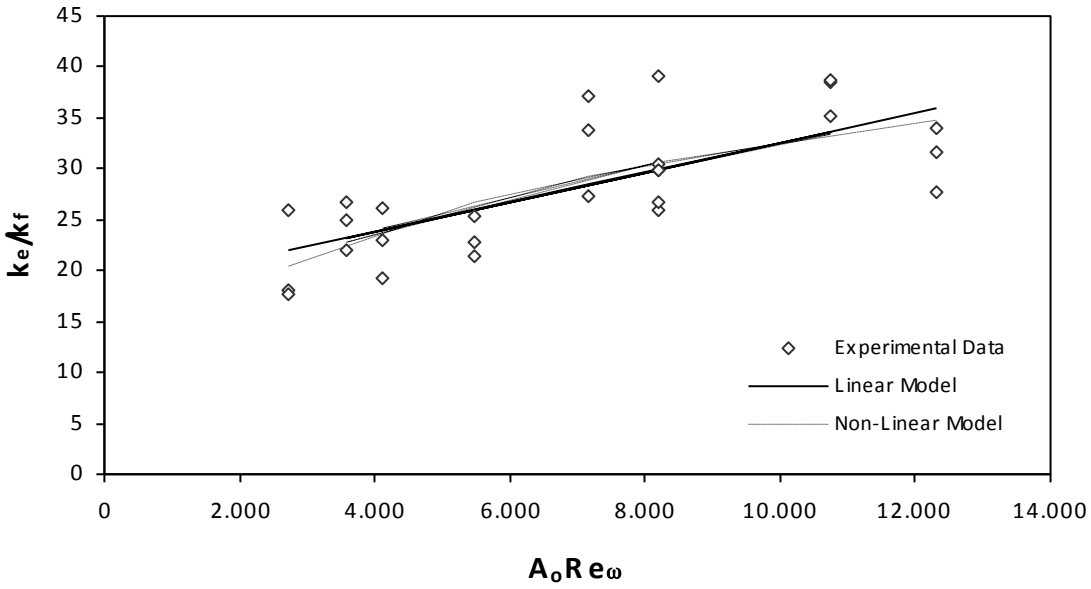

Figure 3 : Variation of effective thermal conductivity vs. A_oRe_ω.

Conclusion

In this experimental study, heat transfer in oscillating flow through porous medium of 3 mm steel balls has been studied. It is shown that the stagnant and dispersion thermal conductivities, thus the effective thermal conductivity of a porous medium of stainless steel balls 3 mm in diameter subjected to oscillating flow can be shown as a linear correlation of A_oRe_ω in the form of $k_e/k_f = C\,(A_oRe_\omega) + k_o/k_f$.

Acknowledgements

We would like to express our thanks to Istanbul Technical University whose financial support and granting access to its laboratory facilities made it possible to realize this project.

Nomenclature

A	cross-sectional area of the test chamber
A_p	cross-sectional area of double acting cylinder
A_o	non-dimensional displacement defined as $A_o = x_{max}/D$
d	ball diameter
D	inner diameter of the test chamber
Da	Darcy number (K/D^2)
h	heat transfer coefficient
K	permeability
k	conduction coefficient
k_d	dispersion conduction coefficient
k_e	effective conduction coefficient
L	length of the porous medium
n	frequency output of A/C drive (1/s, Hz)
N	rotational speed of moto-reductor (rpm)
$Nu(z)$	local Nusselt number
Nu_L	space-cycle averaged Nusselt number
q	joule heating obtained from ribbon heaters (IV Watt)
q''	heat flux at the wall (W/m^2)
r	radial distance from the centerline the test chamber
r_o	radius of the test chamber ($D/2$)

R	radius of flywheel
Re_d	particule based Reynolds Number ($\rho u_m d/\mu$)
Re_ω	kinetic Reynolds Number ($\rho\omega D^2/\mu$)
t	time
t_o	time scale of the variation of the flow or thermal boundary condition
t_p	time scale concerning the thermal inertia of the porous media
$T(t,r,z)$	temperature at radial location r, axial location z at time t
u_m	cross-sectional mean fluid velocity
u_{max}	amplitude of mean fluid velocity
x_p	maximum displacement of the piston (stroke)
x_m	temporal fluid displacement at the inlet of the test chamber
x_{max}	maximum fluid displacement at the inlet of the test chamber

Greek Symbols:

α	heat diffusion coefficient
ρ	density
ω	angular frequency
ν	kinematic viscosity
μ	dynamic viscosity

Subscripts:

f	fluid
m	medium
max	maximum
p	piston
s	solid
w	wall
z	longitudinal direction

References

Byun, S.Y., Ro, S.T., Shin , J.Y., Son, Y.S., Lee, D.-Y. (2006). Transient thermal behavior of porous media under oscillating flow condition, International Journal of Heat and Mass Transfer 49, 5081–5085.

Figliola, Richard S., Beasley, Donald E. (2006). Theory and Design for Mechanical Measurements, John Wiley.

Hsieh, W.H., Lu, S.F. (2000). Heat-transfer analysis and thermal dispersion in thermally-developing region of a sintered porous metal channel, International Journal of Heat and Mass Transfer 43, 3001-3011.

Kaviany, Massoud (1995). Principles of Heat Transfer in Porous Media, Springer.

Kuznetsov, A.V. (2000). Investigation of the effect of transverse thermal dispersion on forced convection in porous media, Acta Mechanica 145, 35-43.

Leong, K.C., Jin, L.W. (2005). An Experimental Study of Heat Transfer in Oscillating Flow Through a Channel Filled Fith Aluminum Foam, International Journal of Heat and Mass Transfer 48, 243-253.

Metzger, T., Didierjean, S., Maillet, D. (2004). Optimal experimental estimation of thermal dispersion coefficients in porous media, International Journal of Heat and Mass Transfer 47, 3341–3353

Nield, Donald A., Bejan, Adrian (2006). Convection in Porous Media, ISBN-3-540-97651-5- Springer-Verlag.

Nield, D. A. (1991). Estimation of the stagnant thermal conductivity of saturated porous media, International Journal of Heat and Mass Transfer Volume 34, Issue 6, June 1991, Pages 1575-1576.

Özgümüş, T., Mobedi1, M., Özkol, Ü., Nakayama, A. (2011). Thermal Dispersion in Porous Media – A Review on Approaches in Experimental Studies, 6th International Advanced Technologies Symposium (IATS'11), 16-18 May 2011, Elazığ, Turkey.

Pamuk, M.T., Özdemir, M. (2012). Heat Transfer in Porous Media of Steel Balls Under Oscillating Flow, Experimental Thermal and Fluid Science, Elsevier (doi:10.1016/j.expthermflusci.2012.04.015).

Vafai, Kambiz (2005). Handbook of Porous Media, Second Edition, CRC Press Taylor & Francis Group.

Yang , C., Nakayama, A. (2010). A synthesis of tortuosity and dispersion in effective thermal conductivity of porous media, International Journal of Heat and Mass Transfer 53, 3222–3230.

Zhao, T.S., Cheng, P. (1998). Heat Transfer In Oscillatory Flows, Annual Review of Heat Transfer, Volume IX.

Comparison of discrete simulation models' results in evaluating the performances of *M/G/C/C* networks

Noraida A. Ghani[1], Mohd. Kamal Mohd. Nawawi[3], Ruzelan Khalid[3]
Luthful A. Kawsar[1, 4], Anton A. Kamil[1], Adli Mustafa[2]

[1]School of Distance Education, Universiti Sains Malaysia, 11800 Penang, Malaysia
[2]School of Mathematical Sciences, Universiti Sains Malaysia, 11800 Penang, Malaysia
[3]School of Quantitative Sciences, Universiti Utara Malaysia, 06010 UUM Sintok, Kedah
[4]Department of Statistics, School of Physical Sciences, Shahjalal University of Science and Technology, Sylhet-3114, Bangladesh

noraida@usm.my, mdkamal@uum.edu.my, ruzelan@uum.edu.my, lakawsar@yahoo.com, anton@usm.my, adli@cs.usm.my

Abstract: An *M/G/C/C* queuing network is a useful tool for modeling entity congestion. However, since its service rates is dependent on the number of entities (e.g. pedestrians, vehicles, etc.) in its system, direct modeling of such dynamic rates is difficult to be implemented in any modern Discrete Simulation System (DES) software. We designed an approach to cater this constraint and implemented it in Arena software to evaluate various performances of the *M/G/C/C* network. Using the models, we have compared their results with analytical results and the results of Cruz, Smith and Medeiros (2005)'s simulation models on the impacts of various arrival rates to the throughput, the blocking probability, the expected service time and the expected number of entities in a single and complex network topologies. Results indicated that there are very small discrepancies between the two DES models. Detail results on how close our simulation results and theirs have been documented and discussed.

Key words: Discrete-event simulation, *M/G/C/C* queuing systems, finite capacity, state dependent.

Introduction

M/G/C/C state dependent queuing networks are useful tools for modeling congestion systems, e.g. pedestrians in a corridor, vehicles on a road, etc. The mathematical background of the systems' behaviors and computation of their common performance measures, etc. have been discussed in details in other papers (e.g. Cruz et al., 2005; Mitchell & MacGregor Smith, 2001; Smith, 2012; Smith & Kerbache, 2012). However, since the systems treat service rates as a function of the number of their residing entities, modeling this condition is difficult in any modern Discrete Event Simulation (DES) software, .e.g. Arena (Altiok & Melamed, 2007; Kelton, 2009; Rossetti, 2010).

Cruz, Smith and Medeiros (2005) designed and constructed an *M/G/C/C* simulation model using C++ (Garrido, 1998; Prata, 2011; Watkins, 1994). The model's essential data structures, algorithms, library structures, etc. have been presented and discussed to support both the basic DES structures (Banks, Carson, Nelson, & Nicol, 2010; Wainer & Mosterman, 2010) and to cater service rates of an *M/G/C/C* network. However, its extension to support more complex or customized congestion models is probably difficult especially for model builders that do not have good experiences in programming; and this may limit its use in modeling congestion systems.

We otherwise used Arena to model *M/G/C/C* networks since it provides many DES facilities (e.g. various simulation modules, animation, statistical instrumentation and reports, etc.). However, since it does not support dynamic updating of servers' service times, we have to design a relevant modeling approach. Thus, this paper presents an approach to handle the problem and discusses how it can be implemented in Arena. Using the models, we then compare their outputs with analytical results and the results of Cruz, Smith and Medeiros's simulation models and document the findings.

We organized this paper as follows. The next Section briefly discusses the main limitation of commercial simulation software in modeling *M/G/C/C* networks and presents ideas how this limitation can be tackled. Further, we focus on the modeling of the networks using modules available in Arena software. In the following section we compare and discuss our simulation results with analytical results and the results of Cruz, Smith and Medeiros's simulation models on a single network and selected topological networks. Finally, the last section summarizes the findings and concludes the paper.

Materials and Method

Designing an *M/G/C/C* Simulation Engine

The essence of *M/G/C/C* state dependent queuing networks is that their service rates are controlled by the number of their current residing entities. Since updating a server's service time is not permitted in the current DES software, we can alternatively use a queue with a relevant buffer size that represents the maximum number of entities in a system and measure the time spent by them in the queue. Any *arrival* or *departure* event to the queue will update all entities' time spent and consequently update their remaining times to leave the queue (that is the remaining distance to cross the space).

To implement this logic, simulation software must have modules for retrieving entities from a queue so that their remaining times can be updated and modules for delaying their delay times so that they can be released whenever their remaining times become zero. Using this logic, the performances of the network can be measured using the relationships listed in Table 1.

Table 1: Model's Variables

$p(c)$ = sumBlockedPedestrians / sumArrivalPedestrians
Θ = sumDepartedPedestrians / simulationLength
L = sumTimeSpentInCorridorbyAllPedestrians / simulationLength
W = sumTimeSpentInCorridorbyAllPedestrians / sumDeparture

Arena as an Implementation Tool

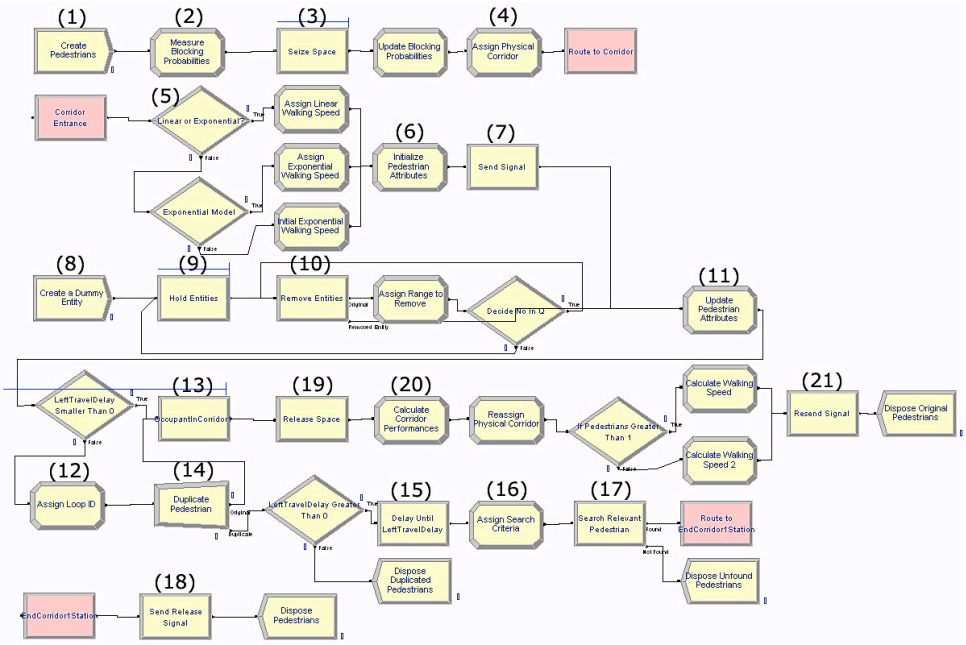

Figure 1: Arena Model for a Single *M/G/C/C* Network

Figure 1 shows our Arena model for a single *M/G/C/C* network. The model starts with the *Create* module (1) to generate a number of entities based on a certain λ arrival rate. We also have to create a dummy entity (the *Create* module (8)) to iteratively activate a mechanism to remove entities from their queue and update their current states. In the *Assign* module (2), we store the number of entering and blocking entities for calculating the network's blocking probability and declare their identification numbers (IDs) for later use in the model.

The *Seize* module (3) allocates a unit of available servers to the entity. If all available units are busy, the entity will automatically be queued until the unit is available to be seized. The *Assign* module (4) defines variables relating to the network that is its area, its capacity and its number of residing entities. These variables are used to calculate the entities' current travel speed. Since there are two mathematical models for modeling the speed (that is linear and exponential models), the *Decide* module (5) offers the option.

The *Assign* module (6) initializes entities' entrance time and current travel distance. Simultaneously, the *Signal* module (7) sends a signal (indicating an arrival event) to force the *Hold* module (9) (that is a type of queue that releases its queued entities when receiving a signal or satisfying a condition) to release the dummy entity and then activate the *Remove* module (10). The *Remove* module then removes entities from their queue (the *Queue* module (13)) to update (the *Assign* module (11)) their current travel distance, their remaining time to exit the corridor and the time points that these events happen. This time will later be used for calculating the entities' new states. We need to update (the *Assign* module (12)) their current number of state changes (loop IDs) to be used later as a search criterion in the model. The dummy entity then flows back to the *Hold* module (9) and waits for the next signal.

The entities cannot calculate their remaining times to stay while in queue. Thus, they have to be duplicated using the *Separate* module (14). The original entities flow back to their queue after updating their states, while their clones perform delay time using the *Delay* module (15). The clones later enter the *Assign* module (16) where the values of their IDs and loop IDs are assigned to new variables and used as a search criteria (accomplished by the *Search* module (17)) to match their original entities that satisfy both values.

The result of the search is either true (found) or false (not found). If the original entity is not found, the clone entity will instantly be destroyed. Else, it will send a signal (the *Signal* module (18)) to the *Hold* module (13) that will release the satisfying entity from its queue and then release (the *Release* module (19)) the network's space. Before destroyed, the entity measures the performances of the network using the *Assign* module (20) and sends a signal (the *Signal* module (21)) to the *Hold* module (13) to force all other entities to update their new states.

The basic model can easily be extended to support *series*, *splitting* and *merging* topologies. The trick is to provide relevant logics to flow entities from corridor to corridor. First, we have to create a unique queue for each corridor so that we can store its residing pedestrians and update them accordingly whenever there is an arrival or a departure event. Second, we have to attach an attribute to the entities (e.g. *toCorridor* that will take their next corridor number) so that we can travel them correctly from corridor to corridor. The value of the attribute must be updated once a relevant pedestrian exits its current corridor and used throughout the model to support the logical statements of the model, e.g. when we want to remove or search relevant entities in their queues. Third, we have to create and send a unique signal number every time the entity enters/exits their network to enable us to update their current states in the network.

Results and Discussion

All results of our simulation models were run for 20000 seconds and 30 replications. The results for a single node's performance measures are presented in Table 2 and Table 3. Table 2 displays results for a corridor 8 meters long and 2.5 meters wide under various arrival rates while Table 3 reports results for a corridor 8 meters long with different width and arrival rates. Note that Simulation[a] denotes Cruz, Smith and Medeiros (2005)'s simulation model while Simulation[b] denotes our simulation model. λ, *p(c)*, *Θ, L* and *W* respectively represent arrival rate, throughput, blocking probability, the expected service time and the expected number of entities of the network.

From Table 2, we can clearly observe that the increase of arrival rates will increase the blocking probabilities, and thus decrease the throughput. Both models display almost the same results unless for λ = 2.7 ped/s where our simulation model reports higher blocking probability compared to the analytical result and the result of Cruz, Smith and Medeiros (2005)'s simulation model. Table 3 also reports almost similar simulation results unless for a corridor width 4.5 meters with λ = 5 ped/s. In this case, our model reports lower blocking probability and this value is close

to the analytical result with 0.00 blocking probability.

Table 2: Single Node Performance Measures Versus Arrival Rate

λ	Model	*p(c)*	*Θ*	*L*	*W*
1.0	**Analytical**	0.00	1.00	6.02	6.02
	Simulation[a]	0.00 [0.00, 0.00]	1.00 [1.00, 1.00]	6.02 [5.99, 6.02]	6.02 [6.02, 6.02]
	Simulation[b]	0.00 [0.00, 0.00]	1.00 [1.00, 1.00]	6.02 [6.02, 6.04]	6.02 [6.02, 6.02]
2.0	**Analytical**	0.00	2.00	14.49	7.24
	Simulation[a]	0.00 [0.00, 0.00]	2.00 [1.99, 2.00]	14.46 [14.42,14.49]	7.24 [7.23, 7.25]
	Simulation[b]	0.00 [0.00, 0.00]	2.00 [1.99, 2.00]	14.46 [14.43,14.49]	7.24 [7.23, 7.25]
2.7	**Analytical**	0.01	2.66	29.90	10.98
	Simulation[a]	0.01 [0.00, 0.02]	2.67 [2.65, 2.68]	27.91 [26.28,29.55]	10.49 [9.81, 11.18]
	Simulation[b]	0.06 [0.03, 0.10]	2.53 [2.43, 2.62]	41.59 [32.29,50.89]	17.76 [12.76,22.75]
3.0	**Analytical**	0.33	2.01	96.96	48.31
	Simulation[a]	0.32 [0.32, 0.33]	2.03 [2.02, 2.04]	95.21 [94.52,95.90]	46.95 [46.37,47.53]
	Simulation[b]	0.34 [0.34, 0.35]	1.97 [1.96, 1.98]	97.44 [96.75,98.14]	49.57 [48.96,50.19]
4.0	**Analytical**	0.51	1.96	99.01	50.53
	Simulation[a]	0.51 [0.51, 0.51]	1.96 [1.96, 1.96]	98.77 [98.75,98.79]	50.43 [50.41,50.45]
	Simulation[b]	0.52 [0.52, 0.52]	1.93 [1.93, 1.93]	99.76 [99.75,99.77]	51.66 [51.65,51.67]

Table 3: Single Node Performance Measures Versus Width

λ	Width	Model	*p(c)*	*Θ*	*L*	*W*
2.5	**1.0**	**Analytical**	0.68	0.79	39.53	50.02
		Simulation[a]	0.68 [0.68, 0.68]	0.79 [0.79, 0.79]	39.46 [39.45, 39.46]	49.98 [49.96, 49.99]
		Simulation[b]	0.69 [0.69, 0.69]	0.78 [0.78, 0.78]	39.93 [39.93, 39.93]	51.42 [51.42, 51.43]
	1.5	**Analytical**	0.52	1.19	59.05	49.69
		Simulation[a]	0.52 [0.52, 0.52]	1.19 [1.19, 1.19]	58.91 [58.90,58.93]	49.59 [49.57, 49.61]
		Simulation[b]	0.53 [0.53, 0.54]	1.16 [1.16, 1.16]	59.87 [59.06, 59.87]	51.55 [51.54, 51.56]
	2.0	**Analytical**	0.36	1.61	77.71	48.32
		Simulation[a]	0.35 [0.35, 0.35]	1.62 [1.61, 1.62]	76.87 [76.63, 77.11]	47.50 [47.23, 47.76]
		Simulation[b]	0.38 [0.37, 0.38]	1.55 [1.55, 1.56]	79.28 [79.10, 79.45]	50.99 [50.79, 51.18]
	2.5	**Analytical**	0.00	2.50	21.07	8.43
		Simulation[a]	0.00 [0.00, 0.00]	2.50 [2.49, 2.50]	21.00 [20.94, 21.06]	8.41 [8.40, 8.43]
		Simulation[b]	0.00 [0.00, 0.00]	2.49 [2.47, 2.51]	22.71 [19.41, 26.01]	9.23 [7.60, 10.85]
	3.0	**Analytical**	0.00	2.50	18.39	7.36
		Simulation[a]	0.00 [0.00, 0.00]	2.50 [2.49, 2.50]	18.35 [18.31, 18.39]	7.35 [7.34, 7.36]

		Simulation[b]	0.00 [0.00, 0.00]	2.50 [2.49, 2.50]	18.38 [18.33, 18.44]	7.36 [7.35, 7.36]
5.0	**2.0**	**Analytical**	0.69	1.56	79.54	51.00
		Simulation[a]	0.69 [0.69, 0.69]	1.56 [1.56, 1.56]	79.40 [79.39, 79.40]	50.95 [50.95, 50.96]
		Simulation[b]	0.69 [0.69, 0.69]	1.55 [1.55, 1.55]	79.86 [79.85, 79.86]	51.67 [51.67, 51.67]
	3.0	**Analytical**	0.53	2.34	119.10	50.86
		Simulation[a]	0.53 [0.53, 0.53]	2.34 [2.34, 2.34]	118.83 [118.81, 118.84]	50.76 [50.75, 50.77]
		Simulation[b]	0.54 [0.54, 0.54]	2.32 [2.32, 2.32]	119.72 [119.72, 119.73]	51.70 [51.69, 51.71]
	4.0	**Analytical**	0.37	3.14	158.24	50.46
		Simulation[a]	0.37 [0.37, 0.37]	3.17 [3.16, 3.17]	156.04 [155.55, 156.53]	49.29 [49.01, 49.57]
		Simulation[b]	0.38 [0.37, 0.38]	3.12 [3.11, 3.13]	157.91 [157.35, 158.47]	50.69 [50.36, 51.03]
	4.5	**Analytical**	0.11	4.45	95.66	21.49
		Simulation[a]	0.00 [0.00, 0.00]	4.99 [4.97, 5.00]	46.80 [45.54, 48.05]	9.39 [9.10, 9.68]
		Simulation[b]	0.04 [0.00, 0.07]	4.99 [4.99, 5.00]	61.67 [48.36, 74.98]	13.66 [9.70, 17.62]
	5.0	**Analytical**	0.00	5.00	40.94	8.19
		Simulation[a]	0.00 [0.00, 0.00]	5.00 [4.99, 5.00]	40.88 [40.80, 40.96]	8.18 [8.18, 8.19]
		Simulation[b]	0.00 [0.00, 0.00]	0.00 [0.00, 0.00]	40.88 [40.80, 40.96]	8.18 [8.18, 8.19]

Table 4, Table 5 and Table 6 respectively report the results for series, splitting and merging network topologies. For both series and splitting topologies, our model measures higher blocking probabilities for the first node compared to analytical and Cruz, Smith and Medeiros (2005)'s results. As a result, our model reports slightly lower throughputs for other consequence nodes. For the merging corridor, our model shows totally different blocking probability that is 0.01 compared to 0.51 (analytical result) and 0.50 (Cruz, Smith and Medeiros (2005)'s result). We believe that our model reports the right blocking probability if we follow the mathematical equation for measuring the throughput that is $\Theta=\lambda(1-p(c))$.

Table 4: Results for 3-Node Series Topology (λ = 3.0)

Measure	**Node 1**		**Node 2**		**Node 3**	
	Analytical	**Simulation[a], Simulation[b]**	**Analytical**	**Simulation[a], Simulation[b]**	**Analytical**	**Simulation[a], Simulation[b]**
p(c)	0.33	0.33 [0.32, 0.33]	0.00	0.01 [0.00, 0.01]	0.00	0.01 [0.00, 0.03]
		0.35 [0.34, 0.35]		0.00 [0.00, 0.00]		0.00 [0.00, 0.00]
Θ	2.01	2.02 [2.01, 2.03]	2.01	2.02 [2.01, 2.02]	2.01	2.02 [2.01, 2.02]
		1.96 [1.95, 1.96]		1.96 [1.95, 1.96]		1.96 [1.95, 1.96]
L	96.96	95.87 [95.35, 96.40]	14.56	16.44 [15.00, 17.88]	16.51	16.51 [15.23, 17.79]
		98.10 [97.61, 98.59]		[14.16, 14.52]		14.33 [14.15, 14.52]
W	48.31	47.53 [47.10, 47.96]	7.26	8.15 [7.44, 8.86]	8.19	8.19 [7.56, 8.81]

		50.16 [49.73, 50.59]		7.33 [7.26, 7.41]		7.33 [7.26, 7.11]

Table 5: Results for 3-Node Split Topology ($\lambda = 3.0$)

Measure	Node 1		Node 2		Node 3	
	Analytical	Simulation[a], Simulation[b]	Analytical	Simulation[a], Simulation[b]	Analytical	Simulation[a], Simulation[b]
p(c)	0.33	0.32 [0.32, 0.33]	0.00	0.00 [0.00, 0.00]	0.00	0.00 [0.00, 0.00]
		0.35 [0.34, 0.35]		0.00 [0.00, 0.00]		0.00 [0.00, 0.00]
Θ	2.01	2.03 [2.02, 2.04]	1.20	1.22 [1.21, 1.23]	0.80	0.81 [0.81, 0.82]
		1.96 [1.95, 1.97]		1.18 [1.17, 1.18]		0.78 [0.78, 0.79]
L	96.96	95.04 [94.23, 95.84]	7.48	7.61 [7.55, 7.67]	4.70	4.76 [4.73, 4.80]
		98.04 [97.38,98.71]		7.30 [7.24, 7.36]		4.58 [4.54, 4.61]
W	48.31	46.82 [46.16, 47.49]	6.21	6.24 [6.23, 6.26]	5.86	5.87 [5.86, 5.88]
		50.12 [49.54, 50.70]		6.21 [6.19, 6.23]		5.85 [5.84, 5.85]

Table 6: Results for 3-Node Merge Topology ($\lambda = \lambda_2 = 3.0$)

Measure	Node 1		Node 2		Node 3	
	Analytical	Simulation[a], Simulation[b]	Analytical	Simulation[a], Simulation[b]	Analytical	Simulation[a], Simulation[b]
p(c)	0.67	0.6 [0.68, 0.68]	0.67	0.68 [0.68, 0.68]	0.51	0.50 [0.50, 0.50]
		0.67 [0.67, 0.68]		0.68 [0.67, 0.69]		0.01 [0.01, 0.01]
Θ	0.98	0.97 [0.97, 0.97]	0.98	0.97 [0.97, 0.97]	1.96	1.93 [1.93, 1.93]
		0.98 [0.96, 1.00]		0.96 [0.93, 0.98]		1.93 [1.93, 1.93]
L	99.51	98.63 [98.60, 98.67]	99.51	98.61 [98.56, 98.67]	99.02	99.76 [99.75, 99.76]
		99.54 [99.48, 99.59]		99.55 [99.19, 99.92]		99.77 [99.76, 99.77]
W	101.6	102.0 [101.8, 102.2]	101.6	101.9 [101.8, 102.1]	50.54	51.70 [51.70, 51.71]
		101.96 [99.76, 104.16]		104.56 [102.25, 106.88]		51.71 [51.70, 51.71]

Conclusions

We managed to design and construct *M/G/C/C* state dependent simulation models using Arena software. We believe it can easily be extended by modelers that are familiar with building DES models using module approaches. We have also presented a comprehensive comparison of the results of single, series and splitting topologies of two *M/G/C/C* simulation models. The results indicated that there are very small discrepancies between the two DES models.

Acknowledgements

This study was supported by the Research University (RU) Grant Scheme, [account number 1001/PJJAUH/811097], Universiti Sains Malaysia. L. A. Kawsar wishes to thank Universiti Sains Malaysia for the financial support (USM Fellowship). The funders had no role in study design, data collection and analysis, decision to publish, or preparation of the manuscript.

References

Altiok, T., & Melamed, B. (2007). *Simulation Modeling and Analysis with ARENA*. Burlington: Academic Press.

Banks, J., Carson, J.S., Nelson, B.L., & Nicol, D.M. (2010). *Discrete-Event System Simulation* (5 edition ed.). New Jersey: Pearson.

Cruz, F.R.B., Smith, J.M., & Medeiros, R.O. (2005). An M/G/C/C State Dependent Network Simulation Model. *Computers and Operations Research, 32*(4), 919 - 941.

Garrido, J. (1998). *Practical Process Simulation Using Object-Oriented Techniques and C++* Norwood: Artech House.

Kelton, W.D. (2009). *Simulation with Arena* (5th ed.). New York: McGraw-Hill.

Mitchell, D.H., & MacGregor Smith, J. (2001). Topological network design of pedestrian networks. *Transportation Research Part B: Methodological, 35*(2), 107-135.

Prata, S. (2011). *C++ Primer Plus* (6th ed.). Indiana: Addison-Wesley Professional.

Rossetti, M.D. (2010). *Simulation Modeling and Arena*. New Jersey: John Wiley & Sons.

Smith, J.M. (2012). Topological arrangements of M/G/c/K, M/G/c/c queues in transportation and material handling systems. *Computers & OR, 39*(11), 2800-2819.

Smith, J.M., & Kerbache, L. (2012). State Dependent Models of Material Handling Systems in Closed Queueing Networks. *International Journal of Production Research*.

Wainer, G.A., & Mosterman, P.J. (2010). *Discrete-Event Modeling and Simulation: Theory and Applications (Computational Analysis, Synthesis, and Design of Dynamic Systems)*. Boca Raton: CRC Press.

Watkins, K. (1994). *Discrete Event Simulation in C*. New York: McGraw-Hill Companies.

Temperature Control in an Industrial SO_2 Converter

Chaouki Bendjaoouahdou[1] and Mohamed Hadi Bendjaouahdou[2]

[1] Department of Industrial Chemistry, Biskra University, Algeria
[2] Department of Mathematics, Constantine Mentouri University, Algeria

Email : chawk052000@yahoo.fr

Abstract: This study addresses the problem of controlling the magnitude of the maximal catalyst temperature, or hot spot, in a four catalyst beds SO_2 converter by manipulating the reaction mixture volumetric flow rate. The control of the maximal catalyst temperature is carried out in order to avoid the occurrence of a hot spot inside the catalyst mass and to keep high catalyst efficiency. Command algorithm used is the generalised predictive control (GPC) with off line process identification. The performance and robustness of the GPC controller are evaluated for the case of a kinetic complex and reversible exothermic reaction. The results obtained by numerical simulation show the possibility of the regulation of the hot spot temperature below a pre-specified value despite the occurrence of strong perturbations.

Keywords: SO_2 converter, packed bed, catalyst, process control, hot spot, simulation.

Introduction

Temperature control is crucial when designing a catalytic reactor for exothermic reactions because hot spots affect conversion, selectivity and lifespan of catalysts. In this study we focus on the control of the catalytic fixed beds reactor because it is very used in the industrial practice for the production of various and important chemicals (Kolios et al.,2000; Vanden Bussche et al.,1993).

The operation of the catalyst fixed beds reactor presents many challenges, such as a strong dependence of temperature and concentration profiles on the inlet conditions, the possible appearance of a maximum in the temperature profile (hot spot) and the possibility of temperature runaway (Varma, 1999). The occurrence of excessive temperatures can obviously have detrimental consequence on the operation of the reactor, such as catalyst deactivation, undesired side reactions, and thermal decomposition of the product. These considerations motivate the need for energy management strategies for such reactor. In this optic, control strategies that regulate the intensity of the hot spot temperature are of crucial importance.

It is well known that the control of the catalytic fixed bed reactors often represents very complex problem. The control problems are due to the process nonlinearity, its distributed nature and high sensitivity of the state and output variables to input changes. In addition, the dynamic characteristics may exhibit a varying sign of the gain in various operating points, the time delay as well as non-minimum phase behavior. Therefore, the process with such properties is hardly controllable by conventional control methods and its effective control requires the application of control advanced methods. It was proposed the use of adaptative control (Oderwater et al,1988), linear optimal control (Kozub et al., 1987) and nonlinear control methods (Hua and Jutan, 2000) based on lumped approximations of the reactor model. Methods for distributed control in hyperbolic partial differential equation systems can be used for this purpose despite the fact that they require multiple heating/cooling zones, and as a consequence they are complex to implement in practice (Christofides and Daoutidis, 1998).

This work is a contribution related to the study of the control of the magnitude of the catalyst hot spot temperature in an industrial SO_2 converter. The studied reactor is running adiabatically with no flow reversal and it is used for the highly exothermic SO_2 oxidation in order to produce the sulfuric anhydride (SO_3). The sulfuric anhydride will be further used for the synthesis of the sulfuric acid (H_2SO_4). In order to reach high degree of SO_2 conversion, a cascade or a serial of catalytic fixed beds must be used. As a consequence, the industrial reactor is constituted, generally, of a serial of four catalytic fixed beds (Gosiewski, 1993). The control of this kind of reactor aims to avoid the occurrence of a hot spot inside the catalyst beds. This can be done by the use of a control loop for each catalytic bed in order to stabilize the maximal catalyst temperature to a specific and fixed value. The control objective is to avoid the occurrence of hot spot inside the catalytic bed and then prevents the catalyst from deactivation or sintering (Trambouze et al., 1984). From the mathematical point of view, this type of reactor belongs to the class of systems with distributed parameters (Gosiewski, 1993). The control of such process by conventional methods with fixed parameters of the controller could be a problem, mainly in the cases

where the operating point changes or reactor dynamic is affected by various changes of the inlet stream parameters. This inconvenience should be overcome with the use of some of recent control strategies such as adaptive control, predictive control etc. On the other hand, the adiabatic catalytic fixed bed is very challenging to control, relatively to cooled catalytic fixed bed, because there are not many control variables available. In this study, the inlet gas volumetric flowrate is used as manipulated variable in order to control this kind of reactor. For this purpose, the dynamic model of the process (adiabatic catalytic bed) will be integrated using the data related to its nominal operating point (Gosiewski, 1993), afterwards, the generalized predictive algorithm (GPC) with off line recursive least -squares identification will be applied to this model.

The industrial SO_2 converter

A schematic flowsheet of the industrial multiple catalytic fixed beds reactor is illustrated in Figure 1 (Gosiewski, 1993). This reactor is a serial of four catalytic fixed beds disposed vertically. Heat exchangers are disposed between two consecutive catalytic beds in order to avoid the decrease of the conversion by cooling the gas before being fed into the next bed. The diameter of each bed is equal to 8.6 m. Each catalytic bed is formed by a compact and fixed stack of vanadium catalyst pellets (Gosiewski, 1993). The inlet gas is fed through the whole reactor from the top to the bottom as illustrated in figure 1. Before the inlet gas is fed, the catalytic beds are preheated to a certain high temperature value which is greater than the catalytic ignition temperature. Then, the inlet gas with low SO_2 concentration is fed into the reactor. Each catalytic stage possesses its nominal run state or operating point specified by the physical parameter values related to the gas (the value of the inlet gas temperature is clearly predefined) and to the catalytic bed (the catalyst mass is rigorously calculated). In order to track the conversion adiabatic path and then to reach the expected conversion value at the exit of each bed, it is necessary to cool the gas at the exit of each bed. Such cooling is done by the use of heat exchangers disposed between two consecutive beds (fig.1). The catalyst bed is made adiabatic by recovering its inside wall by a thermal insulating (firebrick) layer (Gosiewski, 1993).

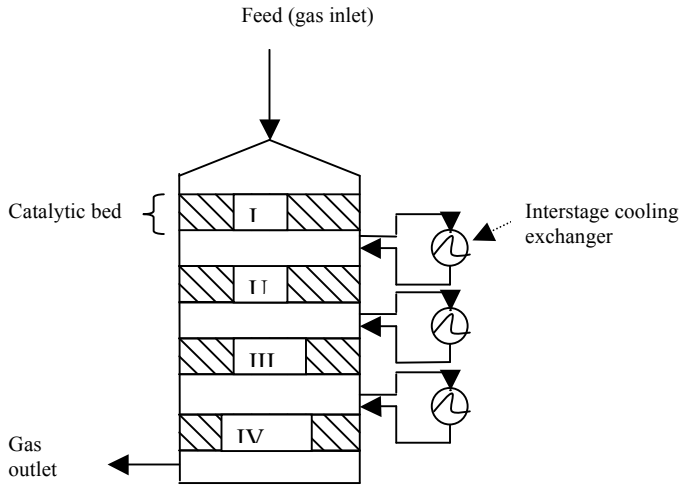

Figure 1. Schematic flowsheet of the industrial multi-staged catalyst fixed bed reactor used for SO_2 oxidation with intermediary cooling.

The catalyst characteristics, reaction rate and inlet gas composition

The SO_2 oxidation is done by the use of a vanadium pentoxyde (V_2O_5) based catalysts. The catalyst pellets have 6 to 8 wt % V_2O_5 (Trambouze et al., 1984). The catalyst is active only between 400 and 650 °C (Gosiewski, 1993). Beyond 650°C, the catalytic efficiency decrease gradually and the catalyst begins to be destroyed (Gosiewski, 1993; Trambouze et al., 1984).

The oxidation of SO_2 is a very exothermic reaction. The enthalpy related to this reaction is approximately constant between 400 and 600 °C (Gosiewski, 1993). The kinetic of SO_2 expression was studied by many authors (Dunn et al., 1999; Villermaux, 1990). In this study, the Calderbank expression rate was used (Calderbank, 1952) in which T (expressed in Kelvin) means the temperature of the catalytic solid phase, the

kinetic constants K_1 and K_2 are expressed in mol^{-1}, the component partial pressure P_i are expressed in atmosphere, and the used value of the perfect gas constant R is 8.31 $J.mol^{-1}.K^{-1}$.

$$\mathbf{r} = K_1.(P_1.P_2/ P_1^{1/2}) - K_2.(P_3. P_2^{1/2}/ P_2^{1/2})$$

$$K_1 = e^{[(130000/R.T) + 12.07)]}$$

$$K_2 = e^{[(220000/R.T) + 22.75)]}$$

In the expression of the reaction rate, the intrinsic kinetic, **r** is expressed in kmol of SO_3/kg.hr. the inlet gas fed to the first catalytic bed must have a temperature greater than 430 °C, and its molar composition is : 79 % of N_2, 11 % of O_2 and 10 % of SO_2 (Gosiewski, 1993). Table I gives additional parameter values related to the reaction rate, catalyst and the reactor.

Table 1. Parameters for SO_2 oxidation in a multiple fixed bed reactor

Parameter	Nominal value
Heat of reaction (J/mole)	$-\Delta H = 8.89 \times 10^4$
Effective heat capacity of particle	$Cp_{keff} = 2.1$ kJ/kmole
Density of catalyst particle	$\rho_u = 620$ kg/m^3
Mean diameter of catalyst pellets	$d_p = 0.0018$ m
Specific outer surface area of catalyst pellets	$S = 568$ m^{-1}
Effective thermal conductivity of catalyst pellets	$\lambda_e = 0.46$ W.m^{-2} K^{-1}
Gas-particle heat transfer coefficient	$\alpha = 151$ W.m^{-1}K^{-1}
Number of catalytic bed	$n = 4$
Depth of the catalytic bed	$L = 0.48$ m
Diameter of the catalytic bed	$D = 8.6$ m
Void fraction of the catalytic bed	$\epsilon_c = 0,5$
Inlet gas superficial molar flow (first bed)	$n_g = 13.24$ mole m^{-2}. s^{-1}
Inlet gas pressure (first bed)	$P_T = 1.2$ atm
Initial bed temperature (first bed)	$T_{co} = 460$ °C
Gas feed temperature (first bed)	$T_{go} = 460$ °C
Steady state SO_2 conversion (exit of first bed)	$X_1 = 68$ %

The dynamic model of the catalytic bed, Boundary and Initial Conditions

Dynamic model of the catalytic bed

In a catalytic fixed bed, the heat transfer between gas and particle phases is the most important, because the cold inlet gas has to be heated by the hot solids near the entrance of the bed and the cold solid is heated by the hot gas near the exit of the bed. As a consequence, in this model, the temperature and concentration differences between the gas and particle phases are accounted. The model equations were derived from the components transient continuity equations and the transient energy balance for both gas and solid phase. The used dynamic model of the catalytic fixed bed is a pseudo-homogeneous one and its related assumptions are those proposed by K. Gosiewski (Gosiewski, 1993).

$$n_g.C_{pg}.\frac{\partial T_g}{\partial x} + \alpha.S.(T_g - T_k) = 0 \qquad (1)$$

$$\lambda_e.\frac{\partial^2 T_k}{\partial x^2} - \rho_u.C_{ps}.\frac{\partial T_k}{\partial t} + \alpha.S.(T_g - T_k) + \Delta H.\mathbf{r}.\rho_u = 0 \qquad (2)$$

$$n_g\frac{\partial C_i}{\partial x} + \nu_i.\mathbf{r}.\rho_u = 0 \qquad (i = 1,2,3) \qquad (3)$$

In the bed dynamic model, the effective axial conduction is taken into consideration since the effective axial conductivity (λ_e) used for the two phases expresses better the heat and mass transfer in the catalytic fixed bed (Gosiewski, 1993; Wakao and Kaguei, 1982; Nodehi and Mousavian, 2006; Toledo et al., 2011).

Boundary and initial conditions

Boundary conditions are (Gosiewski, 1993) :

- For x = 0

$C_1(0, t) = C_{1in}(t)$

$C_2(0, t) = C_{2\,in}(t)$

$C_3(0, t) = 0$

$$\lambda_e \left(\frac{\partial T_k}{\partial x}\right)_{x=0} = (1 - \epsilon_c).\alpha.[T_k(0, t) - T_{g\,in}(t)]$$

$T_g(0, t) = T_{gin}(t)$

- For x = L

$T_g(L, t) = T_{g\,out}(t)$

$$\left(\frac{\partial T_k}{\partial x}\right)_{x=L} = 0$$

Initial conditions are (Gosiewski, 1993) :

$T_k(x, 0) = T_{co}(x) \qquad (0 \le x \le L)$

$T_g(x, 0) = T_{go}(x) \qquad (0 \le x \le L)$

$C_i(x, 0) = 0 \qquad (0 \le x \le L)$

Solution of the dynamic model equations

The equations (1) and (2) are, respectively, the gas phase and the solid phase energy balance. The equation (3) expresses the component mass balances. The Equations (1) and (3) represent Cauchy differential problems, hence readily solvable by the fourth order Runge-Kutta method (Finalyson, 1980). The equation (2) represents a boundary values differential problem. This equation was solved by the Crank Nicholson method using an implicitness factor equal to 1/2 (Necati Özisik, 1993). Indeed, the equation (6) does not belong to the convection-diffusion problems, so, the convective numerical instability will not take place with our difference scheme. A uniform computational grid was used. The catalytic bed depth was divided into N_z equivalent parts (N_z = 100), therefore, the spatial discretization step (ΔX) used was equal to 0.49 mm. The time discretization step (Δt) used was equal to 1 second. The matrix coefficients resulting from the discretization of the equation (6) is tri-diagonal. Therefore, at each time step, the tri-diagonal Thomas algorithm ((Patankar, 1980) was applied.

GPC Algorithm

The objective of the generalized predictive control (GPC) law is to compute, at each sample time t, a control signal u(t) whom the objective is to lead the future plant output y(t+j) (j = N_1, N_2) close to the set point w(t+j) (Clarke et al.,1987). The control signal is then computed so to minimize a cost function J of the form (Clarke et al., 1987):

$$J(N_1,N_2) = \sum_{j=N_1}^{j=N_2} [y(t+j)-w(t+j)]^2 + \sum_{j=N_1}^{j=N_2} \lambda(j).[\Delta u(t+j-1)]^2$$

with $\Delta u(t) = u(t) - u(t-1)$

From the expression of the cost function J, it is clear that the objective of GPC control law is twice. On one hand, the control law minimizes, to least squares sense, the sum extended to the entire prediction horizon (j = N_1, N_2) of the future errors; on the other hand, this objective is realized so that to minimize the energy consumption. The control weighting vector $\lambda(j)$ is introduced into the control law in order to limit every activity excess of the command signal by a judicious choice of its components. Sometimes, to simplify it is assumed that $\lambda(j) = \lambda$ and therefore, λ will be called the control weighting coefficient. The coefficients λ, Nu, N_1 and N_2 are the main conception parameters of the GPC control algorithm (Clarke et al., 1987).

Results and Discussion

In this study we focused only on the control of one catalytic bed (first bed) of the industrial reactor (fig. 1), but, it is obvious that the results found are easily applicable to the other catalytic beds. The control of the catalytic stage

aims to stabilize the intensity of the hot spot in order to prevent the runaway or shutdown of the chemical reaction temperature. In this study, the controlled variable is the maximal catalyst temperature and the manipulated variable is the inlet gas volumetric flowrate. The perturbations considered were the inlet gas temperature, the reactant (SO_2 and O_2) inlet concentrations and the inlet gas pressure.

Open loop catalytic fixed bed

Figures 2 and 3 show that despite the occurrence of an intense perturbation related to SO_2 and O_2 inlet concentrations, the maximal catalyst temperature reaches (fig. 2) or does not exceed 650 °C (fig. 3). This last value is generally the maximal temperature supportable by the V_2O_5 based catalysts. The results given by these figures can be explained by the fact that the reactants are strongly diluted by the inert component (N_2) in the inlet gas. These last figures show that after the inlet reactant concentrations have been turned back to the normal operating value, the maximal catalyst temperature reaches its original value.

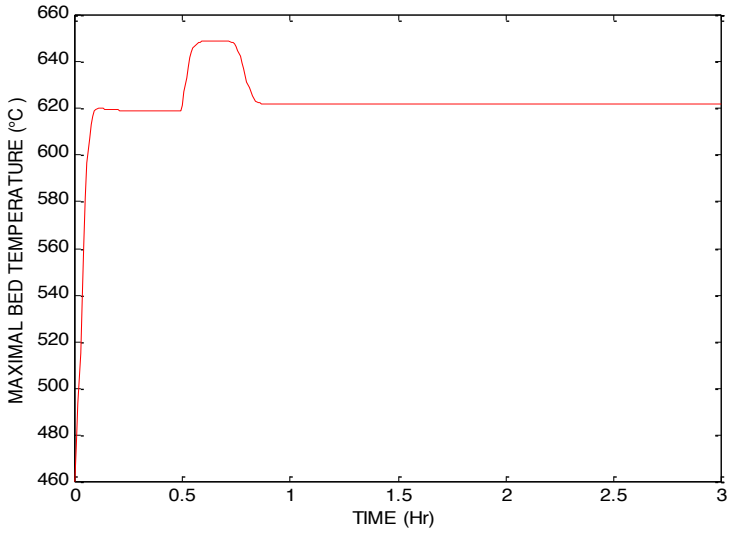

.

Figure 2. Process response to + 25 % step change of C_{1in} (C_{1in} = 0.1) occurring at 0.5 hour during 10 minutes

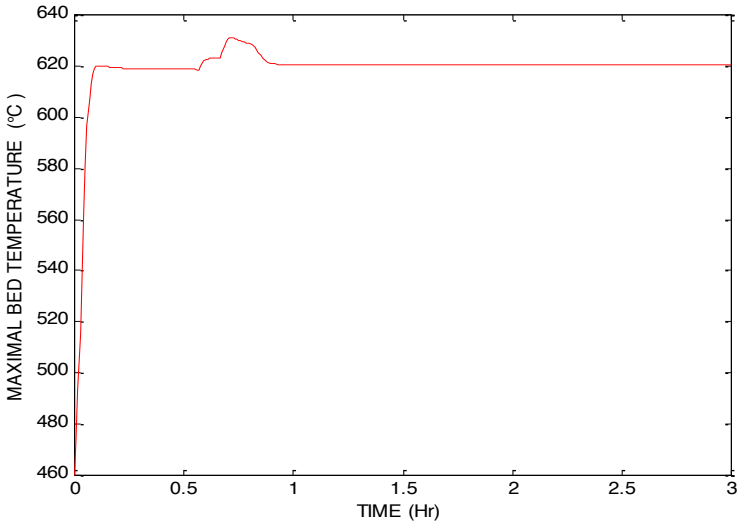

Figure 3. Process response to +25 % step change of C_{2in} (C_{2in} = 0.11) occurring at 0.5 hour during 10 minutes.

Fig. 4 shows that an intense perturbation related to the total pressure does not induce an important increase of the maximal catalyst temperature, (the maximal catalyst temperature remain less than 650 °C), this can be explained, according to Le Châtelier principle (Villermaux, 1990), by the weak value of the difference of the total molecules or moles number of the reaction between reactants and products, which is equal to ½ (SO_2 + ½ O_2 ⟶ SO_3).

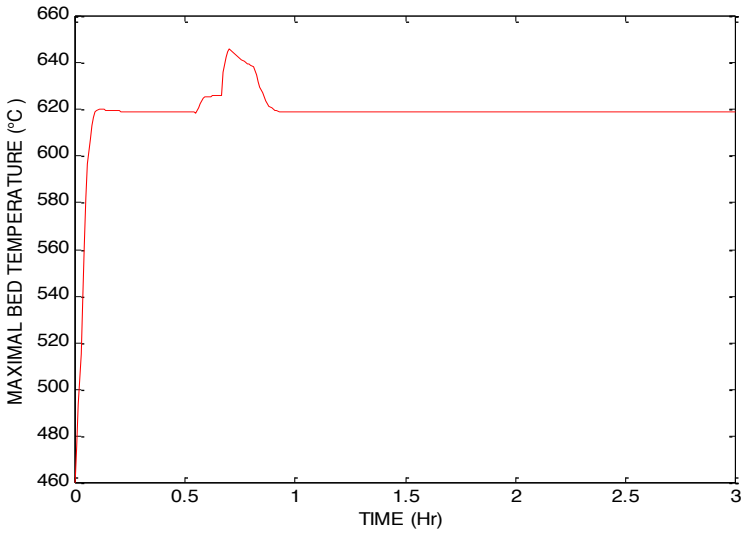

Figure 4. Process response to + 25 % step change of P_T (P_T = 1.2 atm) occurring at 0.5 hour during 10 minutes.

Figures 5 and 6 illustrate the strong influence of gas inlet temperature on the value of the maximal catalyst temperature; this can be explained by the high exothermic effect of the reaction and also by the adiabatic run of the catalytic bed. It can be seen from these figures, that the maximal catalyst temperature exceed largely 650 °C, and consequently, the production capacity of the bed is expected to decrease due to the catalyst deactivity or sintering.

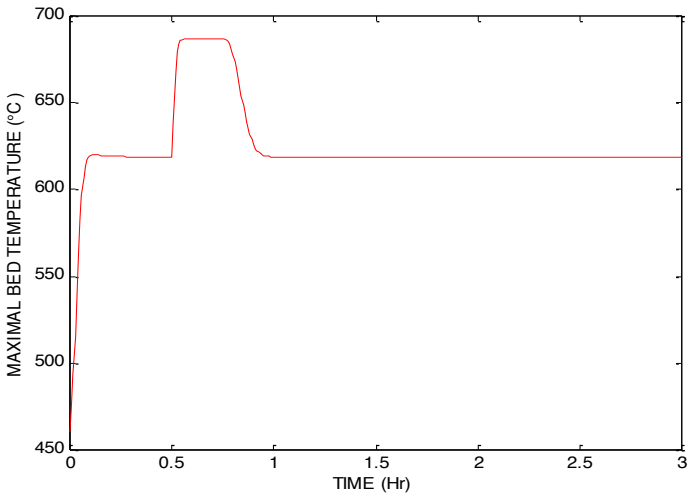

Figure 5. Process response to + 25 % step change of Tg_{in} (Tg_{in} = 440 °C) occurring at 0.5 hour during 10 minutes.

In figure 6, the phenomenon of the inverse response is observed, although it is of a small magnitude. This means that a very special care has to be taken if the gas inlet temperature is used as manipulated variable in a control loop. The inverse response can be explained by the fact that a sudden decrease in the inlet temperature will affect the bed temperature by two mechanisms: by the migration of temperature waves in the bed, which is a slow process; and by the changes in the concentration of chemical components, which is a relatively fast process

(Quina and Qinta Ferreira, 2000). As a consequence, there will be a loss of conversion in the whole bed and the bed temperature decreases (Morud and Skogestad, 1993). The inverse response usually causes difficulties of the stability in a control loop and a such phenomenon was observed for the SO_2 converter (Xiao and al., 1999). The prediction of the heterogeneous and the pseudo-homogeneous dynamic models are quite similar. The pseudo-homogeneous model assumes the same local temperature for the gas and the solids and hence, the time scale for heat transfer between the two phases is zero, whereas reaction time is finite. Thus the pseudo-homogeneous model can predicts better the inverse response or wrong way behavior when compared to the heterogeneous model (Quina and Qinta Ferreira, 2000). Since in the industrial practice, the magnitude of the perturbation of the parameters process does not exceed ± 20 % (Luyben, 2007; Toledo and al., 2001), so, it can claimed that for this kind of industrial reactor, the inlet gas temperature is the only parameter to be considered as a main perturbation for control purposes.

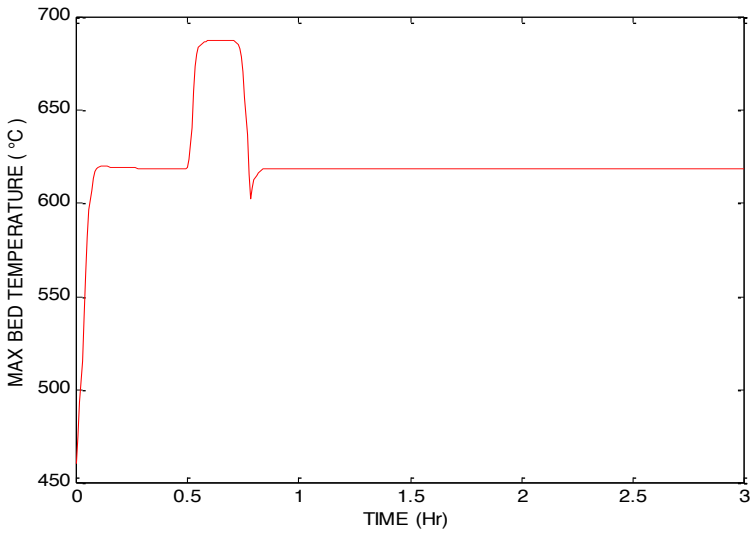

Figure 6. Process response to – 25 % step change of Tg_{in} (Tg_{in} = 440 °C) occurring at 0.5 hour during 10 minutes.

Closed loop catalytic fixed bed

The system (catalytic fixed bed) was identified in open loop mode using a pseudo-random binary sequence (PABS) with a sampling time equal to 20 seconds and a forgetting factor equal to the unity. The recursive least - squares identification method was applied to determine the discrete transfer function. It was found that the system is a second order one and its transfer function is as follows:

$G(z^{-1}) = z^{-1}(0.417 + 0.34.z^{-1}) / (1 - 0.988.z^{-1} + 0.02.z^{-2})$

In order to control the maximal catalyst temperature, the GPC algorithm was used with the following values of its main parameters N_1 =1; N_2 = 8; λ = 4; Nu = 2. These last values were determined by a trial and error procedure. The controlled variable (maximal catalyst temperature) will be given by a set of thermocouples disposed axially along the bed because the hot spot can move inside the bed (Yakhnin and Menzinger, 1998). The maximal catalyst temperature will be selected by a high selector device. This configuration of the thermocouples is frequently used in the practice and has been proven to give good measurements results (Cho and al., 1993; Chin et al., 2002). The control signal (inlet gas flow rate) will be given by a control valve disposed at the entrance of the bed. For all the simulations, the sampling period value used was equal to 30 seconds, the set point of the maximal catalyst temperature was 610 °C and the control signal or the manipulated variable was limited between 5 and 37.45 m^3/s. This control configuration is applicable for the four bed of the converter, and the results obtained for the first bed will be applicable for the other beds.

Figure 7 illustrates that the GPC controller successfully maintains the maximal catalyst temperature at its set value (610°C) despite the occurrence of perturbation. Furthermore the controller attenuates the disturbance very fast and the overshoots caused by this last one are minimal (figure 7 is to be compared with figure 2). From figure 8 it is shown that the GPC controller effectively regulates the maximal bed temperature to the set point value despite the occurrence of an perturbation related to the total operating pressure (P_T). The control signal varies regularly without the presence of dangerous peaks, detrimental for the control valve (figure 8 is to be compared with figure 4).

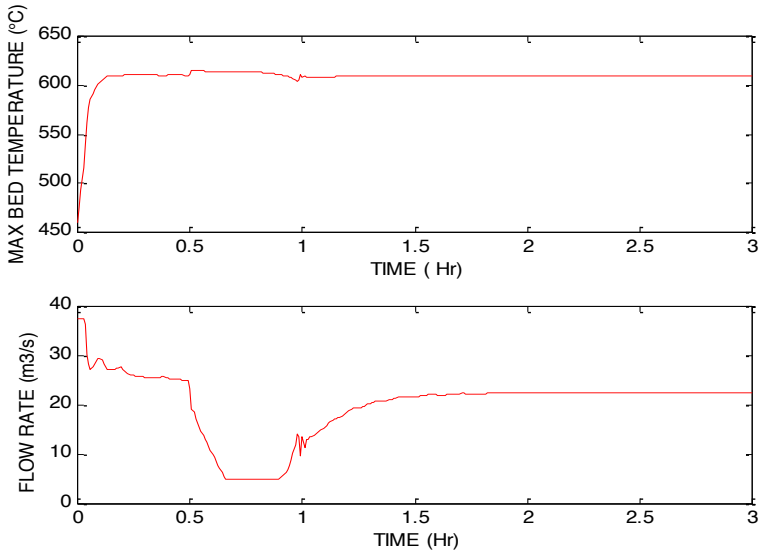

Figure 7. Process response and control signal to + 25 % step change of C_{1in} (C_{1in} = 0.1) occurring at 0.5 hour during 10 minutes with regulation of the temperature at 610 °C.

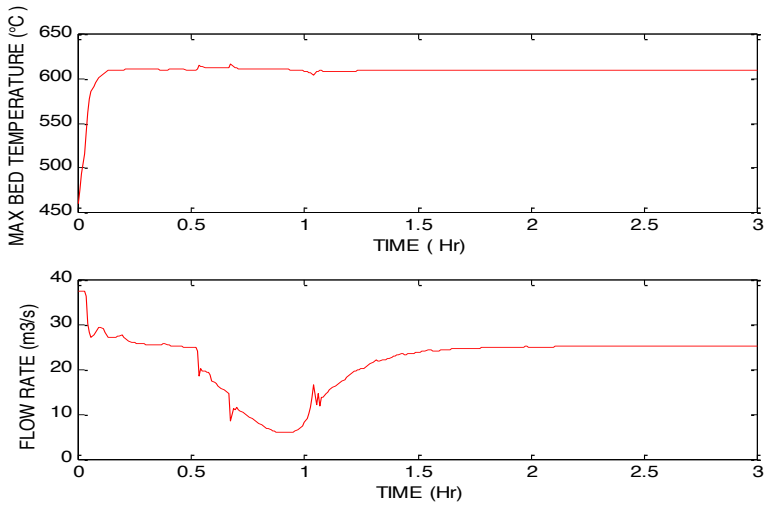

Figure 8. Process response and control signal to + 25 % step change of P_T (P_T = 1.2 atm) occurring at 0.5 hour during 10 minutes with regulation of the temperature at 610 °C.

Figures 9 and 10 show that the GPC controller efficiently stabilizes the maximal bed temperature with a great disturbance rejection capability and the control signal does not present very excessive variations (figures 9 and 10 are to be compared respectively with figures 5 and 6). Figure 11 shows the set point tracking of the maximal bed temperature when the desired temperature changes from 610 °C to 590 °C. It can be seen that the maximal catalyst temperature effectively follows the new value of the desired temperature and the control signal varies regularly. However, the new value of the desired temperature is not reached rapidly; this can be explained by the important thermal inertia of the bed conferred by its great thermal capacity due to the important catalytic mass.

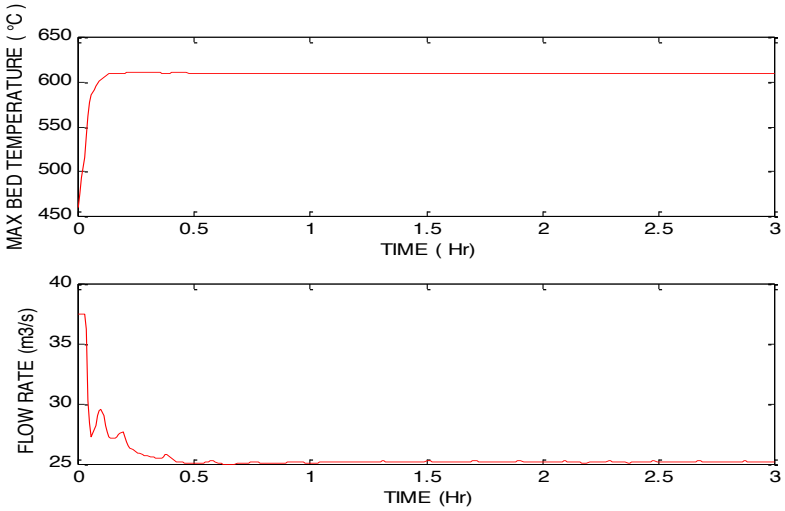

Figure 9. Process response and control signal to +25 % step change of Tg_{in} (Tg_{in} = 440 °C) occurring at 0.5 hour during 10 minutes with regulation of the temperature at 610 °C.

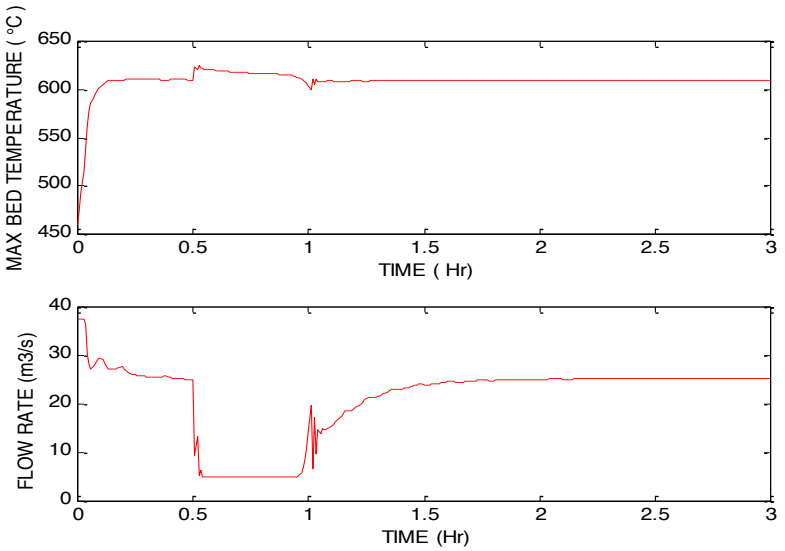

Figure 10. Process response and control signal to -25 % step change of Tg_{in} (Tg_{in} = 440 °C) occurring at 0.5 hour during 10 minutes with regulation of the temperature at 610 °C

Conclusion

The results obtained in this study can be resumed as follows.

1. The finite difference method based on the Crank-Nicolson scheme was used to solve the dynamic model equations on uniform grid. This scheme was stable and provides satisfactory numerical results.
2. The controlled process (catalytic bed) was identified using a pseudo-random binary sequence (PABS) and the recursive least -squares identification method was applied to determine its discrete transfer function.
3. The open loop results showed that the maximal catalyst temperature or hot spot is very sensitive to the inlet temperature gas and insensitive to the inlet reactant concentration and total pressure of the gas. On the other hand, the inlet temperature gas cannot be used as a manipulated or control variable due to the inverse response phenomenon.
4. The closed loop results showed that the generalized predictive control (GPC) successfully and satisfactory controls the maximal catalyst temperature (hot spot) in regulation and set point tracking mode.

5. The control of the magnitude of the hot spot for a catalytic fixed bed is possible, by manipulating the inlet volumetric gas flow, in order to avoid the temperature runaway and the deactivation of the catalyst.

Nomenclature

C_i	molar fraction of species i, in the bulk phase gas, mole
C_{pg}	heat capacity of gas, J/mole.K
C_{ps}	heat capacity of solid, J/mole.K
D	catalytic bed diameter, m
j	predictive index
J	objective function or cost function
K_1, K_2	reaction rate constants
L	catalytic bed depth, m
n_g	superficial molar flow of gas, mole/m^2.s
N_1	minimum prediction horizon
N_2	maximum prediction horizon
Nu	control horizon
N_z	subdivision number of bed depth
p	Laplace variable
P_i	partial pressure of specie I, atm
P_T	total pressure, atm
r	intrinsic rate reaction, kmole of SO_3/(kg.hr)
S	specific outer surface area of catalyst pellets, m^2/m^3
T_g	temperature of the gas phase, (K)
T_k	temperature of the solid phase, K
$T_{g\ in}$	temperature of the gas at the entrance of the first bed, K
$T_{g\ out}$	temperature of the gas at the exit of the first bed, K
$T_{co}(x)$	initial bed temperature profil, K
$T_{go}(x)$	initial gas temperature profil, K
t	time, s
u	control signal
w	set point or reference signal
x	spatial coordinate computed from the entrance of gas phase in the catalytic bed, m
y	output or response process
z	sampling variable

Greek letters

ρ_u	density of solid, kg/m^3
εc	voidage of catalyst bed
α	gas –solid heat transfer coefficient, W/m^2.K
ΔH	heat of reaction, J/mol
Δt	step size of time discretization, s
Δx	step size of spatial discretization, m
Δu(t)	control signal increment at the current instant
λ_e	axial effective thermal conductivity of solid, Watt/(m. K)
λ	control weighting vector of the control signal
$\nu_{i.}$	stoichiometric coefficient of specie i

Subscripts

1	sulfur dioxyde (SO_2)
2	molecular oxygen (O_2)
3	sulfuric anhydride (SO_3)
4	molecular nitrogen (N_2)
g	gas phase
in	entrance of the first catalytic bed
i	chemical specie
k	catalytic or solid phase
out	exit of the first catalytic bed

References

Calderbank P. H. (1952). The mechanism of the catalytic oxidation of sulphur dioxide with a commercial vanadium catalyst: A kinetic study. J. App. Chem., 2(8), 482-492.

Cho C. K., Chang K. S., Cale T. S. (1993). Thermal runaway prevention in catalytic packed bed reactor by solid temperature measurement and control, Kor. J. Chem. Eng., 10(4), 195-202.

Christofides P. D., Daoutidis P. (1998). Robust control of hyperbolic PDE Systems, Chem. Eng. Sci. 53(1), 85-105.

Clarke D. W., Mohtadi C., Tuffs P. S. (1987). Generalized predictive control - Part I. The basic algorithm, Automatica, 23(2), 137-148.

Dunn J. P., Stenger H. G. Jr,. Wachs I. E (1999). Oxidation of SO_2 over supported metal oxide catalysts. J. Catalys. 181(2), 233-243.

Finalyson B. A. (1980). Non linear analysis in chemical engineering, McGraw-Hill New York.

Gosiewski K. (1993). Dynamic modelling of industrial SO_2 oxidation reactors part I. model of 'hot' and 'cold' start-ups of the plant, *Chem.* Eng. Proces : Proces. Intensif, 32(2), 111-129.

Hua X., Jutan A. (2000). Nonlinear inferential cascade control of exothermic fixed-bed reactors, AIChE J. 46(5), 980-996.

Kolios, G., Frauhammer J., and Eigenberger G. (2000). Autothermal fixed –bed reactors concepts, Chem. Eng. Sci,. 55, 5945-5967.

Kozub D. J., Macgregor J. F., Wright J. D. (1987). Application of LQ and IMC controllers to a packed-bed reactor, AIChE J. 33 (9), 1496-1506.

Luyben W. L. (2007). Chemical reactor design and control, 2nd ed, John Wiley & sons, New Jersey.

Morud J., Skogestad S. (1993). The dynamics of chemical reactors with heat integration, paper presented at AIChE Annual Meeting, St Louis, (paper 26e).

Necati Özisik M. (1993). Heat conduction, 2nd ed, John Wiley & Sons New York.

Nodehi A., Mousavian M. A (2006). Simulation and Optimization of an Adiabatic Multi-Bed Catalytic Reactor for the Oxidation of SO_2, Chem. Eng. Tech. 29(1), 84-90.

Oderwater D., Macgregor J. F, Wright J. D (1988). Use of nonlinear transformations and a self-tuning regulator to develop an algorithm for catalytic reactor temperature control, *Can. J. Chem. Eng.* 66**,** 478-484.

Patankar S. V. (1980). Numerical heat transfer and fluid flow, Hemisphere Washington DC.

Quina M. M. J., Qinta Ferreira R. M (2000). Start-up and wrong way behavior in a tubular reactor: dilution effect of the catalytic bed, Chem. Eng. Sci. 55**,** 3885-3897.

Toledo E. C. V., Morais E. R., Melo D. N. C, Mariano A. P.,Meyer J. F. C. A, Maciel
Filho R. (2011). Suiting dynamics models of fixed bed catalytic reactors for computer based applications, Engineering, 3(7), 778-788.

Toledo E. C. V., Sanatana P. L., Wolf Maciel M. R., Maciel Filho R (2001). Dynamic modeling of a three-phase catalytic slurry reactor, Chem. Eng. Sci., 56**,** 6055-6061.

Trambouze P., Van Landeghem and H., Wauquier J. P. (1984). Les réacteurs chimiques conception /calcul /mise en œuvre, Technip, Paris.

Vanden Bussche K. M., Neophytides S. N., Zolotarski I. A., and Froment G. F., (1993). Modeling and simulation of the reversed flow operation of a fixed-bed reactor for methanol synthesis, Chem.Eng. Sci. 48**,** 3335-3345.

Varma A., Morbidelli M., and Wu H. (1999). Parametric sensivity in chemical systems, Cambridge University Press.

Villermaux J. (1990). Génie de la réaction chimique, conception et fonctionnement des réacteurs, Lavoisier, Paris.

Wakao N., Kaguei S. (1982). Heat and mass transfer in packed beds, Gordon and Breach, London.

Xiao W. D., Wang H., Yuan W. K (1999). An SO_2 converter with flow reversal and interstage heat removal : from laboratory to industry, Chem. Eng. Sci, 54, 1307-1311.

Yakhnin V. Z., Menzinger M. (1998). Resonance and moving hot spots in adiabatic packed bed, AIChE. J., 44**,** 1222-1225.